UNIVERSITY OF KWAZULU-NATAL ™

INYUVESI YAKWAZULU-NATALI

Betulinic acid enhances the antioxidant profile in a hyperglycaemic model

BY

Gopala Maharaj

B. Med. Sc. (Hons) (UKZN)

Submitted in fulfilment of the requirements for the degree of

Master of Medical Science

in the Discipline of Medical Biochemistry

School of Laboratory Medicine and Medical Sciences

College of Health Sciences

University of Kwa-Zulu Natal

Durban

2019

PLAGIARISM DECLARATION FORM

I, **Gopala Maharaj**, student number: 215034643, declare that:

i.   The research reported in this dissertation, except where otherwise indicated, is my original work.
ii.   This dissertation has not been submitted for any degree or examination at any other university.
iii. This dissertation does not contain other persons' data, pictures, graphs or other information, unless specifically acknowledged as being sourced from other persons.
iv.   This dissertation does not contain other persons' writing, unless specifically acknowledged as being sourced from other researchers. Where other written sources have been quoted, then:
       a. Their words have been rewritten but the general information attributed to them has been referenced.
       b. Where their exact words have been used, their writing has been placed inside quotation marks, and referenced.
v.   Where I have reproduced a publication of which I am an author, co-author or editor, I have indicated in detail which part of the publication was actually written by myself alone and have fully referenced such publications
vi.   This dissertation does not contain text, graphics or tables copied and pasted from internet, unless specifically acknowledged, and the source being in the dissertation and in the Reference sections

The research described in this study was carried out in the Discipline of Medical Biochemistry, School of Laboratory Medicine and Medical Science, College of Health Sciences, University of Kwa-Zulu Natal, under the supervision of Prof. A. Chuturgoon and Dr N. Sheik-Abdul.

Signed: _____   Date: _08 December 2019_

ACKNOWLEDGEMENTS

CONTENTS

LIST OF ABBREVIATIONS:

1,3-DPG	1,3-diphosphoglycerate
AGE	Advanced Glycation End-products
AO	Antioxidant
APS	Ammonium persulphate
ARE	Antioxidant Response Element
ATP	Adenosine triphosphate
BA	Betulinic Acid
BCA	Bicinchoninic acid
BHT	Butylated hydroxytoluene
BSA	Bovine serum albumin
CAT	Catalase
CCM	Complete culture media
cDNA	Complementary deoxyribonucleic acid
CHO-IR	Chinese hamster ovary cell line transfected with insulin receptor
CREB	cAMP response element-binding protein
CT	Cycle threshold
Cu	Copper
Cu1+	Cuprous ions
Cu2+	Cupric ions
CVD	Cardiovascular disease
CVS	Cardiovascular System
DCFH	2,7-dichlorofluorescein
DMEM	Dulbecco's modified eagle medium
DMSO	Dimethyl sulfoxide
DNA	Deoxyribonucleic acid

DNP	2,4-dinitrophenylhydrazones
DNPH	2,4-dinitrophenylhydrazine
dNTPs	Deoxynucleoside triphosphates
dsDNA	Double stranded DNA
e-	Electrons
EMEM	Eagle's Essential Minimal Media
ERRα	Estrogen-related receptor alpha
ETC	Electron transport chain
FA	Fatty acid
FAD	Flavin adenine dinucleotide
FADH$_2$	Flavin adenine dinucleotide (reduced)
FCS	Foetal calf serum
Fe	Iron
G3P	Glyceraldehyde 3-phosphate
G6PD	Glucose-6-phosphate dehydrogenase
GIT	Gastrointestinal tract
GPx	Glutathione peroxidase
GPx1	Glutathione peroxidase 1
GR	Glutathione reductase
GSH	Glutathione (Reduced)
GSSG	Glutathione (Oxidised)
GST	Glutathione-s-transferase
H	Hydrogen
H$_2$DCF	2,7-dichlorodihydrofluorescein
H$_2$DCF-DA	2,7-dichlorodihydrofluorescein-diacetate
H$_2$O	Water
H$_2$O$_2$	Hydrogen peroxide

H₃PO₄	Phosphoric acid
HCl	Hydrogen chloride
HepG2	Human hepatoma
HFD	High fat diet
HG	Hyperglycaemic
HO₂•	Hydroperoxyl
HOCl	Hypochlorous acid
HRP	Horse radish peroxidase
Hrs	Hours
IDF	International Diabetes Federation
IDH2	Isocitrate dehydrogenase 2
IL1β	Interleukin 1 β
IR-β	Insulin Receptor β-Subunit
IRS-1	Insulin receptor substrate 1
KEAP1	Kelch-like ECH associated protein 1
LDH	Lactate dehydrogenase
LONP1	Lon protease
MAPK	Mitogen-activated protein kinase
MDA	Malondialdehyde
MetS	Metabolic Syndrome
miR124	Micro-RNA 124
miRNA	Micro-RNA
Min	Minutes
mRNA	Messenger ribonucleic acid
MTT	3-(4,5-dimethylthiazol-2-yl)-2,5-diphenyl tetrazolium bromide
NAD⁺	Nicotinamide adenine dinucleotide
NADP⁺	Nicotinamide adenine dinucleotide phosphate

NADPH	Nicotinamide adenine dinucleotide phosphate (reduced)
NOX2	NADPH oxidase 2
NFκB	Nuclear factor κB
nfH$_2$O	Nuclease free water
NRF2	Nuclear-factor-erythroid 2 p45-related factor 2
O$_2$	Oxygen
O$_2{}^{\bullet-}$	Superoxide radicals
O$_3$	Ozone
OH$^{\bullet}$	Hydroxyl radical
OS	Oxidative stress
OXPHOS	Oxidative phosphorylation
PBS	Phosphate buffered saline
PCA	Protein carbonyl assay
PCR	Polymerase chain reaction
PGC1-α	PPARγ Coactivator 1α
PI3K	Phosphoinositide 3-kinase
PIP$_3$	Phosphatidylinositol (3,4,5)-trisphosphate
PKB	Protein kinase B
PKC	Protein kinase C
pNRF2	Phosphorylated nuclear-factor-erythroid 2 p45-related factor 2
PPARγ	Peroxisome Proliferator-Activated Receptor Gamma
PPRE	peroxisome proliferator hormone response elements
PUFA	Polyunsaturated fatty acids
PY20	Phospho-tyrosine
qPCR	Quantitative polymerase chain reaction

RAGE	Receptor for Advanced Glycation End-products
RBD	Relative band density
RLU	Relative light units
RNA	Ribonucleic acid
ROOH	Alkyl hydroperoxide
RO$^{\bullet}$	Alkoxyl
RO$_2^{\bullet}$	Alkperoxyl
ROS	Reactive oxygen species
RT	Room temperature
SDS	Sodium dodecyl sulphate
SDS-PAGE	Sodium dodecyl sulphate–polyacrylamide gel electrophoresis
SIRT3	Sirtuin 3
SOD	Superoxide dismutase
SOD2	Superoxide dismutase 2
ssDNA	Single stranded Deoxyribonucleic acid
T2DM	Type 2 Diabetes Mellitus
TBA	Thiobarbituric acid
TBA/BHT	Thiobarbituric acid/butylated hydroxytoluene
TBARS	Thiobarbituric acid reactive substances
TCA	Tricarboxylic acid
TEMED	Tetramethylethylenediamine
TTBS	Tween 20-Tris buffered saline
UCP2	Uncoupling protein 2
WHO	World Health Organization

LIST OF FIGURES

CHAPTER 2: LITERATURE REVIEW

CHAPTER 3: METHODS AND MATERIALS

CHAPTER 4: RESULTS

CHAPTER 5: DISCUSSION

APPENDIX A

APPENDIX B

LIST OF EQUATIONS

LIST OF TABLES

CHAPTER 2: LITERATURE REVIEW

CHAPTER 3: METHODS AND MATERIALS

APPENDIX A

ABSTRACT

Type 2 diabetes mellitus (T2DM) is a global pandemic, with prevalence rapidly rising in South Africa. T2DM is characterized by insulin resistance, leading to hyperglycaemia which induces oxidative stress (OS) and inflammation with subsequent complications. Betulinic acid (BA), a ubiquitous plant triterpenoid, has many proven benefits including antioxidant (AO) properties. Peroxisome proliferator-activated receptor γ (PPARγ) is a nuclear receptor which binds to triterpenes and promotes glucose uptake and stimulates cytoprotective and anti-inflammatory effects. This study investigated the potential of BA to modulate cytoprotective responses through PPARγ in response to hyperglycaemic (HG) induced OS in a human hepatoma (HepG2) liver cell model. HepG2 cells were cultured under normoglycaemic (NG) and HG conditions and subsequently treated with 5µM and 10µM BA. Spectrophotometric [3-(4,5-dimethylthiazol-2-yl)-2,5-diphenyl tetrazolium bromide (MTT) and lactate dehydrogenase (LDH) assays] and luminescent (ATP assay) principles were employed to assess viability of the chosen BA concentrations. Phosphorylation of the insulin receptor β-subunit (IRβ) was assessed via Western blot to confirm BA's anti-HG effects. Intracellular reactive oxygen species (ROS) levels were assessed via fluorescence using the 2′,7′-dichlorodihydrofluorescein-diacetate (H$_2$DCF-DA) assay, and oxidative stress biomarkers were quantified spectrophotometrically, via use of the thiobarbituric acid reactive substances (TBARS) assay for lipid peroxidation, and protein carbonyl assay (PCA). Intracellular AO potential was measured via luminometric quantification of reduced glutathione (GSH). Western blots quantifying protein expression of PPARγ, nuclear factor erythroid 2-related factor2 (NRF2), phosphorylated NRF2 (pNRF2), sirtuin3 (SIRT3), PPARγ coactivator 1α (PGC1α), superoxide dismutase 2 (SOD2), catalase (CAT), uncoupling protein 2 (UCP2), lon protease (LONP1) and nuclear factor κ-B (NFκB) as well as quantitative polymerase chain reaction (qPCRs) assessing gene expression of glutathione peroxidase (GPx1), NRF2, SIRT3, PGC1α and micro-RNA 124 (miR124) were run to elucidate the molecular mechanism behind the cytoprotective response of BA. The MTT, ATP and LDH assays confirmed cell viability, lack of toxicity and stable energy output, while TBARS, DCF and PCA confirmed a reduction of ROS and its biomarkers. A preliminary Western blot of IRβ confirmed BA's anti-hyperglycaemic actions at a prime concentration of 5µM BA. Further, Western blots also confirmed an AO-induced protective mechanism at 5µM BA originating from the PPARγ/NRF2 positive feedback loop, further involving SIRT3 ($p<0.0001$), PGC1α ($p=0.0025$), LONP1 ($p<0.0001$), and AOs: SOD2 ($p<0.0001$), CAT ($p=0.0003$) and UCP2 ($p<0.0001$). The GSH assay and mRNA levels of PGC1α ($p<0.0001$), NRF2 ($p<0.0001$), SIRT3 ($p<0.0001$) and GPx1 ($p<0.0001$) further confirmed the mechanism, while miR124 levels ($p=0.0093$) hinted at epigenetic regulation between the transcription factors. Additionally, BA was found to downregulate NFκB ($p<0.0001$) in the HG state possibly combatting ROS-induced inflammation.

In conclusion, BA illustrated cytoprotective effects on HG induced OS at an optimum concentration of 5µM, by upregulating the AO response and reducing ROS. Thus, BA may be considered an alternate and cheap adjunctive therapy to mitigate complications of T2DM.

CHAPTER 1: INTRODUCTION

Diabetes is a global pandemic, with more than 90% of cases identified as type 2 (Wu et al., 2014). Hyperglycaemia due to insulin resistance is a prominent feature of T2DM, promoting inflammation and excessive ROS formation, with consequent diabetic complications (Collins et al., 2018).

Basal levels of ROS occur under physiological conditions, albeit minimally, as a result of electron leakage from various complexes within the electron transport chain (ETC), functioning as signalling molecules (Collins et al., 2018). Hyperglycaemic conditions partially inhibit complex 3 of the ETC, exacerbating ROS production (Rolo and Palmeira, 2006). An increase in ROS beyond the capacity of the AO system, results in a phenomenon known as OS, leading to lipid and protein oxidation, and mitochondrial dysfunction (Appari et al., 2018). Excessive and prolonged OS has been one of the earliest identified pathological mechanisms implicated in diabetic complications, which include vascular disorders, neuropathy, nephropathy and cardiovascular disease amongst others (Appari et al., 2018). Recent studies suggest that addressing OS is a strategic therapeutic intervention to address diabetic complications (Guzik and Cosentino, 2018, Saha and Ghosh, 2012, Li et al., 2014).

Of particular concern is the aberrant AO system brought about by the diabetic state. Glycation results in impaired activity of many AO enzymes including SOD2, GPx1 and CAT (Szaleczky et al., 1999). SOD2 enzymatically converts superoxide radicals into the less deleterious hydrogen peroxide. This peroxide is further detoxified into unreactive H_2O via the action of the predominantly cytosolic enzyme CAT, and the predominantly mitochondrial enzyme GPx1, aided by the non-enzymatic cofactor, glutathione (Birben et al., 2012). In addition to the impaired AO activity, high levels of both intramitochondrial and cytosolic ROS, induced by diabetes, further depletes any remaining AO reserves (Phaniendra et al., 2015).

Uncoupling protein 2, a mitochondrial membrane protein, has a somewhat distinctive modulation of both AO response as well as ROS production, making it particularly advantageous in the diabetic setting. UCP2 is a protein that uncouples the ETC from oxidative phosphorylation (OXPHOS), dissipating the energy potential across the inner mitochondrial membrane, thus mitigating ROS production (Pierelli et al., 2017). UCP2 indirectly regulates the AO response by altering the NAD^+/NADH ratio to promote SIRT3 AO activity (Sosa-Gutiérrez et al., 2018).

Sirtuin 3 is a NAD-dependant deacetylase, which activates many AO-related proteins, e.g. SOD2 (Chen et al., 2011). Additionally, SIRT3 activates LONP1, which plays a role in degradation of oxidatively damaged proteins, thus preventing further ROS-induced toxicity (Gibellini et al., 2014).

Different theories explore PGC1α's role in the transcriptional regulation of SIRT3, with one of them involving NRF2 as a transcription factor (Song et al., 2017). Earlier literature reports of a positive feedback loop existing between SIRT3 and PGC1α, with both potentiating each other, as well as the AO profile (Kong et al., 2010).

Under OS conditions, the cell attempts to modulate the AO response via transcriptional regulation. Transcription factor NRF2, along with its positive feedback partner PPARγ, and its co-activator PGC1α, transcribe for a plethora of AO proteins including SOD2, GPx1, CAT and UCP2 (Valle et al., 2005, Lee, 2017).

The phenomenon of epigenetics has been extensively studied in relation to AO modulation. Epigenetics involves the alteration of a gene's expression without altering the genetic code, and includes mechanisms such as methylation, deacetylation and microRNA (miRNA) regulation. MiRNAs are a class of small noncoding RNAs that post-transcriptionally regulate gene expression (Guzik and Cosentino, 2018). MiR124 is relevant because of its association with PPARγ, NRF2 and NFκB. The AO and anti-inflammatory effects of miR124 are due to this association. Thus, miR124 acts to further potentiate the cytoprotective profile.

Exogenous compounds may be used to speed up or heighten the AO-response. Certain secondary plant metabolites, e.g. triterpenes, display various pharmacological benefits, including AO effects, while being devoid of pronounced toxicity (Jäger et al., 2009). Betulinic acid, a ubiquitous, pentacyclic triterpene, which has been used commonly in natural healing, exerts its AO response via binding to PPARγ (Brusotti et al., 2017). Furthermore, triterpenes are proven to directly phosphorylate and activate NRF2 (Loboda et al., 2012). Betulinic acid is found in white birch bark, in the easily convertible form of betulin (Yogeeswari and Sriram, 2005). A wide range of research has proven numerous pharmacological benefits of BA, including antioxidant, anti-diabetic and anti-inflammatory effects (Szuster-Ciesielska and Kandefer-Szerszeñ, 2005, Wang et al., 2016, Silva et al., 2016).

A deleterious repercussion of OS is the activation of the inflammatory pathway. These phenomena are tightly linked via a positive feedback loop, with HG induced ROS being an activation signal for inflammation and vice versa (Sharma et al., 2018). Reactive oxygen species also indirectly promote inflammation via NFκB activation (Morgan and Liu, 2011). NFκB activation is considered a central event early in the pathophysiology of diabetes, and is responsible for the transcription of cytokines, chemokines and other pro-inflammatory molecules (Patel and Santani, 2009).
As an extension of their AO effect, multiple proteins, including NRF2, PPARγ and PGC1α, act to inhibit NFκB, thus reducing ROS driven inflammation (Wahli, 2008, Eisele et al., 2015, Guzik and Cosentino, 2018). Furthermore, PPARγ modulates miR124 expression to exert its anti-inflammatory action via targeting NFκB (Wang et al., 2017).

The liver plays a central role in energy homeostasis with regards to regulation of carbohydrate and lipid metabolism, derangements of which contribute to the pathophysiology of T2DM. Studies show that the HepG2 cell line, despite being a cancer cell-line, closely mimics the *in vivo* situation with regards to glucose metabolism and hence is ideal for generating a HG model (Sefried et al., 2018).

Given the central role of mitochondrial dysfunction and OS in diabetic pathogenesis, the described cytoprotective networks are highly relevant in identifying novel therapies. With multiple lines of research revealing BA's antidiabetic nature, as well as separately proving its AO identity, a conjunctive idea was generated, to assess BA's AO capabilities in the presence of hyperglycaemia. Thus, this study's unique approach to BA combatting OS induced by HG conditions may provide a basis for future ubiquitous, natural methods of intervention to limit resultant T2DM complications, especially in low and middle-income countries.

Research Questions

- Does BA exert cytoprotective properties in HepG2 cells under HG conditions?
- What is the underlying mechanism of BA-induced cytoprotection in HepG2 cells during HG conditions?

Aim

To determine the cytoprotective effects of BA on HG-induced OS in HepG2 cells, by assessing mitochondrial maintenance, ROS repercussions, and the AO-response.

Objectives:

1) To determine an ideal BA concentration in HepG2 cells that does not negatively affect energy output, viability or metabolism via:

- Assessment of cell viability and energy output using the MTT and ATP assays.
- Assessment of cytotoxicity/necrosis (membrane leakage) via the LDH assay.

2) To assess BA's anti-HG effects by determining tyrosine phosphorylation of IR via a PY20 western blot.

3) To determine ROS:

- Using the H_2DCF-DA assay.
- And its effect on oxidative damage to macromolecules via malondialdehyde (MDA) and protein carbonyl quantification.
- And how it influences protein expression of NFκB p65.

4) To determine the AO response of BA in a HepG2 model by measuring:

- Protein expressions of NRF2, pNRF2, PGC1α, SOD2, Catalase, SIRT3, PPARγ, LONP1, UCP2, using western blots.

- Gene expressions of *PGC1α, SIRT3, GPx1, NRF2*, using qPCR.

- Reduced GSH levels via luminometry.

- Expression of miR124 (involved in epigenetic regulation of AO pathways) using qPCR.

Hypothesis

It was hypothesized that BA, via modulation of the PPARγ/NRF2 positive feedback loop, elevated cytoprotective machinery, thus mitigating HG induced oxidative stress in the HepG2 cell line.

CHAPTER 2: LITERATURE REVIEW

2.1) Diabetes

Metabolic diseases are a major cause of morbidity and mortality in both developed and developing countries and place an enormous burden on healthcare. Metabolic syndrome (MetS) results from several factors that increase an individual's risk for diabetes and cardiovascular disease (CVD), including obesity (visceral), dyslipidaemia, hypertension and elevated fasting glucose (Collins et al., 2018). This necessitates efforts towards the development of new and innovative mechanisms to prevent and combat this worldwide epidemic, by specifically looking at ubiquitous and renewable sources of intervention.

Diabetes is a global pandemic, with more than 90% of cases being T2DM (Wu et al., 2014). The International Diabetes Federation (IDF) estimated 451 million adult diabetics in 2017, predicted to escalate to 693 million by 2045 (Cho et al., 2018). A similar trend is being observed in South Africa. In the year 2000, the prevalence of T2DM in South Africa was 5.5% of the population above 30 years of age, rising to 9% in 2009 (Pheiffer et al., 2018). The number of patients has quadrupled in the past 30 years, and diabetes is recorded by World Health Organisation (WHO) as the seventh leading cause of mortality (2018). Globally, 1 in 11 adults has diabetes mellitus, and almost half of this population is undiagnosed (Cho et al., 2018). Furthermore, diabetes mellitus accounts for 12% of global health expenditure, creating enormous economic burden (Zhang et al., 2010).

T2DM is distinguished from type 1 diabetes (an autoimmune disorder characterised by compromised pancreatic insulin secretion) in that insulin may still be sufficiently produced; however, the muscle, fat, and liver are unable to respond to insulin and hence fail to reduce blood glucose levels. This phenomenon is known as insulin resistance and increases circulating glucose levels (hyperglycaemia) which contributes to the pathogenesis of T2DM (Aronoff et al., 2004).

2.2) Glucose uptake and disposal

Glucose cellular uptake is facilitated by binding of insulin to the insulin receptor. The insulin receptor is a transmembrane tyrosine kinase receptor, which after insulin binding, triggers auto-phosphorylation of the tyrosine residues within the β subunit (Czech, 1985). Phosphorylation facilitates the recruitment of adaptor proteins (insulin receptor substrate, protein phosphatases), promoting glucose homeostasis (Berg et al., 2002). Autophosphorylation generates an insulin receptor substrate 1 (IRS-1) binding site. Phosphorylation of IRS-1 results in a phosphoinositide-3-kinase–protein kinase B/Akt (P13K/PIP3/PKB) transduction pathway. Protein kinase B promotes Glucose Transporter 4 (GLUT4) glucose uptake and inhibits glycogen synthase kinase, thus promoting glycogenesis (Berg et al., 2002).

The insulin receptor, in conjunction with other regulatory proteins including PPARγ and PGC1α, are implicated in promoting glucose uptake and in some cases disposal (Berg et al., 2002, Wu et al., 2014, Bonen et al., 2009). This mechanism of glucose disposal is generally facilitated by insulin and is hence impaired in T2DM. Insulin promotes glucose entry into cells via recruitment of glucose transporters, and promotes glycogenesis, glycolysis and entry of acetyl coenzyme A (acetyl-CoA) into the mitochondria to promote lipogenesis (Aronoff et al., 2004). Prolonged HG conditions, however, have the potential to glycate the IR (Rhinesmith et al., 2017).

2.3) Hyperglycaemia and oxidative stress

In T2DM, hyperglycaemia can enhance production of free radicals, including ROS. This disruption to redox balance contributes to diabetic complications (Nishikawa et al., 2000). Enhanced glycolysis results in increased oxidation of glyceraldehyde-3-phosphate to 1,3 diphosphoglycerate, due to increased $NADH/NAD^+$ ratio redox imbalance. Enhanced polyol pathway results in an increase in fructose and sorbitol, also increasing the $NADH/NAD^+$ ratio (Phaniendra et al., 2015). Furthermore, auto-oxidation of glucose generates ketoaldehydes and various ROS (H_2O_2, $OH^\bullet$, $O_2^{\bullet-}$). To further compound the situation, the HG state increases methylglyoxal levels, forming advanced glycation end-products (AGEs) (Brownlee, 2001, Nishikawa et al., 2000).

2.3.1) Advanced Glycation End-products

In T2DM, the excess glucose in circulation covalently binds to cellular macromolecules (proteins, fats, DNA, and RNA) leading to AGE formation, which bind to receptors for advanced glycation end products (RAGE), promoting ROS formation and diminishing the AO capacity (Collins et al., 2018) (Figure 2.1). AGE/RAGE binding impairs muscle healing and contractile function and promotes metabolic disturbance, insulin resistance, adipokine expression, fibrosis and collagen cross-linking, all contributing to the multitude of complications of T2DM. Furthermore, AGE/RAGEs promote increases in inflammation, apoptosis and necrosis via the NFκB/mitogen-activated protein kinase (MAPK) pathway and also via alteration of OS status (Collins et al., 2018) (Figure 2.1).
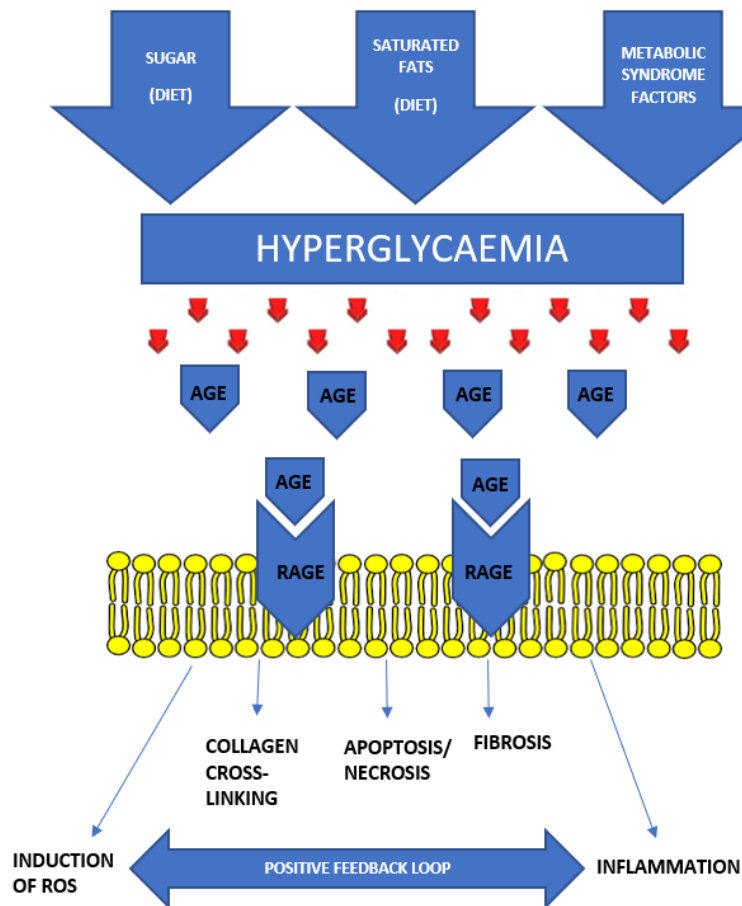
Figure 2.1 : Causation and adverse outcome of AGE/RAGE formation and binding (prepared by author).

2.3.2) Mitochondrial-derived reactive oxygen species

Mitochondria are referred to as metabolic hubs of cells; they harbour the bulk of oxidative and redox processes, ensuring an abundant supply of ROS. The ETC is a source of endogenous ROS. Electron leakage out of the ETC occurs mainly at complexes I and III resulting in superoxide anion radical formation (Andreyev et al., 2005) (Figure 2.4). Hyperglycaemic conditions promote mitochondrial dysfunction; the tricarboxylic acid (TCA) cycle produces excess electron transfer donors that enter the ETC, resulting in partial inhibition of complex III, amplifying superoxide radical levels (Rolo and Palmeira, 2006). Other components within the organelle also contribute to ROS production e.g. monoamine oxidase and α-ketoglutarate dehydrogenase (Phaniendra et al., 2015).

2.4) Reactive oxygen species and Oxidative stress

Oxygen in molecular form is more susceptible to e^- transfer, due to the presence of two unpaired electrons. O_2 forms a reactive anion, known as superoxide, when it accepts an electron, which can form hydroxyl radicals and H_2O_2 via sequential reduction (Apel and Hirt, 2004). ROS can thus be defined as

unstable, O_2-derived molecules (Gorrini et al., 2013). Table 2.1 lists the most physiologically abundant ROS, as well as classifies their radical status.

Despite its pathological associations, basal levels of ROS are essential for cell maintenance. ROS are signalling molecules involved in gene transcription, protein synthesis, post-translational modifications, cellular differentiation, apoptosis and defence. A fine balance exists between pro-oxidants and antioxidants in every cell. However, due to either diminished AO capacity or an increase in ROS, the balance can be disrupted, favouring pro-oxidants. This is known as oxidative stress (Appari et al., 2018).

2.5) Effects of reactive oxygen species

Recent research has identified ROS as playing a pivotal role in various physiological processes, and has linked excess ROS to a diverse group of pathological manifestations, including liver damage, asthma, neurodegenerative diseases, cancer and aging (Phaniendra et al., 2015). High ROS levels initiate inflammation via NFκB. Increased ROS and concomitant inflammation are proven to stimulate MetS, with concomitant diabetes and cardiovascular disease (Collins et al., 2018).

ROS accumulation can result in endoplasmic reticulum (ER) stress. ER stress results in protein misfolding/unfolding, interfering with protein synthesis and calcium homeostasis, and prevents removal of irregular proteins, thus initiating necrosis/apoptosis (Collins et al., 2018). ROS accumulation is also associated with lipid peroxidation and resultant protein carbonylation.

Table 2.1: Most physiologically abundant ROS classified according to radical status (prepared by author).

Non-radicals	Radicals
Hydrogen Peroxide: H_2O_2	**Superoxide: $O_2^{\bullet-}$**
Ozone : O_3	**Hydroxyl: $OH^{\bullet}$**
Hypochlorous acid: HOCl	**Hydroperoxyl: $HO_2^{\bullet}$**
Singlet Oxygen: O_2	**Alkoxyl: $RO^{\bullet}$**
Alkyl hydroperoxide: ROOH	**Alkperoxyl: $RO_2^{\bullet}$**

2.5.1) Lipid peroxidation and protein carbonylation

An important mechanism to consider in free radical mediated cell injury is lipid peroxidation and concomitant protein carbonylation. The autocatalytic uncontrolled process of lipid peroxidation's consequences are 2-fold: this involves the direct attack of cell membrane structures, and indirect mechanisms of release of reactive products (Hauck and Bernlohr, 2016).

Peroxidation alters the biophysical properties of membranes by attacking polyunsaturated fatty acids (PUFAs), and is associated with aging and metabolic diseases. Peroxidative PUFA attack compromises the membranes ability to act as both a simple and selective barrier (Cheeseman, 1993). Proteins involved in active transport are affected; loss of calcium pump activity and hence calcium homeostasis was observed in a hepatocyte model due to lipid peroxidation (Albano et al., 1991, Cheeseman, 1993). Furthermore, the inner mitochondrial membrane is particularly susceptible to lipid peroxidation. Here, cardiolipin maintains cristae structure and stabilizes the ETC and, understandably, oxidation of this lipid is associated with impaired respiration and mitochondrial dysfunction, linked to atherosclerosis and obesity (Hauck and Bernlohr, 2016, Zhong et al., 2014).

The indirect effects of lipid peroxidation stem from the reactive nature of the products and/or intermediates of peroxidation. Amongst oxidative species, lipids, due to high stability and diffusibility, have a large functional boundary, with some lipid aldehydes even diffusing extra-cellularly. These reactive lipid aldehydes post translationally modify cysteine , histidine and lysine residues, resulting in protein carbonylation (Hauck and Bernlohr, 2016). Frohnert and Bernlohr (2013) labelled this lipid peroxidation-induced protein carbonylation as being the determining factor in mitochondrial dysfunction (Frohnert and Bernlohr, 2013).

Mitochondria are particularly vulnerable to carbonylation. Substantial carbonylation of ETC complexes as well as ATP synthetases has been observed in various models resulting in reduced ATP generation capacity (Wen and Garg, 2004). Furthermore, protein carbonylation of mitochondrial α-ketoglutarate dehydrogenase and aconitase are implicated in TCA cycle disruption (Yarian et al., 2005).

Carbonylation results in protein misfolding due to its effects on chaperones and machinery regulating polypeptide conformations. Alterations in protein folding may prevent proper cellular localization as well as the function of interacting partners. These proteins form toxic aggregates, (Dalle-Donne et al., 2006). Tissue deposition of protein aggregates are being increasingly associated with metabolic disorders, with Mukherjee et al. (2015) describing T2DM as a 'protein misfolding disease' (Mukherjee et al., 2015).

Generally, moderately carbonylated proteins are proteasomally degraded, whereas, proteins that are heavily carbonylated, form high molecular weight aggregates, thus resisting degradation and hence accumulate. Excess oxidation potentiates cross linking, providing a structural constraint preventing entry into the catalytic sites of the proteasomal enzymes (Dalle-Donne et al., 2006). Aggregation and inhibition of degradation may result in apoptosis (Powell et al., 2005). Under high stress conditions, however, the mitochondria use a specific proteolytic digester of oxidized proteins known as LONP1 (Ngo et al., 2013).

2.6) Lon Protease

Lon protease is a nuclear-encoded, mitochondrial, ATP dependant, serine peptidase that indirectly complements the AO response by degrading oxidized proteins (Bota and Davies, 2016).

Pinti et al (2016) described LONP1 as a "master-regulator of mitochondrial functions". Mitochondrial DNA replication and mitogenesis as well as chaperone systems have been implicated in LONP1 function (Bota and Davies, 2016). Furthermore, a decrease in LONP1 activity affects the levels of proteins involved in the stress response, ATP production and ribosomal assembly (Pinti et al., 2016). Cells with decreased/deficient LONP1 activity experience a decrease in the level of ETC complexes I, III and IV which leads to defects in cellular respiration (Key et al., 2019).

In OS conditions, nuclear transcription of LONP1 occurs, followed by translation into a precursor polypeptide. This polypeptide contains a mitochondrial target sequence, allowing it through the mitochondrial membranes into the matrix. The target sequence is then cleaved off, producing a newly processed protein (Venkatesh et al., 2012). Gibellini et al., (2014) stated that changes in LONP1 mRNA levels, protein activity, and gene expression are not always correlated, implying high levels of post-translational modification (Gibellini et al., 2014). During oxidative stress, SIRT3 deacetylates LONP1, post-translationally activating it, which in turn eliminates damaged proteins due to oxidative stress via proteolysis (Gibellini et al., 2014). If these proteins are not removed they may cross link and lead to toxicity (Gounden and Chuturgoon, 2017).

2.7) Inflammation and reactive oxygen species

Metabolic changes observed in diabetes involving hyperglycaemia, hyperlipidaemia and insulin resistance with an associated increase in OS and inflammation, drive diabetic complications such as nephropathy , atherosclerosis, cardiomyopathy, neuropathy and retinopathy (Sharma et al., 2018).
A cyclical process exists between inflammation and oxidative stress. Increased pro-inflammatory cytokine expression stimulates ROS levels. Reciprocally, high ROS levels result in increased pro-inflammatory cytokine expression (Figure 2.1) (Sharma et al., 2018). This positive feedback loop drives a highly pro-inflammatory and pro-oxidant state, proven deleterious to T2DM, exacerbating complications. Integral to this positive feedback loop, is the role of NFκB (Morgan and Liu, 2011).

2.7.1) Nuclear factor κ B

In T2DM, HG-induced ROS is an important inflammasome activating signal. This direct role is well researched, however another role also exists, in which ROS, via its actions on NFκB, indirectly stimulates inflammation (Figure 2.2) (Sharma et al., 2018).

In its inactive state, NFκB is sequestered within the cytoplasm by its inhibitor, IκB. When this inhibitor undergoes phosphorylation and resultant degradation, NFκB (p65 subunit) is activated and translocates into the nucleus (Nishikori, 2005). Previously, it was concluded that high levels of hydrogen peroxide activate NFκB, however more recently, Kim et al. (2008) demonstrated that ROS indirectly activates NFκB via activation of AKT. AKT activation, and subsequent IKK phosphorylation, results in oxidation and dissociation of IκBα inhibitory proteins, thus allowing phosphorylation of ser-276 and hence NFκB translocation (Kim et al., 2008, Schreck et al., 1991).

NF-κB is a rapidly inducible transcription factor that affects a wide range of cellular responses via gene induction. It is considered integral in inflammation as it is involved in transcriptional activation of cytokines, chemokines, and various inflammasome components (Sharma et al., 2018). However, NFκB plays a dual role. Besides being activated by ROS, for inflammatory purposes, NFκB also further enhances ROS production by inducing expression of various proteins. NFκB directly upregulates NADPH oxidase 2 (NOX2), a devoted ROS producer, and cyclo-oxygenase 2 (COX2), an enzyme producing superoxide by-products, thus promoting OS (Figure 2.2) (Morgan and Liu, 2011).

NFκB's pivotal role in both ROS and inflammation warrants its need to be regulated by various antioxidant transcription factors and co-factors. Collino et al. (2005) demonstrated that agonist binding to PPARγ successfully controlled oxidative stress and inflammation via direct suppression of NFκB and its downstream ROS generators (Collino et al., 2005). Furthermore, PPARγ's co-activator, PGC1α, has been implicated in promoting an anti-inflammatory environment in skeletal muscle cells via reduction of NFκB activity (Figure 2.9) (Eisele et al., 2015). Interestingly, Wardyn et al. (2015) reported a form of molecular crosstalk existing between NFκB and the well-known AO-regulator NRF2. He noted that absence of NRF2 is linked to an upsurge in oxidative stress, exacerbating NFκB-induced cytokine production (Figure 2.2) (Wardyn et al., 2015). NFκB's direct link to ROS and involvement in many proteins within the cytoprotective network emphasises the need to further study this transcription factor in an HG induced OS model.
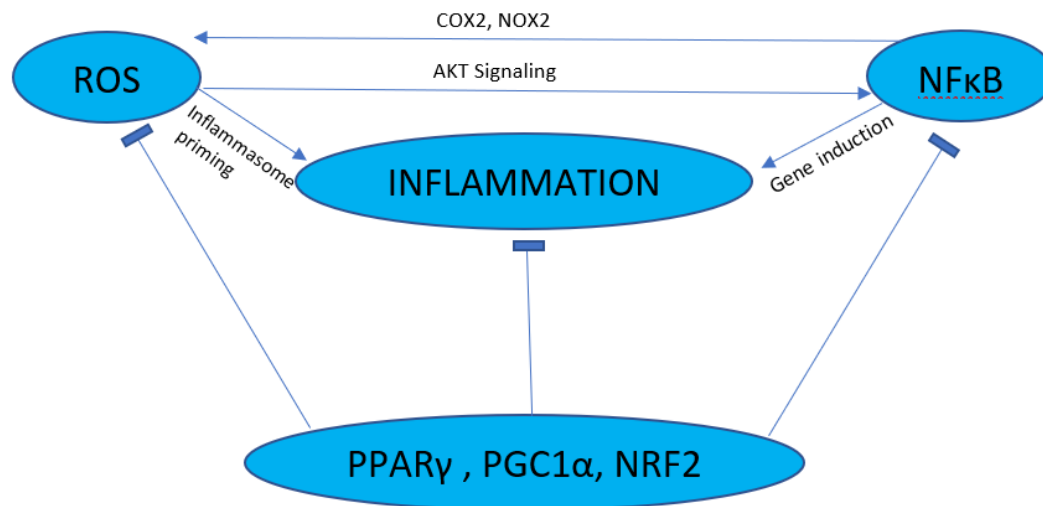
Figure 2.2: Relationship between NFκB, ROS and inflammation and its regulation by antioxidant-related proteins (prepared by author).

2.8) Intramitochondrial Antioxidant defence systems

Due to their high susceptibility to redox damage, mitochondria possess an innate antioxidant system. Antioxidants are phenol containing compounds, which inhibit substrate oxidation, thus neutralizing the harmful effects of ROS (Noori, 2012). Antioxidants prevent free radical producing oxidation reactions by being oxidized themselves, thus removing other radical intermediates and are thus known as reducing agents (Lü et al., 2010). These free radical scavengers may be enzymatic (SOD, GPx1) or non-enzymatic (GSH) (Noori, 2012).

2.9) Reactive oxygen species detoxification

Detoxification of ROS occurs both intra- and extra-mitochondrially. SOD2, located in the mitochondrial matrix, is the first line of defence that plays a crucial role in detoxifying free superoxide radicals ($O_2^{\bullet-}$) (Figure 2.3). It is an AO metalloenzyme with a manganese centre which catalyses portioning of the superoxide radical. SOD2 thus, transforms the superoxide radical into either H_2O_2 or diatomic oxygen, ensuring that basal ROS levels are maintained (Ighodaro and Akinloye, 2018). SOD2 has been proven vital for mitochondrial function in oxidative tissue, however, superoxide detoxification does occur in the absence of SOD2, albeit at a lower rate (Ighodaro and Akinloye, 2018).

Due to its important role, SOD2 is well regulated. Both NRF2 and PPARγ transcribe for SOD2 and, SIRT3 deacetylates the protein, in response to hyperglycaemia, thus enhancing its AO-activity (Lee, 2017, Gounden et al., 2015). Additionally, PGC1α associates with the SOD2 promoter, thus inducing its expression (Figure 2.3 and Figure 2.7)(Valle et al., 2005).

Hydrogen peroxide is not as toxic as $O_2^{\bullet-}$, however, it can oxidize iron-sulphur centres and thiol groups, as well as be converted to mutagenic $OH^{\bullet}$ (Sharma et al., 2012). Thus, the mildly reactive H_2O_2 is further detoxified by either CAT or GPx1 into water (Figure 2.3). Catalase is an AO protein, found most abundantly in peroxisomes and cytosol, which has the capability to detoxify millions of hydrogen peroxide molecules. It structurally contains 4 long polypeptide chains and 4 porphyrin haem rings, which detoxify the H_2O_2 (Kabel, 2014). According to Kabel (2014), CAT detoxifies H_2O_2 in a basic catalytic manner and a peroxidatic manner (Kabel, 2014). The catalytic reaction generates H_2O and O_2 while peroxidatic detoxification uses the O_2 from H_2O_2 to oxidize H-donors and also produces H_2O (Kabel, 2014). Transcription factors PPARγ, NRF2, and PGC1α (Figure 2.9) are implicated in the transcriptional activation of CAT (Lee, 2017, Valle et al., 2005).

2.9.1) Glutathione peroxidase 1/glutathione (reduced) antioxidant mechanism

Yet another enzyme implicated in H_2O_2 detoxification, is GPx1. GPx1 can be located within the cytoplasm, mitochondria, and the nucleus. Both NRF2 and PGC1α are implicated in its transcriptional upregulation (Lee, 2017, Valle et al., 2005). A unique amino acid by the name of selenocysteine, located on GPx active sites, utilises low molecular weight thiols to detoxify lipid peroxides and H_2O_2. GSH is one of the most common thiols utilised when metabolizing H_2O_2 to water (Birben et al., 2012).

GSH is a nonenzymatic AO located both in the mitochondrial matrix and the cytoplasm (Lushchak, 2012). This free radical scavenger exists in reduced and oxidised forms and is a substrate for GPx1 activity (Lushchak, 2012). Reduction of H_2O_2 results in oxidation of GSH to GSSG by GPx1. GSSG is reduced back to 2GSH molecules via the action of glutathione reductase (GR) and the cofactor, NADPH (Figure 2.3) (Lushchak, 2012). Research has shown that T2DM patients display lower levels of GSH synthesis (Sekhar et al., 2011).
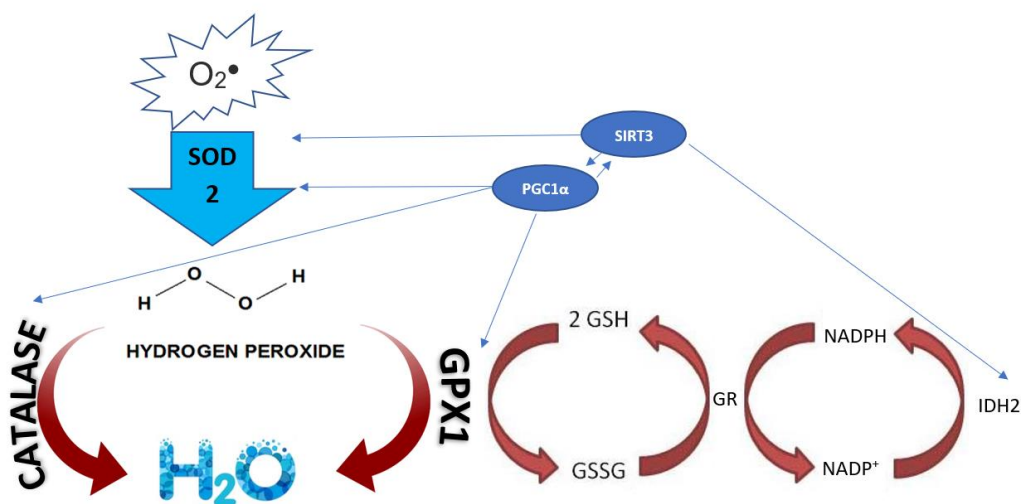
Figure 2.3: SIRT3 and PGC1α's involvement in antioxidant mechanisms (prepared by author).

2.10) Diabetes and its antioxidant implications

Of equal importance in the pathological setting, to enhanced ROS, is that of diminished AO capacity. In the diabetic case, this extends beyond the concept of excess ROS levels merely depleting the AO supplies, leaning toward a more direct effect on antioxidants.

Numerous studies confirmed the diabetic state as a causal agent in lowering AO levels of CAT, SOD and GPx (Loven et al., 1986, Wohaieb and Godin, 1987, Sukalski et al., 1993). Research into this avenue provided us with two theoretically firm explanations to the adverse effects of diabetes on AO mechanisms.

The first theory revolves around glycation, the non-enzymatic binding of glucose to proteins bringing about functional and structural changes. Szaleczky et al. (1999) speculated that the HG state could result in a reduction of AO enzyme capability via enhanced glycation (Szaleczky et al., 1999).

The second theory involves diabetic-induced modulation of the micronutrient environment. Antioxidant enzymes require certain cofactors and micronutrients to express their functionality; CAT requires haem, GPx requires selenium and superoxide dismutase utilises copper, zinc or manganese. It was suggested that in the diabetic state, alterations of the micronutrient environment affected cofactor/enzyme ratio, thus influencing activation statuses of AO enzymes (Szaleczky et al., 1999). Thus, an aberrant AO profile and high ROS levels are induced by diabetes. In a possible attempt to offset both these aberrations, UCP2 expression is found to be upregulated in the HG state (Sosa-Gutiérrez et al., 2018).

2.11) Uncoupling Protein 2

The uncoupling proteins are a family of 5 carriers unique to mammals (Pierelli et al., 2017). They consist of 3 U-shaped membrane units of 100 amino acids each, and exist in the mitochondrial inner membrane (Su et al., 2017). UCP2 is distributed widely in various tissues, including kidney, spleen, pancreas, and is responsible for regulating redox status (Liu et al., 2013). The UCP2 promoter region bears putative response elements for the AO-transcriptional protein, PPARγ (Pierelli et al., 2017) and also senses energy levels and aids in mitochondrial maintenance (Su et al., 2017).

UCP2 aids in rectifying the spatiotemporal imbalance between ROS and AO, most uniquely, by both lowering ROS levels and enhancing AO machinery. Although unconventional in its methods, uncoupling is considered an AO mechanism (Sosa-Gutiérrez et al., 2018).

Attenuation of ROS production

ATP and the ETC are coupled processes. Reducing donors such as NADH and $FADH_2$ provide the ETC with substrates. Electron flow is conveyed along the chain, generating energy, forcing H^+ ions out of the membrane. High levels outside the inner mitochondrial membrane promote re-entry via ATP synthase, thus stimulating OXPHOS. The ETC, however, generates small amounts of ROS via interactions between electrons and free O_2 (Figure 2.4). In HG conditions, tight mitochondrial coupling

results in high proton motive force, leading to excess reduction of ETC subunits, and hence increased ROS (Souza et al., 2011).

Uncoupling protein 2 functions as a transmembrane proton channel, thus enabling H^+ ions to flow back through the membrane instead of through ATP synthase. This proton leakage dissipates the electrochemical proton gradient across the inner membrane, uncoupling the ETC from OXPHOS (Figure 2.4) (Pierelli et al., 2017). Uncoupling substrate oxidation from ATP production prevents defects of one of the processes from affecting the other. This mild uncoupling prevents further superoxide production as well as decreases oxidative damage (Pierelli et al., 2017).

<u>Enhancing antioxidant activity:</u>
UCP2 indirectly regulates SIRT3 activity. The uncoupling ability of UCP2 allows it to modulate the $NADH/NAD^+$ ratio, due to its effects on the ETC. This innate ability is of relevance in HG conditions, favoring NADH. The intrinsic ability of NAD+-dependent SIRT3 to sense the ratio then results in an increase of SIRT3 activity, which then promotes AO-protein activity to combat ROS (Sosa-Gutiérrez et al., 2018).
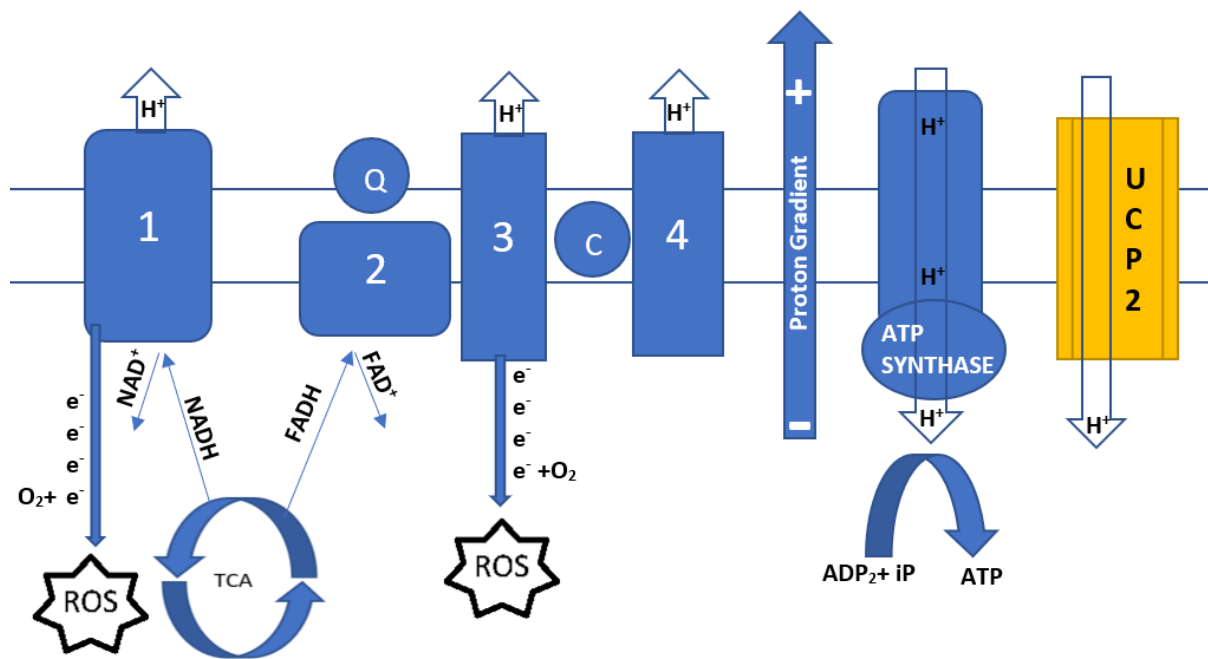
Figure 2.4: The electron transport chain; endogenous ROS generation; uncoupling of OXPHOS from the ETC (prepared by author).

2.12) Sirtuin 3

Sirtuin 3 is a member of the sirtuin family of deacetylases. It is a soluble protein which is located in the matrix of the mitochondria and plays a vital role in many body processes. Hence it is found in abundance in many active organs, such as the liver (Hirschey et al., 2011a).

Initially, SIRT3 is produced enzymatically inactive within the cytosol, and is only activated when translocated into the mitochondrial matrix by mitochondrial peptidase. Upon translocation into the mitochondrion, SIRT3 undergoes proteolytic cleavage, becoming an active 28kda protein. SIRT3 functions as a deacetylase, removing the acetyl groups of acetyl-lysine residues on amino acids. This reaction requires NAD^+ as a cofactor (Hirschey et al., 2011a).

Transcriptional activation

A positive feedback loop exists between SIRT3 and PGC1α (Flick and Lüscher, 2012). PGC-1α induces SIRT3 expression (Figure 2.5) by allowing transcription factor estrogen-related receptor α (ERRα) to bind to the promoter region of SIRT3. Reciprocally, SIRT3 activates cAMP response element-binding protein (CREB) which in turn stimulates PGC1α activation. Interestingly, Song et al. (2017), proposed another mechanism of activation in which NRF2 transcribes for SIRT3 with the aid of PGC1α to enhance the cellular AO status (Song et al., 2017).

Oxidative stress

Sirtuin 3 plays a major role in oxidative stress by increasing AO capacity as well as promoting proteolytic digestion of oxidized proteins.

Sirtuin 3 is regulated in accordance with the oxidative status of the cell; high oxidative stress increases SIRT3 expression whereas decreased ROS decreases SIRT3 expression (Chen et al., 2014). During OS, SIRT3 directly targets AOs: SOD2 and isocitrate dehydrogenase (IDH2), activating them by deacetylation (Chen et al., 2011, Yu et al., 2012). SIRT3 also indirectly affects AOs: GPx1, SOD2, CAT and UCP2 via PGC1α (Fig. 2.3; Fig. 2.5) (Gounden et al., 2015). Furthermore, Someya et al. (2010) concluded that SIRT3 reduces oxidative DNA damage via upregulation of the GSH AO mechanism (Someya et al., 2010).

SIRT3 also deacetylates and hence modulates LONP1, which aids in the breakdown of proteins that are oxidatively damaged within the mitochondrial matrix (Chen et al., 2014).

Mitochondrial Metabolism

Sirtuin 3, considered a metabolic sensor, plays a beneficial role in the regulation and procession of mitochondrial metabolism, via direct interaction with many of its aspects e.g. TCA, OXPHOS, ETC.

Within the ETC, SIRT3 deacetylates complexes I and II, resulting in precession of the ETC (Liu et al., 2002). SIRT3 regulates OXPHOS by activating acetyl-CoA synthetase 2 and glutamate dehydrogenase (Ahn et al., 2008).

In the TCA cycle, SIRT3 deacetylates the enzyme aconitase (allowing conversion of citrate to isocitrate), succinate dehydrogenase (allowing conversion of succinate to fumarate and allowing electrons to transfer to FAD converting it to $FADH_2$), isocitrate dehydrogenase (allowing oxidative decarboxylation of isocitrate), as well as GDH and acetyl-CoA synthetase 2 (Fernandes et al., 2015, Finley et al., 2011, Yu et al., 2012, Ansari et al., 2017).

<u>Diabetes and Sirtuin 3</u>

With regards to the HG state, Gounden et al. (2015) concluded that hyperglycaemia resulted in increased expression of SIRT3 to combat the higher levels of ROS associated with this state (Gounden et al., 2015). Additionally, SIRT3 also plays an integral role in directly combatting the hyperglycaemia by increasing insulin sensitivity and glucose entry into the cell (Hirschey et al., 2011a). Furthermore, a series of metabolic abnormalities extrapolated to mimic MetS were observed in mice, following SIRT3 disruption (Hirschey et al., 2011b).
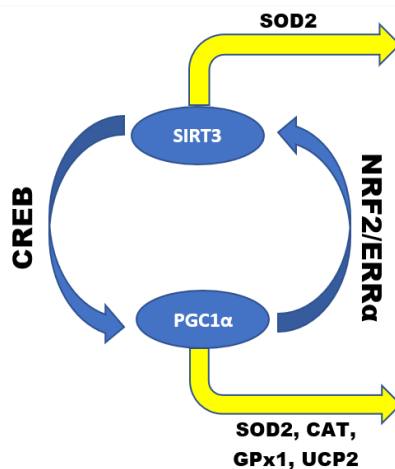
Figure 2.5: SIRT3/PGC1α positive feedback loop in potentiation of the antioxidant profile (prepared by author).

2.13) Epigenetics

Epigenetics involves the study of post-translational or post-transcriptional modification of gene expression as an alternative to alteration of the true genetic code. This concept of chromatin remodelling has proven to be an important gene modulator without affecting the DNA sequence, thus resulting in heritable changes in cellular phenotype (Guzik and Cosentino, 2018). The epigenetic concept is particularly relevant in this case due to its regulation of proteins involved in the AO response.

The major mechanisms of epigenetics involve DNA methylation, post-translational histone modifications (acetylation/deacetylation) and RNA regulating molecules such as miRNAs (Guzik and Cosentino, 2018).

2.13.1) MicroRNA-124

MicroRNAs are small non-coding RNAs that post-transcriptionally regulate gene expression. They alter mRNA stability and inhibit translation via complementary binding to the 3'-UTR of mRNA (Guzik and Cosentino, 2018). Alterations of miRNA expression have been noted in diabetes and some miRNAs have even been identified as biomarkers for several human diseases. Recent studies highlight a link between several miRNA and diabetic-induced OS in the potentiation of T2DM complications (Yu et al., 2015, Yildirim et al., 2013). Furthermore, many anti-inflammatory miRNAs have been downregulated in T2DM, thus promoting a pro-inflammatory phenotype (Guzik and Cosentino, 2018).

MiR124 is involved in many processes including AO, immunity, apoptosis, inflammation, cell differentiation, survival, apoptosis, and OS (Yao et al., 2018, Mokabber et al., 2019). Wang et al. (2017) revealed that PPAR-γ binds directly to the PPRE on the miRNA124 promoter region, inducing its expression. Furthermore, Wang et al. (2017) states that PPARγ activation can inhibit production of pro-inflammatory cytokines via upregulation of miR124 (Wang et al., 2017). MiR124 exerts its anti-inflammatory actions by inhibiting translation of the inflammatory signaller, NFκB (Qiu et al., 2015). Shu and Zhang (2019) suggests that miR124 stimulates the p13K/AKT/NRF2 pathway, resulting in NRF2 transcribing for AO-proteins that combat oxidative stress. However, its regulatory mechanism is not fully elucidated (Shu and Zhang, 2019).
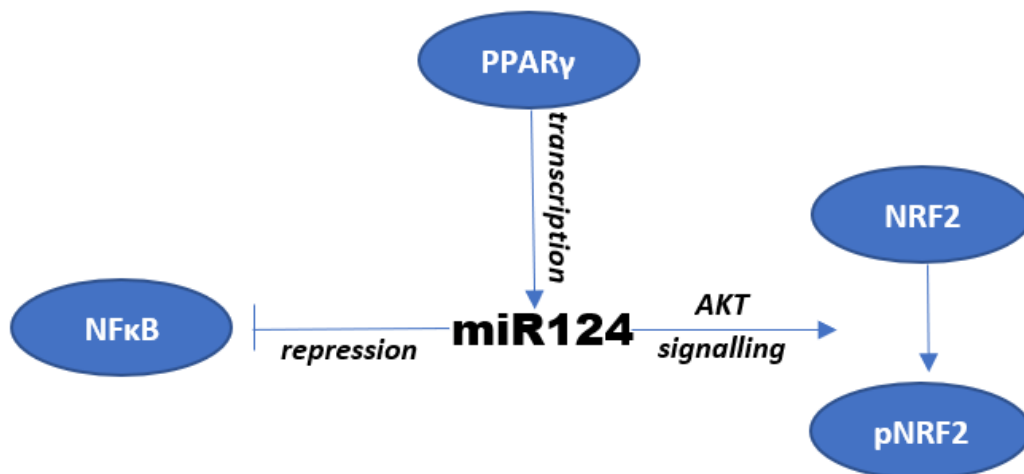
Figure 2.6: Relation of miRNA124 to transcription factors and involvement in reducing ROS-induced inflammation and potentiating the antioxidant response (prepared by author).

2.14) Nuclear factor erythroid 2-related factor 2

Nuclear factor erythroid 2-related factor 2 is a transcription factor, regarded as a pivotal modulator of the AO response. NRF2 is normally bound to Kelch-like-ECH-associated protein 1 (KEAP1) in the cytoplasm and is targeted for ubiquitination and degradation, thus supressing its antioxidant capabilities. In the presence of ROS, cysteine residues of KEAP1 conjugate to ROS inducing agents inhibiting ubiquitination. This results in nuclear translocation of NRF2 (Figure 2.5) (Lee, 2017). In the nucleus, NRF2 interacts with small maf proteins and other coactivators and binds to the antioxidant response element (ARE), transcriptionally activating a plethora of AO-related genes including PPARγ, SIRT3, retinoid X receptor (RXR), CAT, GPx1, SOD2 (Cho et al., 2010, Chorley et al., 2012, Jeong et al., 2016, Jin et al., 2016, Cho et al., 2005, Song et al., 2017).

More recent research, however, explores alternate regulatory mechanisms of NRF2, including phosphorylation. Protein kinase C phosphorylates NRF2 in the Neh2 domain at ser-40, thus disrupting the NRF2-KEAP1 association promoting translocation and AO-related activity (Bryan et al., 2013).

The role of the NRF2 pathway in the prevention, delay, and/or reversal of diabetic complications has been elucidated. Murine models of NRF2 overexpression indicate that NRF2 activation improves insulin sensitivity and can ameliorate diabetes and obesity (David et al., 2017). Furthermore, NRF2 has been shown to have an anti-inflammatory role by reducing ROS-dependent inflammation; and a recent study by Liu et al. (2017) indicated that an NRF2 activator reduced ROS levels, subsequently reducing inflammasome activation, cleavage of caspase 1 and production of interleukin 1β (IL1β) (Liu et al., 2016).

2.15 Peroxisome proliferator-activated receptor gamma

PPARs are a group of nuclear receptors that regulate metabolic pathways including those involving the pathophysiology of diabetes and obesity (Brusotti et al., 2017). Steroid/thyroid hormone ligands, eg. cortisol, bind to nuclear receptors, functioning in conjunction with proteins to regulate gene expression. This binding causes a conformational change that results in either an up-or-downregulation of gene expression (Sever and Glass, 2013).

PPARγ is a nuclear receptor that, once ligand bound, enters the nucleus, heterodimerizes with RXR and binds to PPAR response elements (PPREs) on the promoter region of genes (Figure 2.7). PGC1α is one of the co-activators required to elicit its action (Figure 2.9). This action recruits a large array of protein coactivators, initiating diverse physiological outcomes, including AO response via NRF2, UCP2, SOD, CAT, GPx (Kvandova et al., 2016, Pierelli et al., 2017, Polvani et al., 2012, Girnun et al., 2002)
In addition to its AO capabilities, PPARγ also modulates certain aspects of carbohydrate and lipid metabolism. PPARγ-regulated gene expression is involved in fatty acid storage via lipid uptake and

adipogenesis as well as improving basal glucose uptake via GLUT4 recruitment (Carvalho, 2017, Rosen and Spiegelman, 2001).

PPARγ also directly influences inflammation. Multiple studies have identified this transcription factor as a negative regulator of OS-induced inflammation. In-depth mechanistic research uncovered that PPARγ suppresses inflammation via transcriptional repression of several pro-inflammatory transcription factors and proteins such as COX2 and NFκB (Wahli, 2008, Polvani et al., 2012, Reddy and Standiford, 2010).

2.16) Crosstalk between PPARγ and NRF2

Various studies investigated links between PPARγ and NRF2, with some studies hinting at a reciprocal regulation between the 2 transcription factors (Reddy and Standiford, 2010, Huang et al., 2010a, Polvani et al., 2012). Lee (2017) further investigated this crosstalk, hypothesizing a positive feedback loop between these 2 factors (Lee, 2017). Lee (2017) based his hypothesis on various findings including: (i) NRF2 binding to the ARE on PPARγ; (ii) PPRE presence on NRF2; (iii) NRF2 inducing RXR upregulation; and (iv) both PPARγ and NRF2 inducing the same AO genes (Figure 2.7)(Lee, 2017, Cho et al., 2010, Kvandova et al., 2016, Chorley et al., 2012). Thus, both transcription factors upregulate each other and have a collaborative action on AO genes, potentiating the AO response to OS.
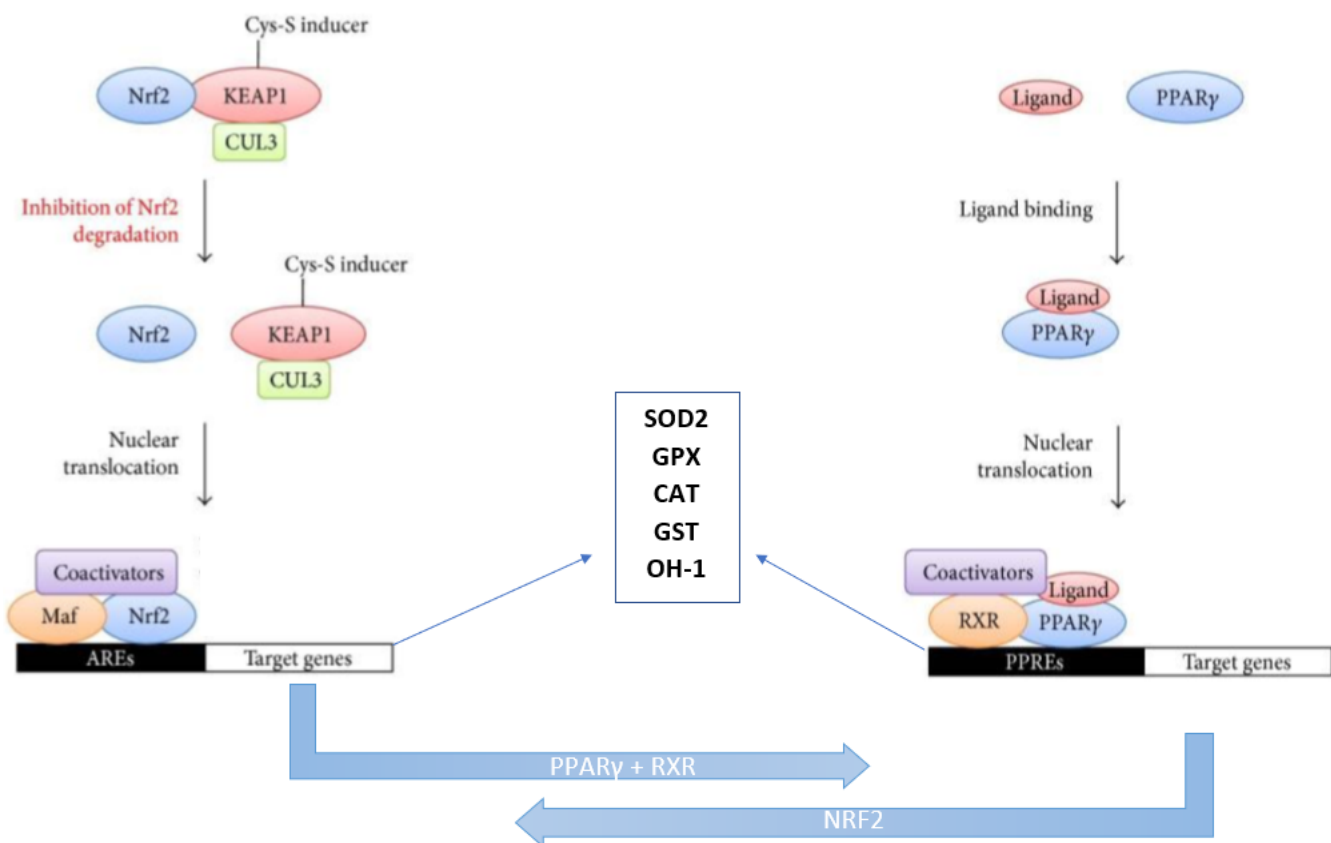
Figure 2.7: Collaborative action of NRF2 and PPARγ [Adapted by author from Lee, (2017)].

2.17) Betulinic Acid

Betulinic acid, a secondary plant metabolite, is ubiquitous in nature, having been identified in many fruit, vegetables and the bark of trees (Brusotti et al., 2017). It has been used therapeutically for centuries across the globe. In the African continent, BA is an important constituent in a traditional medicinal plant, *Peltophorum africanum* (Theo et al., 2009). Native Americans used bark containing BA to treat diarrhoea and dysentery whereas Russians have reportedly used BA therapeutically since 1834 (Yogeeswari and Sriram, 2005).

Betulinic acid is found abundantly in the barks of some trees like the white birch, *Betula alba*, in the form of betulin, which can be easily converted to BA (Yogeeswari and Sriram, 2005). Currently, BA can be prepared via various means such as using the yeast *Saccharomyces cerevisiae* (baker's yeast), and by recombinant plant and microbial cultures (Zhang et al., 2016). Sousa et al. (2019) explored simple transformations to BA, including amination, esterification, sulfonation and alkylation to medicinally functionalize BA (Sousa et al., 2019).

Betulinic acid ((3β)-3-Hydroxy-lup-20(29)-en-28-oic acid)(Fig. 2.8) is a naturally occurring penta-cyclic triterpenoid with a lupane skeleton containing two functional groups: 3OH and 17COOH (Yogeeswari and Sriram, 2005, Sousa et al., 2019). Pentacyclic compounds have 5 rings of atoms in their structure (Yogeeswari and Sriram, 2005). A triterpene is a hydrocarbon with no heteroatoms.

Pentacyclic triterpenes, particularly lupane-type, display various pharmacological effects, while being devoid of prominent toxicity (Jäger et al., 2009). Betulinic acid, being a triterpenoid acid, has a structure similar to that of cholesterol, and can thus bind to receptors, e.g. PPARγ, that normally bind to endogenous steroid hormones (Heiss et al., 2014).
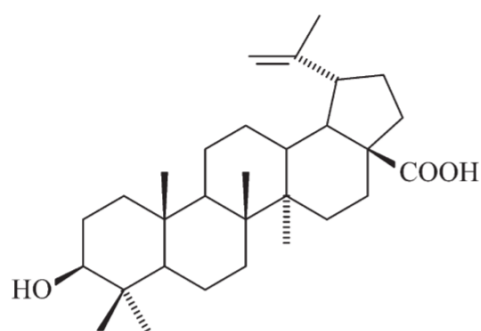
Figure 2.8: Chemical Structure of Betulinic Acid (de Melo et al., 2009).

2.17.1) Betulinic Acid and Peroxisome Proliferator-Activated Receptor Gamma

Betulinic acid is a PPARγ antagonist. An agonist response typically involves ligand binding stimulating gene expression. An antagonist usually competitively binds at the same active site, thus preventing agonist binding (Brusotti et al., 2017). PPARγ agonists can exert insulin sensitizing actions in T2DM. Thiazolidinediones are agonists currently in use for diabetes, with serious side effects of weight gain and cardiac failure (Bermudez et al., 2010). New synthetic agonistic ligands were identified, but were later withdrawn due to toxicity, with new antagonistic ligands developed to fill this gap. Furthermore, studies show that use of PPARγ antagonists with agonists ameliorate agonist side effects, thus providing a niche for BA (Leyvraz et al., 2010). Betulinic acid is the first PPARγ antagonist with a solved crystal structure. The crystal structures of the BA/PPARγ complex suggest that another molecule can be modelled at a second alternative site. (Brusotti et al., 2017).

Betulinic acid antagonistically binds with high affinity to its receptor, PPARγ, requiring no transactivation. Therefore, it is utilised for its insulin sensitizing and antidiabetic properties (Brusotti et al., 2017). Betulinic acid increased basal glucose uptake in adipocytes insulin-independently by up to 50% (Brusotti et al., 2017).

2.17.2) Pharmacological benefits

Betulinic acid has many biological and pharmacological benefits (Zhang et al., 2016). It has been proven to possess antimalarial, antiretroviral, immunomodulatory, antiangiogenic, antifibrotic, antioxidant, hepatoprotective and anti-inflammatory effects (Zhang et al., 2016).

Betulinic acid's thoroughly researched anti-diabetic properties stem from its phosphorylation of IR. Castellano et al. (2013) demonstrated that oleanolic acid and triterpenoid analogues synergistically enhance IR phosphorylation in Chinese hamster ovary (CHO-IR) cells and that, in the absence of insulin, at high concentrations, they can duplicate auto-phosphorylated receptors, concluding that triterpenes bind not to the insulin site but onto the β subunits (Castellano et al., 2013). Insulin receptor signalling may result in GLUT4 membrane localization. A separate study by Castro et al. (2014) demonstrated BA's effect on GLUT4 membrane localization for resultant glucose uptake (Castro et al., 2014). Many of the anti-diabetic effects of the triterpenes involve the repression of the polyol pathway, AGEs production and are related to activation of NRF2 (Castellano et al., 2013).

Betulinic acid and other triterpenes act as anti-diabetic agents via alternate pathways including through decreased gastro-intestinal glucose absorption, decreased endogenous glucose production and through increased insulin biosynthesis, secretion and sensitivity. Triterpenes further improve lipid homeostasis. Experimental studies have revealed that these positive effects on glucose and lipid metabolism occur at a dose that is not hepatotoxic as evidenced by normal levels of liver enzymes (Silva et al., 2016). Most

recently, Kim et al (2019) uncovered BA's amelioration of hyperglycaemia in a HFD mice model via decreased plasma glucose and increased insulin secretion (Kim et al., 2019).

Wang et al. (2016) proved BA's anti-inflammatory effect to diabetic-induced renal inflammation via interactions with NFκB signalling (Wang et al., 2016). In this study, HG conditions promoted the activation and translocation of NFκB, with BA exerting its effect via blocking the translocation of NFκBp65 into the nucleus, thus inhibiting the promotion of inflammation.

Betulinic acid and UCP2

Betulinic acid's effect on the uncoupling response is not well researched. Heiss et al., (2014) published a glycolytic switch study, in which they demonstrated the upregulations of UCP1 and 2 by BA in the mouse embryonic fibroblast (MEF) cell line. The authors, however, suggested that future studies are warranted to test UCP2 expression in other cell types as UCP2 is expressed differentially in different tissues. They further mentioned that the molecular mechanism behind UCP induction by BA is still to be elucidated (Heiss et al., 2014).

Betulinic acid and NRF2

Links between triterpenoids and NRF2 have previously been explored. Loboda et al., (2012) indicated that triterpenoids are able to regulate NRF2 via oxidative modification of -SH groups and signalling pathway phosphorylation (Loboda et al., 2012). Reisman et al., (2009) concluded that oleanolic acid, a triterpenoid like BA, protects against hepatoxicity via induction of NRF2 and its downstream targets (Reisman et al., 2009).

Antioxidant properties

The AO properties of BA have been researched, though not as comprehensively as BA's other pharmacological properties. In rat models, BA had a protective effect against redox imbalance (Adeleke and Adaramoye, 2017). More relevantly, Yi et al. (2014) confirmed BA's stimulation of the AO system (SOD2, GPx1, GSH) in response to alcohol-induced hepatotoxicity (Yi et al., 2014). Furthermore, Szuster-Ciesielska and Kandefer-Szerszen. (2005) proved, in a HepG2 cell model, that BA prevents excess superoxide production against ethanol-induced cytotoxicity. Szuster-Ciesielska and Kandefer-Szerszen. (2005) also confirmed that the AO activity of BA and other triterpenes was dependent on ROS induction (Szuster-Ciesielska and Kandefer-Szerszeñ, 2005). Thus, taking into account BA's selective AO activity and antidiabetic actions, there is a niche for evaluating BA's ability to combat HG-induced ROS.
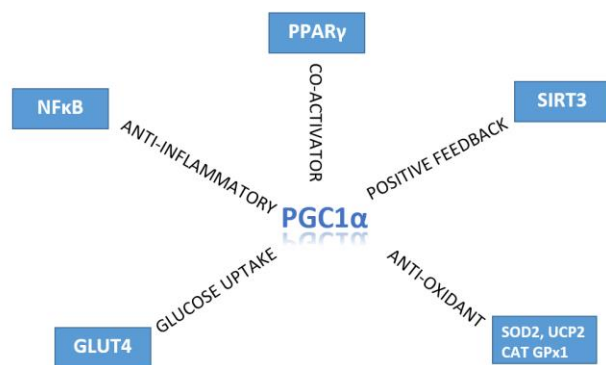
Figure 2.9: The various effects of PGC1α (prepared by author).

2.18) The human hepatoma cell line

The liver, possessing insulin-requiring tissue, plays a central role in energy homeostasis with regards to the regulation of carbohydrate and lipid metabolism, and is often deemed the metabolic hub of the body (Rui, 2011). Following a meal, glucose, lipid and protein are shunted primarily to the liver via the portal circulation. Within the liver, AKT insulin signalling occurs, resulting in various outcomes such as glycogenesis, and excess glycolysis and amino acid degradation fuel fatty acid (FA) synthesis. During starvation, the liver is the primary site of glycogenolysis and gluconeogenesis, helping in the maintenance of normal blood glucose (Rui, 2011). The liver is also central to diabetic pathophysiology, in that high levels of gluconeogenic precursors, like glycerol and lactate, fuel a drastic increase in gluconeogenesis, which plays a primary role in hyperglycaemia associated with T2DM (Consoli, 1992). Primary hepatocytes, however, are rarely accessible for experimental culture models, possessing an unstable phenotype, and can only be cultured for a short time span (Shulman and Nahmias, 2012).

HepG2 cells are an easily accessible, immortal cell line, whose characteristics have been thoroughly examined, possessing a stable phenotype, revealing many differentiated hepatic functions. Donato et al. (2015) described their functions as follows: cholesterol/triglyceride metabolism, glycogen synthesis, lipoprotein metabolism, insulin signalling, amongst others (Donato et al., 2015). Further, studies comparing HepG2 cells and primary hepatocytes show that, despite being a cancer cell line, the HepG2 cell line closely mimics the *in vivo* situation with regards to glucose metabolism (Sefried et al., 2018). However, this *in vitro* model does not mimic all the metabolic processes that are present in the *in vivo* state. Additionally, Kamalian et al. (2015) concluded that HepG2 cells are a suitable cell line to detect toxicity levels at different glucose concentrations (Kamalian et al., 2015).

Furthermore, HepG2 cells also demonstrate high expression of AO systems and are therefore, suitable for evaluating stress response (Mersch-Sundermann et al., 2004). The HepG2 cell line has been proven to accurately detect early changes in ETC via ATP measurement, which is indicative of respiration and mitochondrial metabolic state (Kamalian et al., 2015). Thus, the easy to handle HepG2 cell line

possesses an advantageous phenotype for this study, given its abilities in detecting glucose toxicity and metabolism, as well as evaluating the AO response.

CHAPTER 3: METHODS AND MATERIALS

3.1) Materials

Human hepatoma cells (HepG2) were obtained from the American Type Culture Collection (ATCC; HB-8065). Betulinic acid (B8936) and glucose (G8270-100G) was purchased from Sigma-Aldrich (St Louis, MO, USA). Western blotting reagents were obtained from Bio-Rad (Hercules, CA, USA). Antibodies were purchased from Cell Signalling Technology (Danvers, MA, USA), Abcam (Cambridge, UK), Sigma-Aldrich (St Louis, MO, USA) and Santa Cruz (Dallas, TX, USA). All other consumables and reagents were purchased from Merck (Darmstadt, Germany) unless otherwise stated.

3.2) Preparation of Betulinic Acid

Betulinic acid (5mM) stock solution was prepared in 0.1M phosphate buffered saline (PBS) and diluted in glucose-free-Eagles minimum essential medium (EMEM) to concentrations between 0-150μM for the MTT assay, and 5μM, 10μM, 25μM, 50μM for all remaining assays.

3.3) Cell Culture

The HepG2 cell line is an adherent cell line with an epithelial-like morphology. HepG2 cells are proven to demonstrate many differentiated hepatic functions as well as the ability to detect toxicity at various glucose levels (Donato et al., 2015, Kamalian et al., 2015).

HepG2 cells were cultured (ethics number: BREC/00000822/2019) in monolayer in a $25cm^3$ cell culture flask at 37ºC with 5% CO_2 in glucose-free Dulbecco's Modified Eagle's Medium (DMEM). Cells were washed with 0,1M PBS on alternate days and thereafter reconstituted with 5ml media.

Glucose free DMEM (Thermo-Fisher, A1443001) was supplemented as follows:

Normal Glucose (NG) media: 5mM glucose, 10% foetal calf serum (FCS), 1mM sodium pyruvate, 1% penstrepfungizone, 5mM 4-(2-hydroxyethyl)-1-piperazine ethanesulfonic acid (HEPES).

High glucose (HG) media: 25mM glucose, 1mM sodium pyruvate, 1% penstrepfungizone, 10%FCS and 2mM HEPES.

3.4) Cell Preparation for assays

HepG2 cells were grown in complete culture media (CCM) and switched to respective HG and NG media at 80% confluency. Cells were then treated with varying BA concentrations and incubated [24hours (hrs), 37ºC]. Thereafter, cells were removed via trypsinization and mechanical agitation. The trypan blue exclusion method was employed for cell counting. Cell numbers differ per assay. All assays were performed twice separately with a minimum of three replicates unless specifically stated otherwise.

3.5) Metabolic Activity

3.5.1) 3-(4,5-dimethylthiazol-2-yl)-2,5-diphenyl tetrazolium bromide (MTT) assay

Principle

The MTT assay is a colorimetric assay used to determine cell viability. It is based on the principle by which metabolically active cells reduce the yellow MTT salt to insoluble purple formazan crystals (Morgan, 1998). The crystals are then solubilised using dimethyl sulfoxide (DMSO), with the intensity of the purple formazan product being quantified using spectrophotometry (Fig. 3.1).

The reduction requires the use of NADH as a cofactor and succinate dehydrogenase as an enzyme. The NADH cofactor is a by-product of the TCA cycle and the enzyme required forms complex 2 of the ETC. Thus formazan intensity is a direct indication of the metabolic state of the mitochondria and cell viability (Riss et al., 2016, Morgan, 1998)(Fig 3.1).

Protocol

HepG2 cells were seeded into 96 well plate (15,000 cells/well) and allowed to adhere overnight. Thereafter, cells were treated with varying concentrations of BA (0µM, 30µM, 50µM, 70µM, 90µM, 110µM, 130µM, 150µM) under NG and HG conditions at 37°C for 24 hrs. Following treatment, cells were rinsed twice with 0.1M PBS and incubated (37°C, 4hrs) with 20µl MTT salt solution (5mg/ml in 0.1M PBS) and 100µl EMEM. Subsequently, supernatants were removed and 100 µl per well DMSO was added to solubilise the formazan (1 hr; 37°C). Optical density was measured at 570nm and a reference wavelength of 690nm using a spectrophotometer (Bio-Tek µQuant). Thereafter, the results were expressed as percentage cell viability versus the concentration of BA.
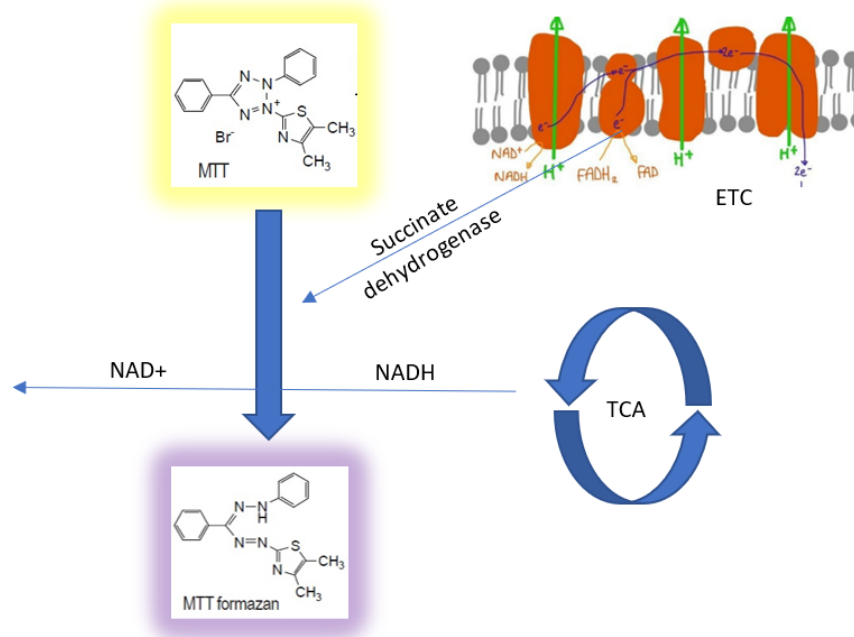
Figure 3.1: Reduction of MTT salt utilising ETC component and TCA by-products (prepared by author).

3.5.2) ATP assay

Principle

The metabolic state of the cell is driven by energy in the form of ATP. This 'molecular energy currency' is obtained from glycolysis as well as substrate level phosphorylation, however, the main source of ATP is obtained from OXPHOS. Oxidative phosphorylation is driven by H^+ flux via the ETC and is hence controlled via such means, making it an ideal assessment of the metabolic state of a cell (Souza et al., 2011) .

The ATP assay employs luminescence techniques to directly determine ATP concentration within a cell, as an extrapolation of cell viability. The reagent lyses the cells, freeing the ATP, which, along with co-factors Mg^{2+} and molecular oxygen, mono-oxygenates introduced luciferin via luciferase activity. This generates a luminescent signal directly proportional to the amount of ATP, and hence metabolically active cells, present in culture (Riss et al., 2016).

Protocol

The CellTiter-Glo® Luminescent Cell Viability Assay (Promega, Madison, USA) was conducted. Following treatment, HepG2 cells (20, 000 cells/well in 0.1M PBS) were seeded into an opaque 96-well microtiter plate in triplicate. 20µL CellTitler-Glo® reagent was added followed by incubation in the dark [30 minutes (min), room temperature (RT)] to allow the reaction to occur. Thereafter,

luminescence was measured on a Modulus™ microplate luminometer (Turner Biosystems, Sunnyvale, USA), and results are represented as relative light units (RLU).

3.5.3) Lactate Dehydrogenase Assay

Principle

Hyperglycaemic-induced OS results in high lipid peroxidation, which directly damages the membrane. The cytotoxicity detection kit is based on quantifying cytoplasmic enzymes released into the supernatant by damaged cells. Lactate dehydrogenase is a stable cytoplasmic enzyme, found in all cells, that is released into the supernatant when membrane integrity is compromised (Kumar et al., 2018).

Extracellular LDH levels are measured enzymatically in cell culture supernatant. In the first step, NAD^+ is introduced into the supernatant, being reduced to $NADH/H^+$, as a co-factor in the conversion of lactate to pyruvate. This reaction is catalysed by LDH. In the second step, an introduced catalyst known as diaphorase transfers an H/H^+ from the $NADH/H^+$ to the INT tetrazolium salt, reducing it to formazan (Kumar et al., 2018).

Protocol

LDH cytotoxicity detection kit (Roche, Manheim, Germany) was used to quantify LDH in cell culture supernatants following treatment as per the manufacturer's instructions. Briefly, 100µl of supernatant was transferred to a 96 well microtitre plate in triplicate followed by 100µL of cytotoxicity detection reagent [catalyst (diaphorase/NAD), dye solution (INT/sodium lactate)]. Plates were then incubated for 25 min at room temperature in the dark. Optical density was measured at a wavelength of 500nm (microplate reader-Bio-Tek µQuant).

3.6) Oxidative Stress

3.6.1) Endogenous ROS: 2′,7′-dichlorodihydrofluorescein-diacetate assay

Principle

This simple, sensitive, fluorometric assay quantifies intracellular ROS. Cells were exposed to the membrane permeable, non-fluorescent $H_2DCF-DA$ probe (Wan et al., 2005). Once it passively diffuses into the cell, it is deacetylated by cellular esterases to non-fluorescent 2',7'-dichlorfluorescein (DCFH). This compound reacts with ROS, and undergoes a $2e^-$ oxidation to form fluorescent H_2DCF (Fig. 3.2). This fluorescence can be measured via many means (flow cytometry, luminometry, microscopy) and is directly proportional to intracellular ROS levels (Kalyanaraman et al., 2012).
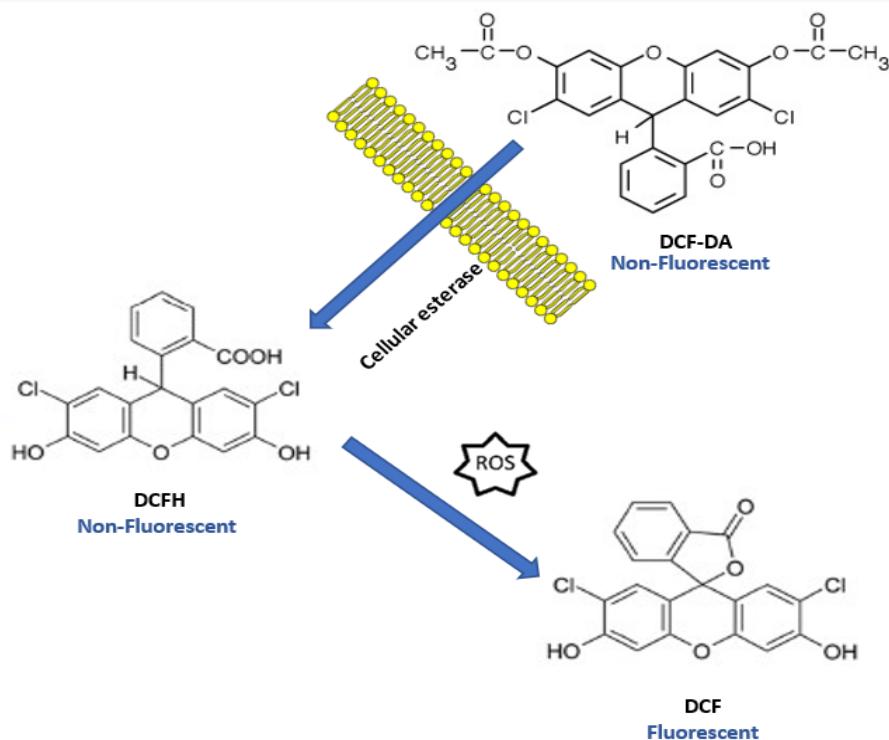
Figure 3.2: Formation of fluorescent DCF for ROS quantification (prepared by author).

Protocol

DCF working solution was made by dissolving 0,5 µL of H$_2$DCF-DA in 25ml DMEM. Cells grown in a 25cm^3 flask (50 000 cells) were centrifuged (400xg; 10 min; RT) to a pellet and incubated in DCF solution (200µL; 30 min; 37ºC). Centrifugation (400xg; 10 min; RT) ensured removal of stain and cells were washed twice in 200µL 0,1M PBS. Cells were then resuspended in 200µL 0,1M PBS and plated in triplicate (96 well opaque microtiter-plate; 50µL per well). A blank of only 0,1 M PBS was also plated in triplicate.

Fluorescence was then measured using a Modulus^{TM} microplate luminometer (Turner Biosystems, Sunnyvale, CA). A blue filter was used at an excitation wavelength of 503nm and an emission of 529nm. Fluorescence was calculated by subtracting average fluorescence of blank from sample fluorescence.

3.6.2) Lipid Peroxidation: Thiobarbituric acid reactive substances assay

Principal

The TBARS assay is utilised to quantify lipid peroxidation as an indication of oxidative damage due to ROS. The assay quantifies MDA, a by-product of lipid peroxidation, via conjugation with two molecules of thiobarbituric acid (TBA), to generate a pink chromogenic adduct which is spectrophotometrically measured (Fig. 3.3).

Reactive oxygen species interact with polyunsaturated fatty acids (PUFAs), removing their hydrogen bond, thus initiating the chain reaction that is lipid peroxidation (Fig. 3.3). Molecular rearrangement follows, forming a conjugated diene. This then reacts with oxygen forming a lipid peroxy-radical which then removes H-bonds from new lipids, restarting the process. Nonradical products can be generated via AO H-atom donation to lipid peroxy-radicals (Devasagayam et al., 2003).

High temperature and low pH conditions are required for this assay. Phosphoric Acid ensures an acidic environment while butyl-4-hydroxybenzoic acid (BHT) prevents non-specific chromophore formation. Butanol is used to extract the MDA-TBA from the sample allowing measurement of the adducts (Grotto et al., 2009).
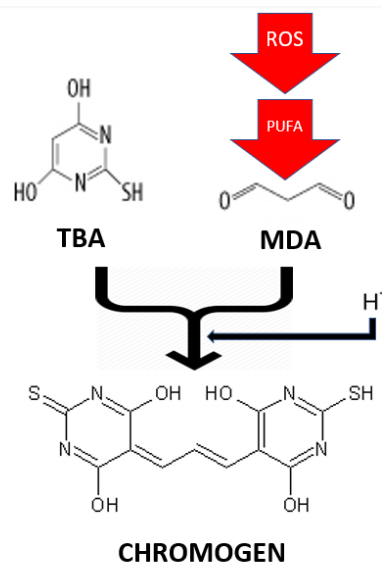
Figure 3.3: TBARS assay reaction. 2TBA reacts with lipid peroxidation by-product malondialdehyde to produce chromophore measured at 532nm (prepared by author).

Protocol

200µl of supernatants from controls and BA-treated cells were added to test tubes, bar the negative and positive controls. 200µl of 2% H_2PO_4 and 200µL of 7% H_2PO_4 were added into each tube. 400µL TBA/butylated hydroxytoluene (BHT) was then added into all tubes except the negative control to which 400 µL of 3M HCl was added. All tubes were then vortexed. 200µl 1M HCl was added to adjust the pH and 1µL MDA was added to the positive control. Thereafter, samples were boiled (15 min, 100°C) and allowed to cool to RT. Butanol (1.5ml) was added to each sample, vortexed (30 sec) and allowed to stand, thus separating into different phases. 100µl of the upper butanol phase was removed and plated into a 96 well microtiter plate in five replicates. Thereafter, the optical density was measured

at 532nm (reference wavelength: 600nm) using a spectrophotometer (Bio-tek µQuant). MDA concentration was calculated using the equation below (equation 3.1) (Devasagayam et al., 2003).

$$MDA_{Concentration} = \frac{\text{Average Absorbance Sample - Average Absorbance Blank}}{156mM^{-1}}$$

Equation 3.1: Calculation to determine the MDA concentration (in mM), where 156mM^{-1} is the extinction co-efficient of the MDA-TBA adduct (Devasagayam et al. 2003).

3.6.3) Protein Carbonyl Assay

Principle

Quantification of intracellular carbonyl groups allows us to measure protein oxidation as a result of oxidative stress. Protein carbonylation is defined as the introduction of aldehyde or ketone carbonyl groups into a protein's molecular structure (Purdel et al., 2014). This can be achieved via many mechanisms, including oxidation directly on specific amino acid residues within a protein chain, interaction between lipid peroxide products and aldehyde groups and interaction between carbonyl groups formed via lipid degradation or glycoxidation. The above-mentioned mechanisms are signs of oxidative stress, hence, high protein carbonyl content is a biomarker of oxidative stress (Purdel et al., 2014).

The process of carbonylation is irreversible, thus making it an ideal, accurate measurement for oxidative stress damage. The standard method for assessing protein carbonylation status involves spectrophotometry. Trichloroacetic acid is used to precipitate protein. Ethanol-ethyl acetate eliminates *dinitrophenylhydrazine* (DNPH) traces and solubilizes residual lipids. Centrifugation is utilised to remove any insoluble material. Carbonyl groups are derivatized with DNPH in order to obtain a DNP-derived protein, which is a yellow colour. This products optical density can be measured at 370nm (Purdel et al., 2014) (Fig. 3.4) .
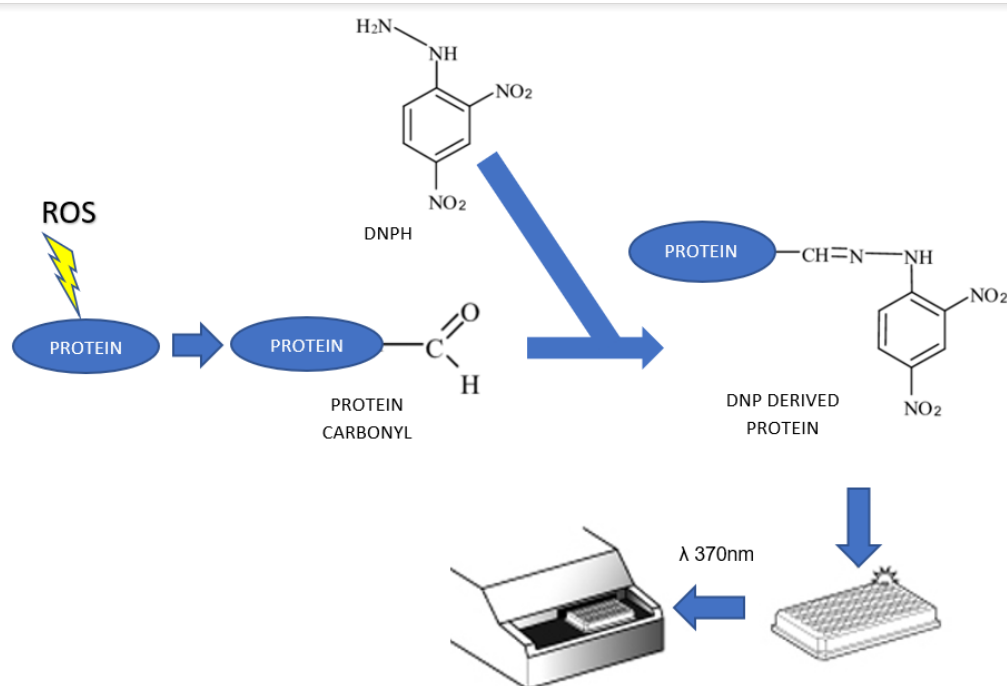
Figure 3.4: DNP-derived protein formation for protein carbonyl-group detection (prepared by author).

Protocol

Protein was isolated using Cell Lysis Buffer (200µL), quantified using the BCA assay, and standardized using cell lysis buffer once again. Standardized proteins were aliquoted into 15ml centrifuge tubes (100µL), along with 400µL of DNPH, and incubated (RT; 1 hr). Samples were vortexed every 15 minutes. 100 µL of control treatment was added to 400µL 2,5HCl to act as a blank. Following this, 500µL of 20% trichloroacetic acid was added to all samples and vortexed. Tubes were placed on ice for 10 minutes, vortexed, and thereafter centrifuged (2000xg;10 min; RT). Protein precipitates were collected and supernatant discarded. Pellets washed (500µL 10% trichloroacetic acid), vortexed and centrifuged (2000xg; 10min; RT). Pellets were thereafter washed twice in 500µL ethyl acetate and final precipitates dissolved in 250µL 6M Guanidine hydrochloride. Incubation (37ºC;10 min) followed by removal of insoluble material via centrifugation (2000xg;10 min; RT) ensued. Supernatants were plated (50µL; triplicate) in a 96 well plate, and absorbance was measured at 370nm, spectrophotometrically. Carbonyl content was calculated using equation below (Equation 3.2) (Mercier et al., 2004)

$$\boldsymbol{Carbonyl\ Concentration}\ (\mu M) = \frac{1cm\ (Absorbance_{sample} - Absorbance_{blank})}{22\ 000 M^{-1} cm^{-1}}$$

Equation 3.2: Equation to determine protein carbonyl concentration in µM where 1cm is the pathlength and 22 000M^{-1}cm^{-1} is the extinction coefficient of the DNP (Mercier et al., 2004).

3.7) Antioxidant detection

3.7.1) GSH Assay
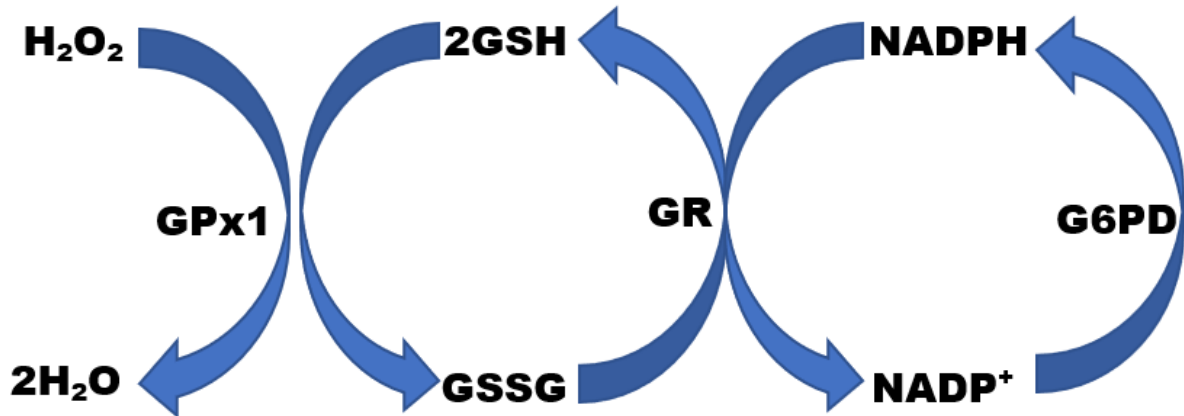
Figure 3.5: The GSH cycle (prepared by author).

Principle

Glutathione is an AO that exists in two states, namely GSH [glutathione (reduced)] and GSSG [Glutathione (oxidized)]. GSH donates an e^- and, in a reaction catalysed by the enzyme glutathione peroxidase (GPx1), detoxifies H_2O_2 into H_2O. It is thus oxidised to GSSG by doing so. Glutathione reductase (GR), with cofactor NADPH, reduces GSSG back to GSH. Glucose-6-phosphate dehydrogenase (G6PD) is an enzyme which reduces $NADP^+$ to NADH, thus providing cofactors for GR action. Thus, the cycle ensues, detoxifying ROS (Fig. 3.5). High levels of GSH thus gives an indication to a sample's AO ability (Rahman et al., 2006).

The GSH-Glo® Glutathione Assay is a luminometric assay that detects and quantifies reduced glutathione as an indicator of AO response and capacity. Introduced luciferin derivative interacts with endogenous GSH, catalysed by GST, to generate luciferin which, via the action of luciferase, produces a light photon. This is quantified via luminometry and is directly proportional to intracellular GSH concentration (Fig. 3.6) (Rahman et al., 2006).
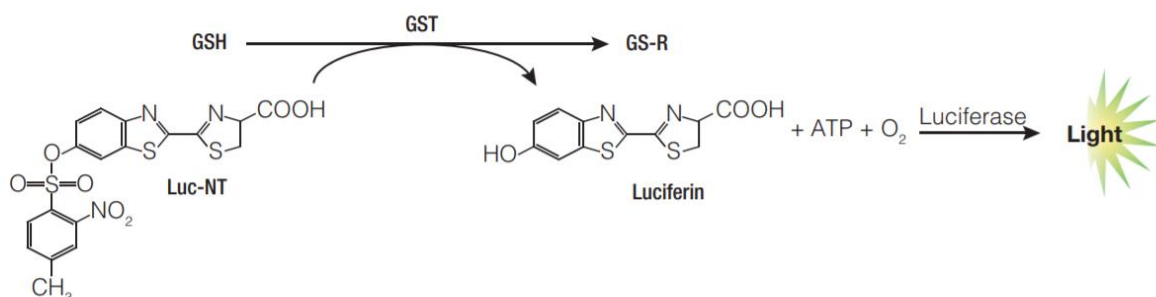
Figure 3.6: GSH reactions involved in generation of a light signal (diagram supplied by manufacturer).

Protocol

The GSH-Glo® Glutathione Assay (Promega, Madison, USA) was conducted to assess AO ability. Following treatment, HepG2 cells (20,000 cells in 0.1M PBS) were plated into a 96-well opaque microtiter plate in triplicate. Standards were prepared from 5mM GSH stock (0µM, 1µM, 2µM, 2,5µM, 3µM, 4µM, 5µM) via dilution of de-ionized water and plated in triplicate. 50µL GSH-Glo® reagent was added followed by incubation in the dark (30 min, RT). 100 µL of Luciferin Detection Reagent was added to each well followed by 15 min incubation (RT). Thereafter luminescence was measured on a Modulus™ microplate luminometer. The standards helped construct a standard curve upon which the GSH-concentration of the sample was extrapolated.

3.8) Protein isolation, quantification and standardization

Principle

Protein lysate from HepG2 cells was required for western blotting. Crude protein concentrations were quantified and standardized to the sample with the lowest concentration to ensure that samples could be compared accurately. Isolation occurred on ice to prevent protein degradation. Both chemical and mechanical lysis methods were utilised (Huang et al., 2010b).

Protein concentration was quantified using the sensitive bicinchoninic acid assay (BCA). This assay was undertaken in alkaline conditions and relies on two reactions based on the biuret reaction. Cu^{2+} reacts with peptide bonds and is reduced to Cu^{1+}. Cuprous ions then engage in chelation with 2BCA generating a purple colour. Colour intensity is directly proportional to protein concentration (Fig. 3.7). Spectrophotometric analysis ensues. A range of standards are generated from protein of known concentration. A standard curve is generated from these results and the sample protein concentration calculated via extrapolation methods (Huang et al., 2010b).
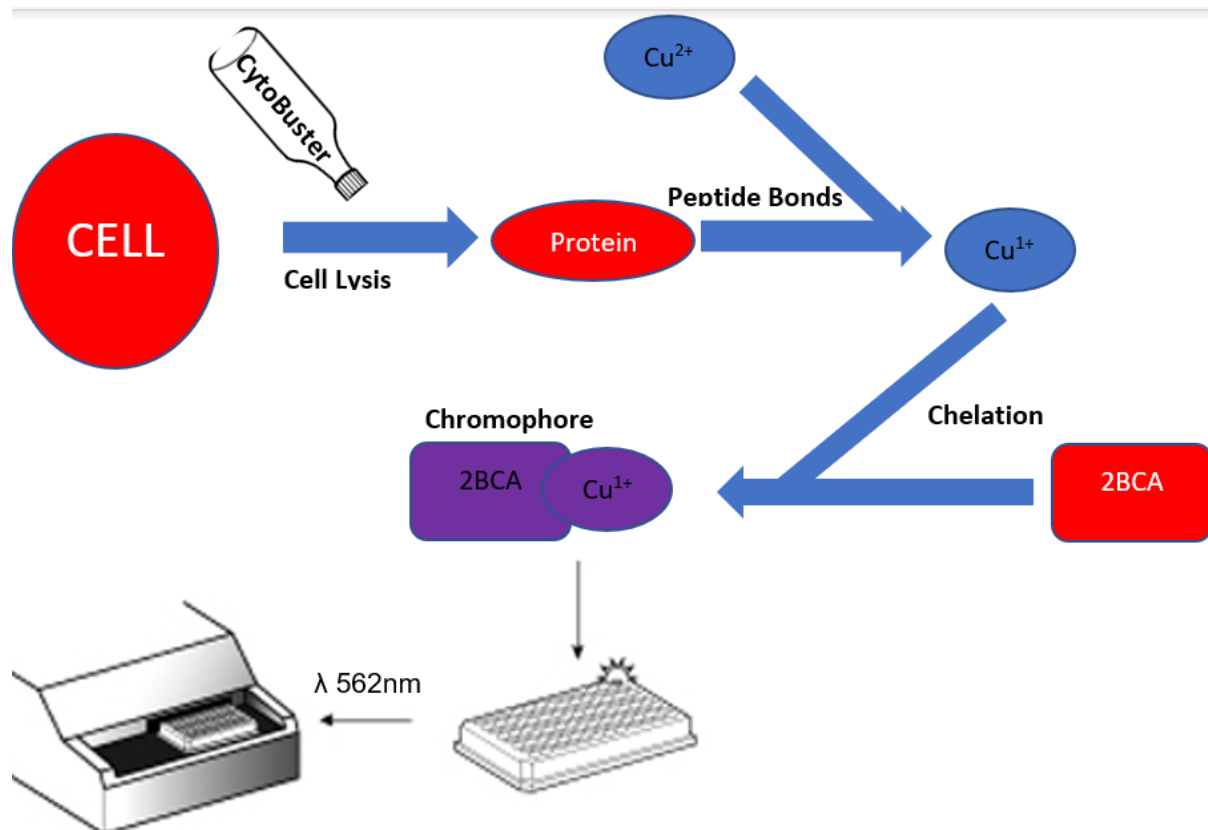
Figure 3.7: Biuret based BCA reaction to quantify protein (prepared by author).

Protocol

Protein samples were isolated using Cytobuster (250µL) lysis reagent (Novagen, USA, catalogue no. 71009) supplemented with protease and phosphatase inhibitors (Roche, 05892791001 and 04906837001, respectively) for western blotting. Adhered cells were incubated on ice (30 min) in Cytobuster and then mechanically scraped to facilitate cell lysis. Proteins were then transferred into micro-centrifuge tubes and subject to centrifugation (10 000xg; 4ºC; 10 min). Newly obtained crude protein was quantified using the BCA assay. Standards of known protein bovine serum albumin (BSA) were prepared (0mg/ml, 0,2mg/ml, 0,4mg/ml, 0,6mg/ml, 0,8mg/ml, 1mg/ml) and plated in triplicate alongside protein samples plated in duplicate (25 µL). 200µL BCA working solution (198µL 2BCA; 4µL $CuSO_4$) was added to each well followed by incubation (37ºC; 30 min). Optical density was measured spectrophotometrically (Bio-Tek µQuant) at 562nm. Absorbance values of standards were used to construct a standard curve and sample concentrations were extrapolated. Quantified proteins for western blot were standardized to lowest protein concentration via dilution with Cytobuster.

3.9) Protein expression: Sodium Dodecyl Sulphate – Polyacrylamide Gel Electrophoresis (SDS-PAGE) and Western Blotting.

Principle

SDS-PAGE and western blotting are widely used techniques to identify and detect protein expression. Proteins are subject to an electric field, separating them based on molecular weight, electro-transferred to a membrane, and immuno-detected (Kurien and Scofield, 2006).

Standardized proteins are boiled (5 min; 100ºC) in 1x Laemmli buffer [Tris-Cl (6.8 pH), glycerol, Bromophenol blue, β-mercaptoethanol, SDS, dH_2O]. These components allow for the efficient migration of protein samples through the gel. Bromophenol Blue is used as a tracking dye for visualization of protein migration; β-mercaptoethanol is a reducing agent which breaks disulphide bonds, thus allowing for protein unfolding; Tris-HCl acts as buffer, maintaining pH during electrophoresis; SDS provides an overall negative charge to the proteins allowing it to be separated according to size rather than its shape and charge; and glycerol adds density to the sample, ensuring that it forms a thin layer in the wells during SDS-PAGE. Heating denatures the higher order of the protein. This ensures that the anionic charge is not neutralized to allow for protein movement within an electric field (Mahmood and Yang, 2012).

Proteins were separated using SDS-PAGE. SDS-PAGE involves the migration of molecules through a gel, under the influence of an electric field, with the negatively charged proteins migrating towards the positively charged cathode. Laemmli buffer ensured that all proteins were in their primary form. Smaller proteins migrate faster and further (towards the cathode) than larger ones. The frictional coefficient is also dependant on the viscosity of buffer and pore size of the medium (Mahmood and Yang, 2012).

A polyacrylamide gel, a cross linked polymer of acrylamide and N, N'-methylene bis-acrylamide, is used along with Tetramethylethylenediamine (TEMED) (free radical stabilizer) and ammonium persulphate (free radical donor) to ensure polymerisation. Two types of gels are used in SDS-PAGE: a high percentage resolving gel allowing for accurate size separation and a low percentage stacking gel above this, ensuring that all proteins start at the exact same line, before the electric field is applied. For efficient separation, constant temperature must be maintained (to prevent denaturing) and convection currents must be avoided. Tris maintains running pH of run and glycine ensures proteins move in a tight band and that none straggle (Mahmood and Yang, 2012).

Following SDS-PAGE, proteins are electro-transferred from a gel to a nitrocellulose membrane. Nitrocellulose membranes possess high binding capacity for protein, are easily stained for protein and do not require pre-activation (Kurien and Scofield, 2006).

An electric field was utilised to elute protein from the gels, transferring them to membranes. The membranes, fibre pads and the gels were equilibrated in transfer buffer. Equilibration helps to reduce

the amount of SDS and other buffer salts in the gel, which can interfere with protein adsorption to the membrane. The gel and membrane were then sandwiched by fibre pads on either side between two electrodes, allowing uniform transfer. The blot transfer system then applied a voltage, generating an electric current perpendicular to the gel surface. This allowed negatively charged proteins to migrate from the gel onto the nitrocellulose membrane (Kurien and Scofield, 2006).

Protein expression was then detected using immunological and chemiluminescent methods. A primary antibody specific to the protein of interest is added to the membrane followed by an enzyme [horse radish peroxidase (HRP)]-conjugated secondary antibody that binds to the primary antibody. A chemiluminescent reagent is added, reacting with the enzyme, releasing a luminescent signal directly proportional to protein intensity, allowing for detection (Fig. 3.8) (Kurien and Scofield, 2006).
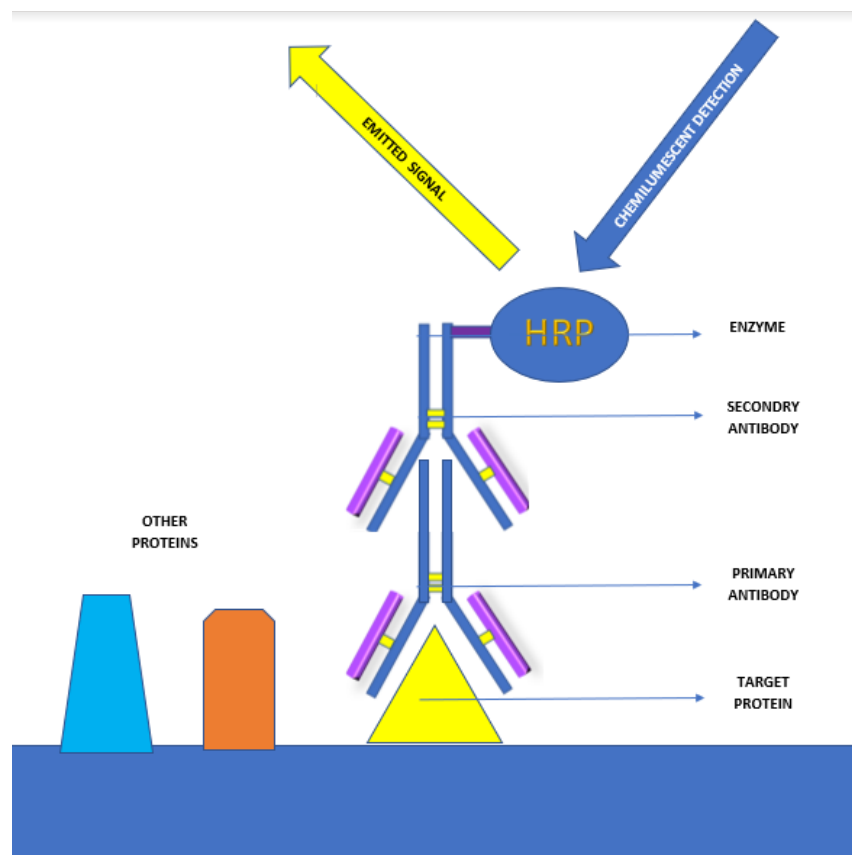
Figure 3.8: Immunoblotting concept employed in western blotting to detect protein levels (prepared by author).

Protocol

Standardized proteins were boiled (100°C) in Laemmli buffer [0.5M Tris-Cl (6.8 pH), glycerol, 1% Bromophenol blue, 5% β-mercaptoethanol, 10% SDS, dH$_2$O] for 5 minutes. Thereafter, gel electrophoresis was used to separate proteins according to molecular weight (4% stacking gel; 10% resolving gel) at 150V for 1 hr (Bio-Rad Mini PROTEAN Tetra-Cell System). This was followed by

electro-transference to a nitrocellulose membrane. The stacking gel was discarded and the resolving gel was carefully removed from the glass plate. Gels, fibre pads and membranes were soaked in transfer buffer (20% methanol, 25mM Tris, 192mM glycine for 10 min) and sandwiched together. The sandwich was placed between electrodes and subject to a current (30 min; 20V) using the Transblot Turbo Transfer System, (Bio-Rad). Membranes were blocked using 5% BSA in Tris buffered saline containing Tween 20 (TTBS: 137mM NaCl, 24mM Tris, 0.5% Tween 20, 2.7mM KCl). Membranes were incubated with primary antibodies (Table 3.1) overnight at 4ºC. The membranes were then washed with TTBS, probed with a HRP-conjugated secondary antibody (Table 3.1), incubated (2 hrs, RT, 1:5 000) and viewed. Membranes were developed using 400µl BioRad Clarity Western ECL Substrate (Bio-Rad, Hercules, USA) and the ChemiDoc XRS+ Molecular Imaging System (Bio-Rad) was used to visualize protein bands. Membranes were stripped via incubation with 5% hydrogen peroxide (37°C, RT). Protein expression was normalised against HRP-conjugated β-actin. Results were displayed as Relative Band Density (RBD) of relevant proteins divided by the RBD of β-actin.

Table 3.1: Antibodies and dilutions utilised for western blotting (prepared by author).

PRIMARY ANTIBODY	CATALOGUE NO.	DILUTION
Anti-pNRF2	ab76026 (Abcam)	1:1000 in 5% BSA
Anti-NRF2	ab31163 (Abcam)	1:1000 in 5% BSA
Anti-SOD2	HPA001814 (Sigma-Aldrich)	1:1000 in 5% BSA
Anti-CAT	C0979 (Sigma-Aldrich)	1:1000 in 5% BSA
Anti-SIRT3	C73E3 (Cell signalling technologies)	1:1000 in 5% BSA
Anti-Lon-P1	HPA002034 (Sigma-Aldrich)	1:1000 in 5% BSA
Anti-IRβ	ab10321 (Abcam)	1:2000 in 3% BSA
Anti-PGC1α	ab72230 (Abcam)	1:1000 in 5% BSA
Anti-UCP2	ab67241 (Abcam)	1:1000 in 5% BSA
Anti-PPARγ	ab59256 (Abcam)	1:1000 in 5% BSA
Anti-NFκB	D14E12 (Cell signalling)	1:1000 in 5% BSA
Anti-β-actin	A3854 (Sigma-Aldrich)	1:5 000 in 5% BSA
SECONDARY ANTIBODY	CATALOGUE NO.	DILUTION

Goat Anti-mouse IgG HRP	Sc-2005 (Santa Cruz)	1:5 000 in 5% BSA
Goat Anti-rabbit IgG HRP	Sc-2004 (Santa Cruz)	1:5 000 in 5% BSA
Donkey anti-goat IgG-HRP:	Sc-2020 (Santa Cruz)	1:5 000 in 5% BSA

3.10) Messenger RNA quantification: Quantitative Polymerase Chain Reaction

Principle

PCR allows for a sensitive, specific and reproducible method to amplify a specific DNA sequence from a template strand. This method enables copies of a DNA template to be made in direct proportion to original amount of target DNA. qPCR simultaneously amplifies and quantifies target DNA. Fluorescent dyes bind to double stranded DNA (dsDNA), emitting fluorescence when bound, thus when DNA is produced the fluorescent signal is amplified and quantified (Pestana et al., 2010).

There are 3 steps in the PCR process (Arya et al., 2005). The initial step involves exposing the DNA template to extreme temperatures (94-98ºC) for 20-30 seconds, resulting in denaturation. The H-bonds between dsDNA are broken producing single stranded DNA (ssDNA) which serves as the template DNA strand. Thereafter, temperatures are lowered to 55-60ºC and two synthesized oligonucleotide primers (forward and reverse) complimentary to the sites adjacent to the target region, are annealed to the template DNA via complimentary base pairing. During extension, the temperature is increased to 72ºC (optimum temperature for *Taq* polymerase activity) and *Taq* polymerase facilitates the attachment of deoxynucleoside triphosphates (dNTPs) complimentary to the ssDNA at the target gene, resulting in a new dsDNA. $MgCl_2$ is a co-factor for Taq Polymerase and is required for primer binding to template DNA (Fig. 3.9). The buffer solution used maintains the pH and ionic strength of the reaction solution suitable for activity of Taq polymerase. The process is repeated for 30-40 cycles to ensure sufficient amplification (Arya et al., 2005).

Housekeeping gene glyceraldehyde 3-phosphate dehydrogenase (GAPDH) was run alongside samples in each run. The amount of target DNA is reported relative to the amount of housekeeping gene for every sample. Housekeeping genes are used because they are expressed constantly, regardless of tissue, at all stages of development, and hence expression levels should remain constant amongst samples (Arya et al., 2005).

In order to measure mRNA expression, RNA is isolated and reverse transcribed into complementary DNA (cDNA) which serves as the starting DNA template in qPCR. RNA isolation utilises Qiazol reagent (containing phenol), which degrades cellular and nuclear membranes, while maintaining the

integrity of RNA; chloroform, which removes DNA, protein, and lipids; isopropanol, which precipitates the RNA; and nuclease free water (nfH$_2$O) , which lacks RNase enzymes allowing the RNA to be dissolved while preventing its degradation (Arya et al., 2005).
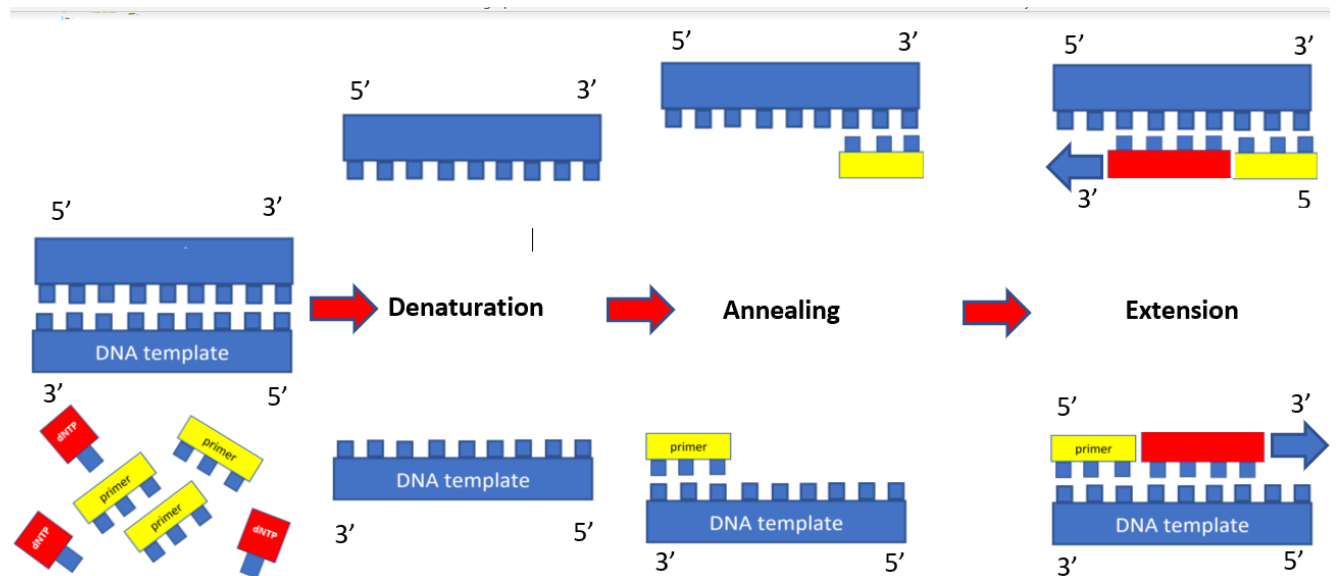
Figure 3.9: 3 steps involved in a single PCR cycle resulting in DNA amplification (prepared by author).

Protocol

Following treatment, HepG2 cells were washed three times in 0.1M PBS; and subsequently incubated in 500µL Qiazol (Qiagen, Hilden, Germany) and 500µL 0,1M PBS (5 min, RT). Cells were mechanically lysed using a cell scraper and lysates were transferred to 2ml micro-centrifuge tubes and stored overnight at -80ºC. Thereafter, samples were thawed, chloroform (100µL) was added and the samples were centrifuged (12,000xg; 4ºC; 15 min). Supernatants were transferred to fresh 2ml micro-centrifuge tubes and 250µL cold isopropanol was added before overnight storage at -80ºC.

Following incubation, samples were thawed and centrifuged (12,000xg; 4ºC; 20 min). Supernatants were removed, RNA pellets were washed in 75% cold ethanol (500µl), and centrifuged (7,400xg; 4ºC; 15 min). The ethanol was removed and the RNA samples were air dried for 10 min at RT. RNA pellets were then resuspended in 15µL of nfH$_2$O and quantified using the Nanodrop2000 spectrophotometer (Thermo-Fischer Scientific).

The A260/280 ratio was used to assess RNA purity. RNA was then standardized to 1,000 ng/µl and reverse transcribed into cDNA using the Maxima H Minus First Strand cDNA synthesis Kit (Thermo-Fisher Scientific; K1652) as per manufacturer's instructions. Briefly, a master mix comprising of 1µL RNA, 0,25µL Oligo(dt) primer; 1µL 10mm DNTP mix; 12,75µL nfH$_2$O was incubated at 65ºC for 5 min in the thermocycler (Bio Rad T100^{TM} Thermal Cycler). Thereafter, 4µL 5X RT Buffer and 1µL

Maxima H minus enzyme was added to each sample and incubated (10 min at 25ºC; 15 min at 50ºC; 5 min at 85ºC). 60µL nfH$_2$O was added to each sample and stored at -80ºC.

Gene expression was analysed according to the manufacturer's instructions using PowerUp SYBR Green Master Mix (Thermo-Fisher Scientific; A25779). Forward and reverse primers of genes of interest (Table 3.2) were diluted down to 25µM with nfH$_2$O. Samples were plated (1µL) with 9µL of mastermix (5µL SYBR Green; 1µL Forward Primer; 1µL Reverse Primer; 2µL nfH$_2$O) in triplicate. *GAPDH* was used as the housekeeping gene to normalise gene expression.

Sample amplification was performed using the CFX96 Touch™ Real-Time PCR Detection System (Bio-Rad). Initial denaturation (95ºC; 8 min) was followed by 37 denaturation cycles (95ºC; 15 sec), annealing (40 sec; temperatures) and extension (72ºC; 30 sec). Calculation demonstrated by Livak and Schmittgen (2001) was used to determine mRNA expression variances. Results are expressed as fold change relative to the control (GAPDH) (Livak and Schmittgen, 2001).

With regards to miRNA, RNA, standardized to 1,000 ng/µl, was reverse transcribed into cDNA using the miScript II RT Kit (Qiagen, 218161) as per manufacturer's instructions. Briefly, a master mix, comprising of 1µL RNA, 4µL 5x miScript HiFlex Buffer, 2µL 10x miScript Nucleics Mix , 11µL RNAse free H$_2$O, 2µL miScript Reverse Transcriptase Mix, was incubated at 37ºC for 60 min, 95ºC for 5 min and 4ºC for 5 min.

MiRNA cDNA was used to determine miR-124 expression using the miScript SYBR Green PCR Kit (Qiagen, 218073). Human *RNU6* (Qiagen, MS000033740) was used as a house keeping gene. Each reaction was carried out in triplicate containing 2X Quantitect SYBR Green (6.25 µl), 10X miScript Universal Primer (1.25 µl), RNase free water (2.25 µl) and template cDNA (1 µl). The qPCR experiments were conducted in the CFX Touch™Real Time PCR Detection System (Bio-Rad) at the following thermal conditions: Initial denaturation (95ºC; 15 min) was followed by 37 denaturation cycles (94ºC; 15 sec), annealing (40 sec; 55ºC) and extension (70ºC; 30 sec). . The cycle threshold (Ct) values were used to analyse changes in miRNA expression and were represented as fold change relative to the house keeping gene RNU6 using the method described by Livak and Schmittgen (2001) (Livak and Schmittgen, 2001).

Table 3.2: Genes of interest with relevant annealing temperatures and primer sequences (prepared by author).

Gene	Annealing Temperature	Primers
GPx1	57.4ºC	F-5'-GACTACACCCAGATGAACGAGC-3' R-5'-CCCACCAGGAACTTCTCAAAG-3'
PGC1α	57.6ºC	F-5'-CCAAACCAACAACTTTATCTCTTCC-3' R-5'-CACACTTAAGGTGCGTTCAATAGTC-3'
SIRT3	57ºC	F-5'-CGGCTCTACACGCAGAACATC-3' R-5'-CAGC GGCT CCCC AAAG GAAC AC-3
NRF2	58ºC	F-5' AGTGGATCTGCCAACTACTC 3' R-5' CATCTACAAACGGGAATGTCTG- 3'
GAPDH	variable	F-5'-TCCACCACCCTGTTGCTGTA-3' R-5'-ACCACAGTCCATGCCATCAC-3'

3.11. Statistical Analysis

Data analysis was performed using the One-way Analysis of Variance (ANOVA) and Bonferroni test for multiple group comparison via GraphPad Prism V5.0 Software. Data was considered significant at $p<0.05$.

CHAPTER 4: RESULTS

4.1) Betulinic acid stabilises mitochondrial output and maintains cell viability

The intracellular energy and metabolism status of BA-treated HepG2 cells were assessed by the MTT and ATP assays.

Betulinic acid is a known anti-cancer agent, and hence non-toxic and low concentrations of BA were used to establish its antioxidant and anti-hyperglycaemic properties (Yogeeswari and Sriram, 2005). Both the MTT and ATP assays measured cell viability and metabolic output.

An MTT assay confirmed that BA (0-150µM) did not significantly impair cell viability and energy output of the HepG2 cell line under NG conditions (Fig. 4.1A) and HG conditions (Fig. 4.1B). No significance was expressed relative to the controls.

In literature, it was found that BA concentrations higher than 21µM exhibit a degree of toxic potential, hence values within the MTT range, but below 21µM were chosen (Fu et al., 2005, Santos et al., 2009). ATP cell viability assays were conducted on 5µM and 10µM treatments as a preliminary measure to determine mitochondrial function. No significant differences were observed in ATP levels in both NG (p= 0.3261; Fig. 4.1C) and HG (p=0.5309; Fig. 4.1D) conditions.
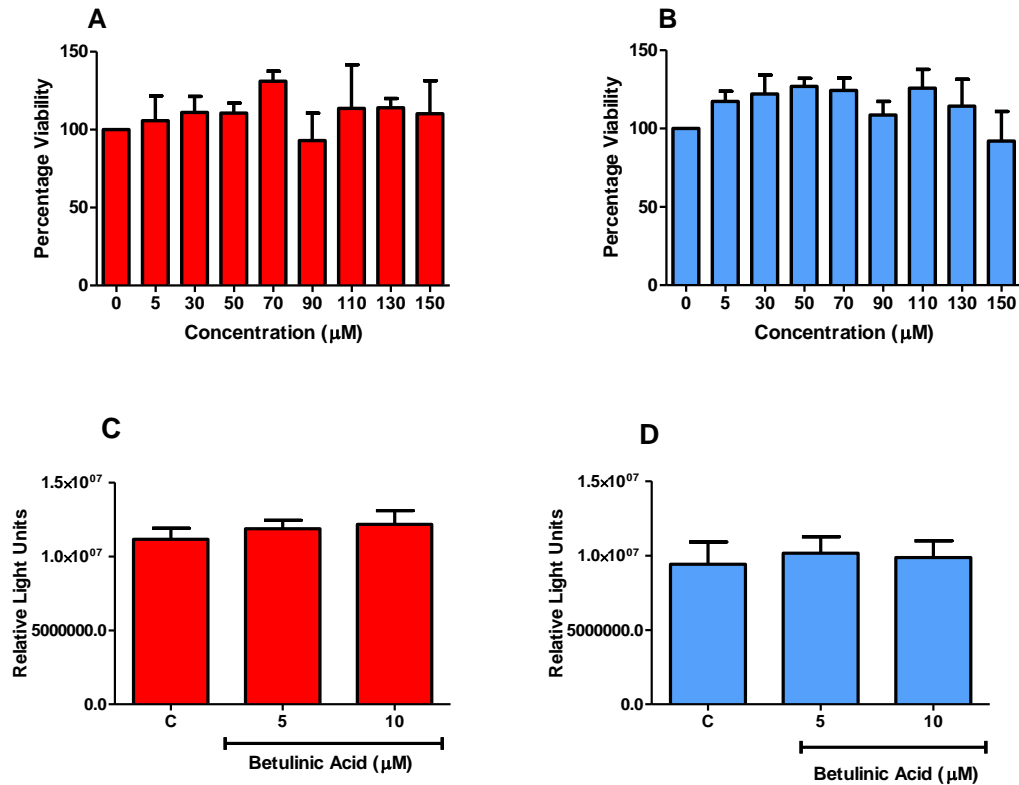
Figure 4.1: MTT assay demonstrating cell viability and constant levels of metabolic activity in both A) normoglycaemic and B) hyperglycaemic media. ATP assay further demonstrating this at given concentrations in both C) normoglycaemic and D) hyperglycaemic media. #p<0.05; ##p<0.001; ###p<0.0001 relative to negative controls.

NORMOGLYCAEMIC CONDITIONS

HYPERGLYCAEMIC CONDITIONS

4.2) Betulinic acid reduces hyperglycaemic-induced toxicity.

Hyperglycaemic conditions induce ROS, which can lead to peroxidation of the cell membrane (Collins et al., 2018). An LDH assay was run to ensure that BA exerted no cytotoxic effect on the cell line, and to assess if BA could combat the HG-induced toxicity.

BA reduced HG-induced LDH levels optimally at 5µM (p<0.0001) and less so at 10µM (p<0.05), in comparison to HG negative control (Fig. 4.2B). Additionally, NG conditions showed no significant change in the LDH levels (Fig. 4.2A).

Thus, BA reduced HG-induced membrane damage. It is noteworthy that LDH levels were most significantly reduced at 5µM in HG conditions.
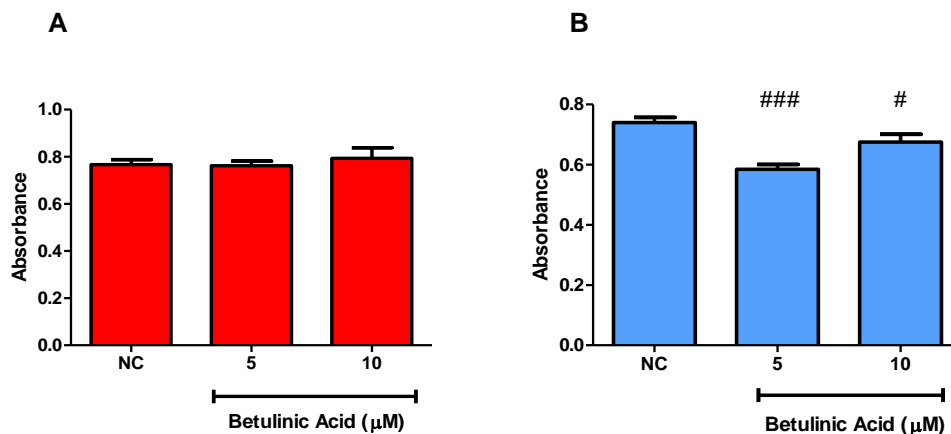
Figure 4.2: LDH quantified in the supernatants, in both A) normoglycaemic (p= 0,1390) and B) hyperglycaemic (p< 0.0001) conditions. #p<0.05; ##p<0.001; ###p<0.0001 relative to negative controls.

NORMOGLYCAEMIC CONDITIONS
HYPERGLYCAEMIC CONDITIONS

4.3) Betulinic acid enhances insulin receptor phosphorylation

To preliminarily assess BA's anti-hyperglycaemic effects on the HepG2 cell line at these specific concentrations, we tested a previously researched anti-diabetic scenario.

Betulinic acid is known to enhance phosphorylation of the β subunit of the insulin receptor (Castellano et al., 2013). Recent studies, however, proved that HG conditions glycate the insulin receptor thus inhibiting binding (Rhinesmith et al., 2017). A PY20 western blot was performed to verify tyrosine residue phosphorylation.

Betulinic acid promoted phosphorylation of IR at 5μM and 10μM ($p<0.0001$) under NG conditions (Fig. 4.3A) Under HG conditions (Fig. 4.3B), BA significantly upregulated IRβ phosphorylation at 5μM ($p<0.05$). Interestingly, similar phosphorylation was observed between the insulin control and 5μM HG conditions.

Thus, it was established that, despite possible HG-induced glycation of the insulin receptor, BA, nonetheless, promoted IR phosphorylation at 5μM, similar to that of insulin.

Figure 4.3: PY20 western blot demonstrating phosphorylation of IRβ in A) normoglycaemic conditions (p=0.0004) and in B) hyperglycaemic (p< 0.0001) conditions. #p<0.05; ##p<0.001; ###p<0.0001 relative to negative controls.

4.4) Betulinic acid downregulates reactive oxygen species and its biomarkers

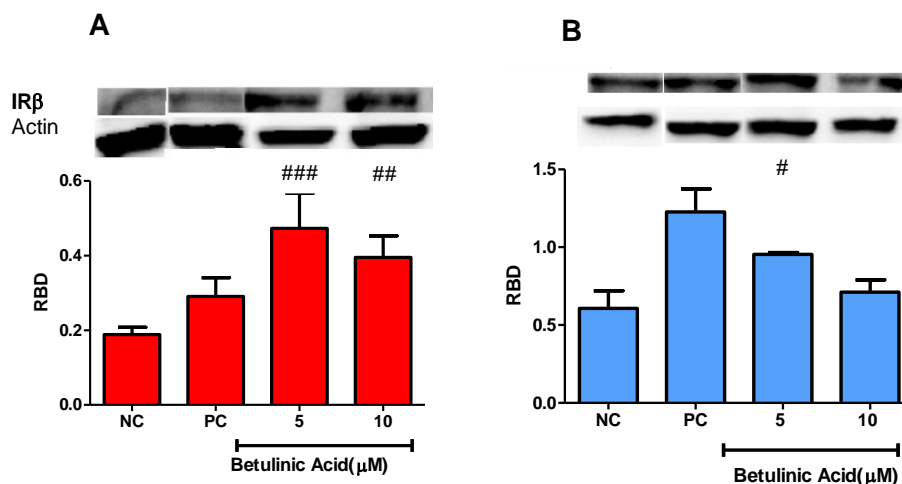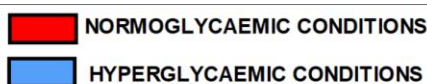Hyperglycaemic conditions promote ROS formation, with consequent lipid peroxidation and protein carbonylation (Nishikawa et al., 2000). The analysis of ROS utilized the DCF assay for endogenous ROS quantification, as well as the PCA and TBARs assay to measure protein carbonyls and lipid peroxides.

Betulinic acid treatment reduced ROS levels in both HG (Fig. 4.4B) and NG (Fig. 4.4A) conditions, at both 5µM and 10µM concentrations ($p < 0.0001$). This peculiar result suggests that BA reduced ROS even in the absence of HG induced OS.

MDA is a lipid peroxidation by-product and high levels are associated with HG-induced OS (Asmat et al., 2016). Expectedly, BA induced a more pronounced ($p < 0.0001$) downregulation of MDA at both concentrations of BA (Fig. 4.4D) in HG conditions. Normoglycaemic MDA levels demonstrated a subtle downregulation at 5µM ($p < 0.001$) and 10µM ($p < 0.05$) of BA (Fig. 4.4C).

Lipid peroxidation by-products are able to post-translationally modify proteins, resulting in irreversible carbonylation (Hauck and Bernlohr, 2016). Further analysis via PCA revealed that BA treatment significantly ($p < 0.0001$) downregulated carbonyl levels in HG media (Fig. 4.4F). Under NG conditions (Fig. 4.4E), BA decreased protein carbonyl levels less significantly ($p < 0.001$).

Taken together, these results suggest that BA downregulates ROS independent of OS-status, however BA understandably reduces OS markers (lipid peroxides and protein carbonyls) more in the toxic HG state, where they are more prominent.
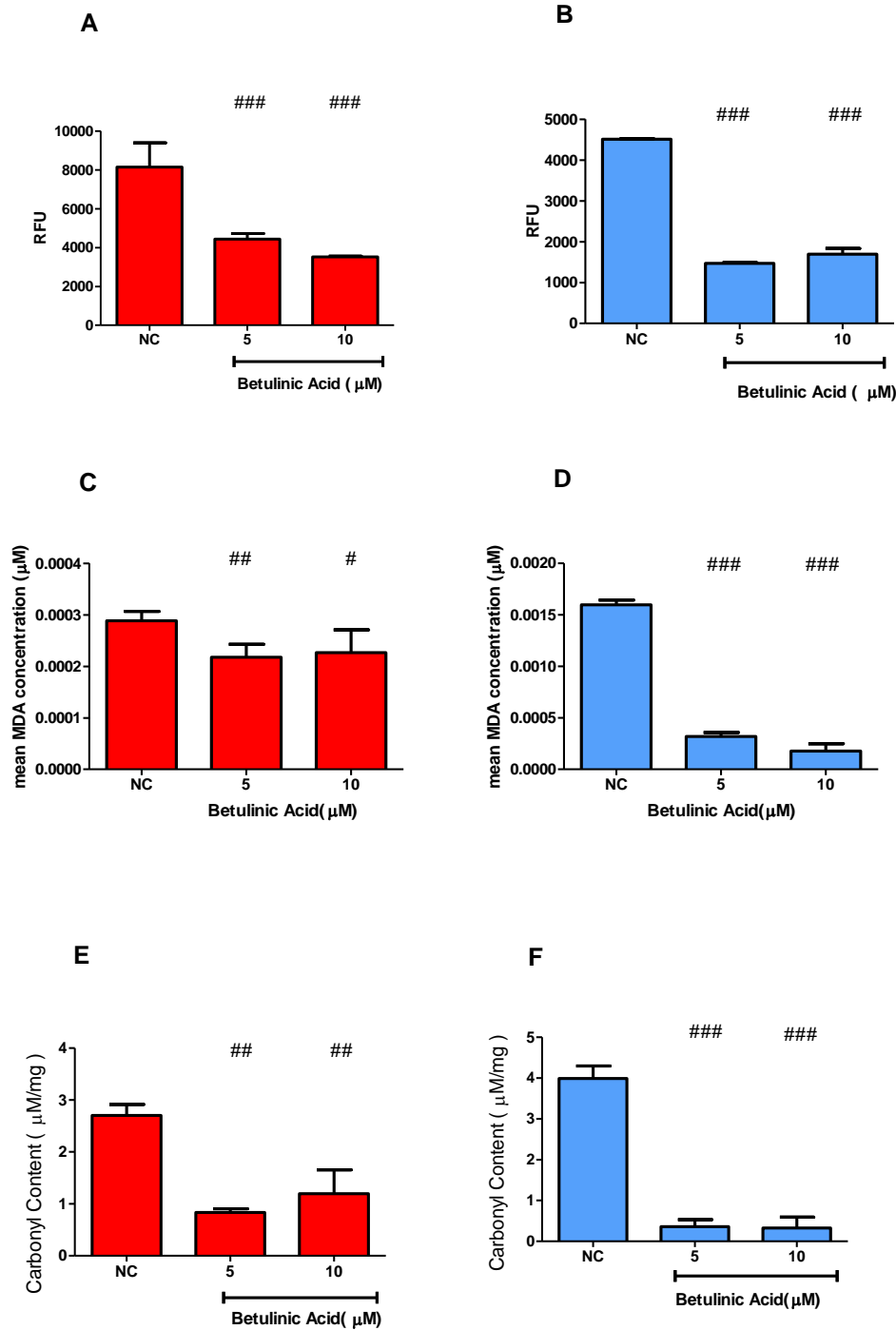
Figure 4.4: The H₂DCF-DA assay quantifying intracellular ROS levels in response to BA administration in a A) normoglycaemic (p<0.0001) and B) hyperglycaemic (p<0.0001) model. Lipid peroxidation by-product, MDA, quantified via a TBARS assay in both C) normoglycaemic (p=0.0037) and D) hyperglycaemic (p<0.0001) media. PCA assay quantifying protein carbonyl concentrations as an effect of ROS and lipid peroxidation, in E) normoglycaemic (p<0.0001) and F) hyperglycaemic (p<0.0001) media. #p<0.05; ##p<0.001; ###p<0.0001 relative to negative controls.
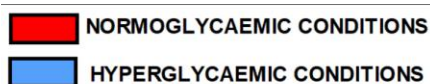
4.5) Betulinic acid promotes PPARγ/NRF2 positive feedback loop in hyperglycaemic conditions.

Multiple studies have linked triterpenes and specifically BA, to AO-related transcription factors PPARγ and NRF2 (Loboda et al., 2012, Brusotti et al., 2017). These transcription factors transcribe for a variety of AOs. Both transcription factors additionally transcribe for each other, by generating a positive feedback loop, and thus potentiate the AO response (Lee, 2017).

Betulinic acid treatment potentiated the expression of PPARγ, in both conditions and both concentrations. Under NG conditions (Fig. 4.5A), BA upregulated PPARγ ($p < 0.05$) in HepG2 cells; whilst under HG conditions (Fig. 4.5B) PPARγ was more significantly upregulated at 10µM BA ($p < 0.001$) and optimally at 5µM BA ($p < 0.0001$).

The enhanced PPARγ levels in HG state coincides with its feedback partner, NRF2. BA potentiated NRF2 protein expression to maximum significance ($p < 0.0001$) at both concentrations in HG conditions (Fig. 4.5D). BA also upregulated NRF2 mRNA levels in HG conditions (Fig. 4.5F) at 10µM ($p < 0.05$) and optimally at 5µM ($p < 0.0001$). BA did not upregulated NRF2 gene (Fig. 4.5E) and protein (Fig. 4.5C) in NG conditions.

Altogether, BA potentiated the AO-associated PPARγ/NRF2 feedback loop, at an optimal concentration of 5µM BA in HG conditions.
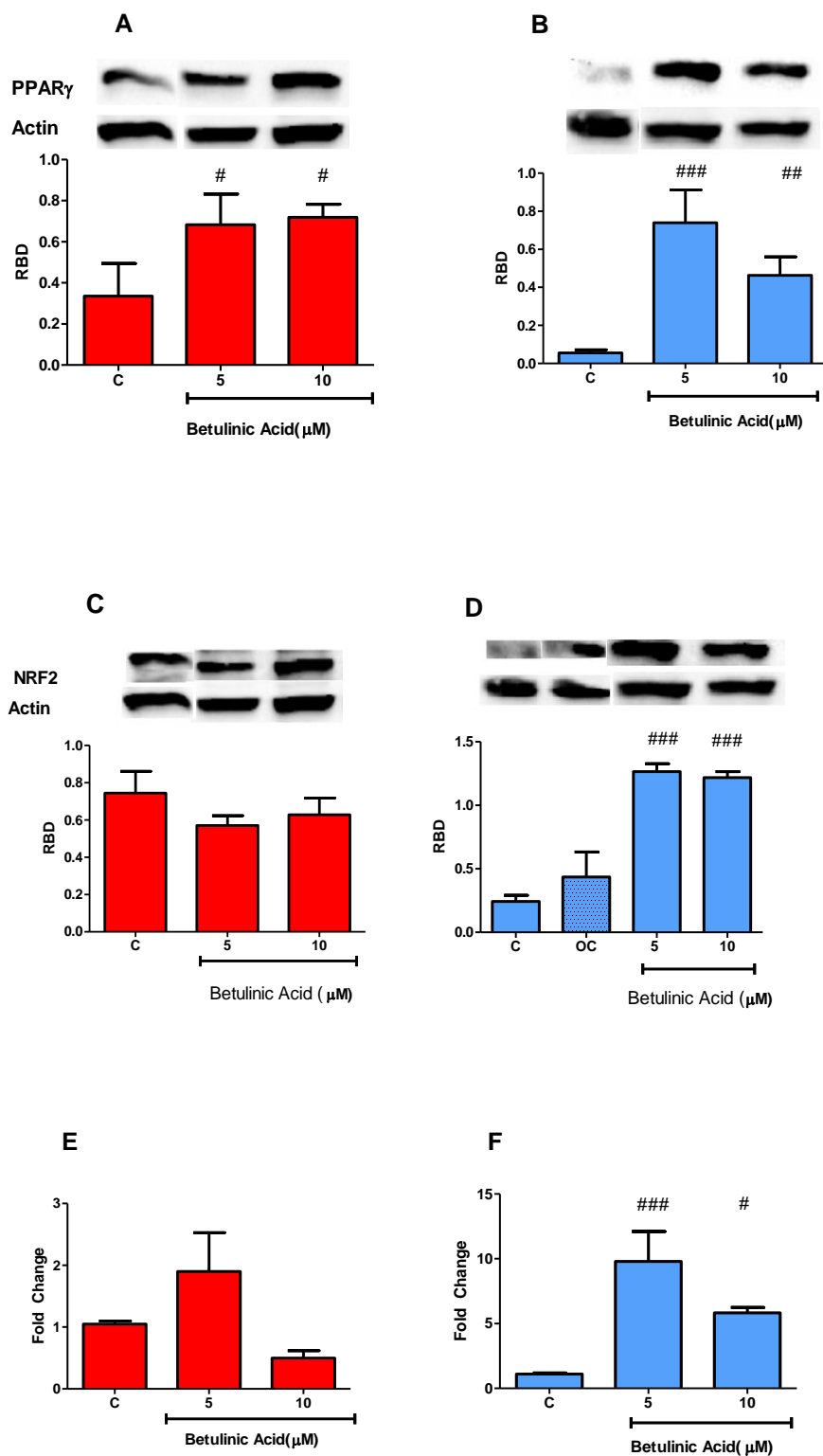
Figure 4.5: PPARγ protein expression in A) normoglycaemic (p=0.0047) and B) hyperglycaemic (p<0.0001) conditions. Protein expression of total NRF2 in C) normoglycaemic (p=0.0868) and D) hyperglycaemic (p<0.0001) conditions, along with mRNA levels of NRF2 in E) normoglycaemic (p=0.0019) and F) hyperglycaemic (p=0.0007) conditions. #p<0.05; ##p<0.001; ###p<0.0001 relative to negative controls.

NORMOGLYCAEMIC CONDITIONS

HYPERGLYCAEMIC CONDITIONS

4.6) Epigenetic control of NRF's phosphorylation

Additionally, we explore miR124 as an epigenetic link between PPARγ and phosphorylation of NRF2. MiR124 is induced by PPARγ, and exerts its effect indirectly via signal pathways, phosphorylating NRF2 (Shu and Zhang, 2019, Wang et al., 2017). Phosphorylation of NRF2 results in activation and nuclear translocation. Multiple studies have also suggested that triterpenes phosphorylate NRF2 directly for AO actions (Loboda et al., 2012).

Betulinic acid increased expression of miR124 (qPCR), at 5μM (p<0.05) in HG conditions (Fig. 4.6B). Furthermore, protein expression of phosphorylated NRF2 was also upregulated at both BA treatments (p<0.0001) in HG conditions (Fig. 4.6D). Betulinic acid did not upregulate miR124 (Fig. 4.6A) and pNRF2 (Fig. 4.6C) levels in NG media.

Betulinic acid indirectly modulates miR124, which promotes phosphorylation of NRF2 at 5μM HG conditions. Additionally, BA may have a direct effect on NRF2 phosphorylation in HG conditions at both concentrations.
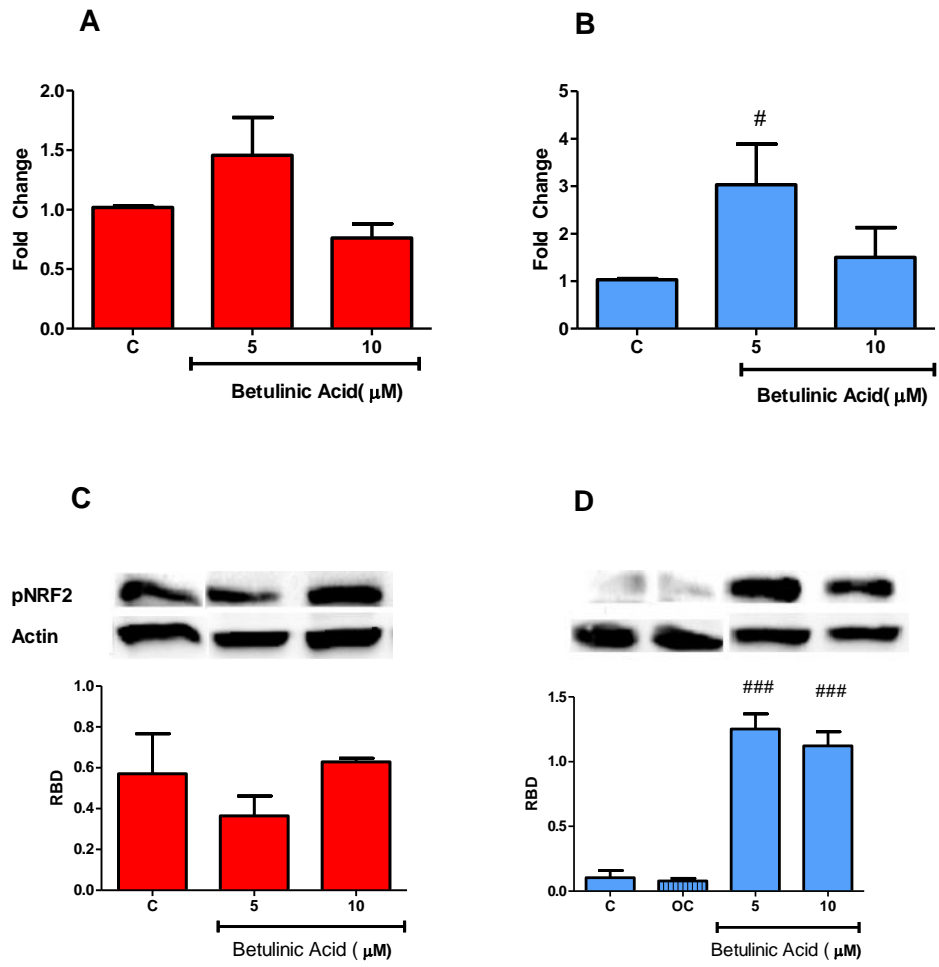
Figure 4.6: qPCR for miRNA124 in A) normoglycaemic (p=0.0866) and B) hyperglycaemic (p=0.0093) conditions along with protein expression of pNRF2 in C) normoglycaemic (p=0.0116) and D) hyperglycaemic (p< 0.0001) conditions. #p<0.05; ##p<0.001; ###p<0.0001 relative to negative controls.
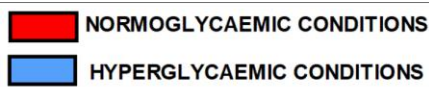
4.7) Betulinic acid upregulates the antioxidant mechanism in hyperglycaemic conditions.

Enhanced PPARγ/NRF2 expression potentiates the AO response. Both transcription factors transcribe for CAT and SOD2, with NRF2 additionally transcribing for GPx1. SOD2 functions to detoxify superoxides into H_2O_2. This H_2O_2 is reduced into harmless H_2O via two enzymes, CAT and GPx1. Furthermore, GPx1 utilises a non-enzymatic cofactor known as GSH (Noori, 2012).

The optimal concentration of 5µM BA (HG conditions; Fig. 4.7B) upregulated SOD2 protein expression ($p < 0.0001$) and CAT ($p < 0.05$) expression (Fig. 4.7D). BA treatment in NG conditions had no effect on both these antioxidants (Fig. 4.7A; Fig. 4.7C).

Further, BA upregulated the GPx1/GSH mechanism in the HG state. BA significantly upregulated *GPx1* mRNA levels ($p < 0.0001$) at both concentrations in HG media (Fig. 4.7F). Luminometry showed increased GSH levels at 5µM ($p < 0.001$) and at 10µM ($p < 0.05$) in HG conditions (Fig. 4.7H).

Taken together, the 5µM BA optimal concentration enhanced expression of the SOD2/CAT/GPx1/GSH AO mechanism to combat ROS in HG conditions.
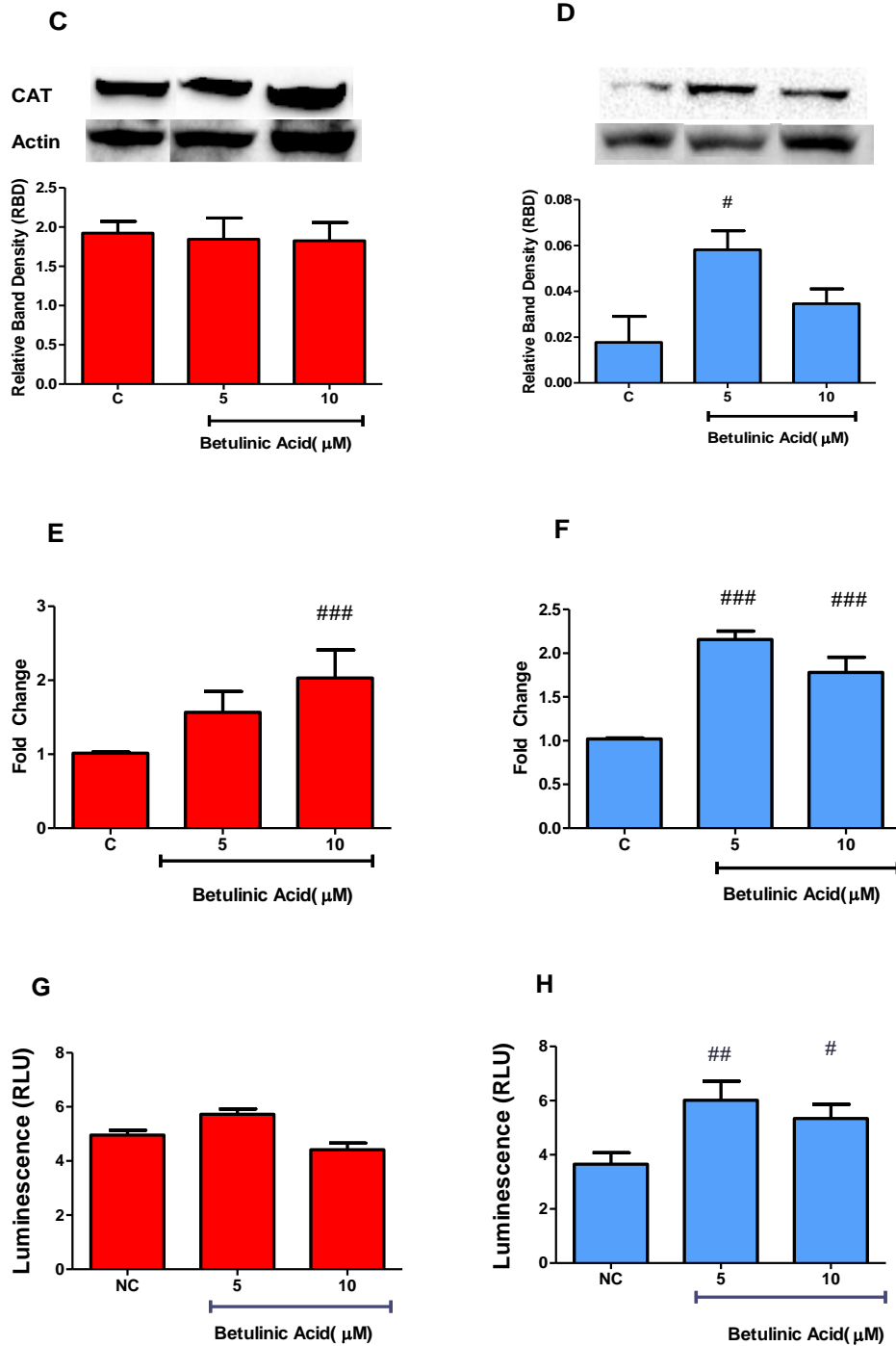
Figure 4.7: SOD2 protein levels in A) normoglycaemic (p<0.0001) and B) hyperglycaemic (p<0.0001) conditions. CAT protein levels in C) normoglycaemic (p= 0,0001) and D) hyperglycaemic (p=0.0003) conditions. GPx1 mRNA levels in E) normoglycaemic (p= 0,0028) and F) hyperglycaemic (P<0.0001) conditions. Luminometric quantification of reduced glutathione levels in G) normoglycaemic (p=0.0010) and H) hyperglycaemic (p=0.0003) conditions. [#]p<0.05; [##]p<0.001; [###]p<0.0001 relative to negative controls.

4.8) Betulinic acid modulates UCP2

PPARγ transcribes for UCP2, which is upregulated in the HG condition, and combats ROS (Pierelli et al., 2017, Sosa-Gutiérrez et al., 2018, Liu et al., 2013).

UCP2 protein levels were upregulated in HG media (Fig. 4.8B) at 5µM BA ($p < 0.05$) treatment. Conversely, BA, in the absence of OS, in NG media (Fig. 4.8A), downregulated UCP2 at both 5µM ($p < 0.0001$) and 10µM ($p < 0.001$). This suggests differential regulation of UCP2 by BA based on the glycaemic and OS status of the cells.
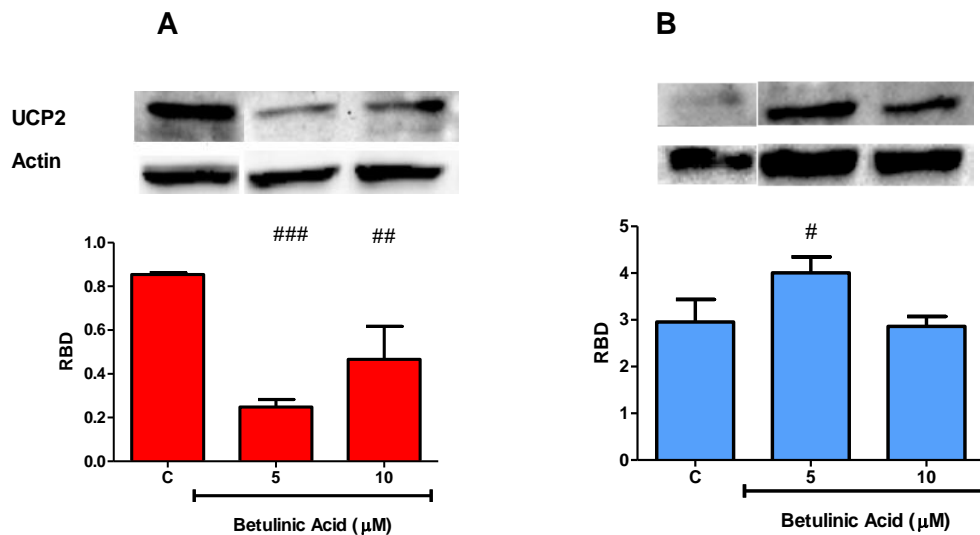
Figure 4.8: Differential regulation of UCP2 protein expression by BA in A) normoglycaemic ($p < 0.0001$) and B) hyperglycaemic ($p < 0.0001$) conditions. #$p < 0.05$; ##$p < 0.001$; ###$p < 0.0001$ relative to negative controls.
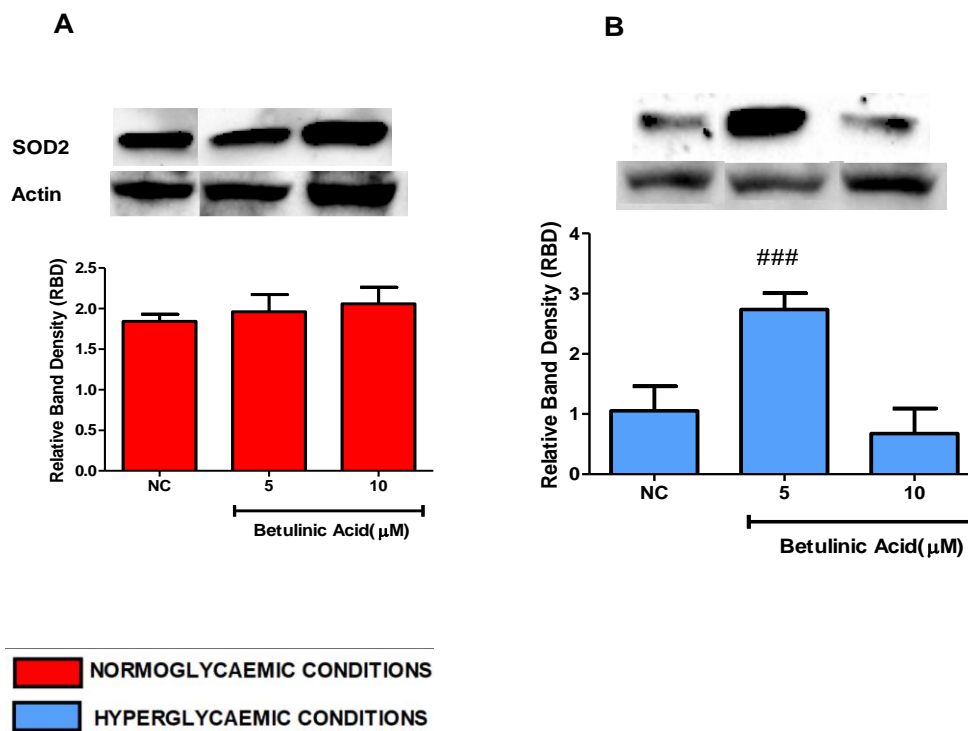

NORMOGLYCAEMIC CONDITIONS

HYPERGLYCAEMIC CONDITIONS

4.9) Betulinic acid differentially regulates NFκB

Transcription factor NFκB promotes ROS-induced inflammation and ROS production (Sharma et al., 2018, Morgan and Liu, 2011). Additionally, NFκB is involved in a wide range of cellular responses via gene induction (Zhang et al., 2017). Many proteins and genes in this study including PPARγ, PGC1α, miR124 and NRF2 have been linked to repression of NFκB, directly targeting NFκB p65 in inflammatory conditions (Wahli, 2008, Wang et al., 2017, Eisele et al., 2015, Wardyn et al., 2015). It was hypothesized that increased expression of these proteins in HG state would downregulate NFκB.

Under HG conditions (Fig. 4.9B), BA markedly downregulated NFκB at both 5µM and 10 µM concentrations (p<0.0001). In contrast, upregulations of NFκB by BA at 5µM (p<0.001) and 10µM (p<0.0001) in non-inflammatory NG conditions suggest that BA differentially modulates NFκB to suit circumstances (Fig. 4.9A).

Thus, BA inhibits NFκB in the HG state, to prevent ROS-induced inflammation and OS.
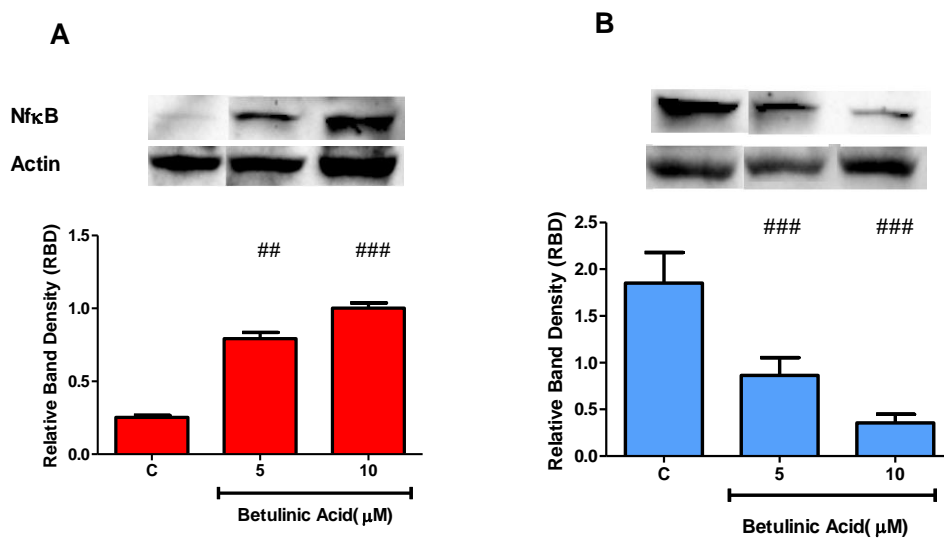
Figure 4.9: Protein expression of NFκB in A) normoglycaemic (p<0.0001) and B) hyperglycaemic (p<0.0001) conditions #p<0.05; ##p<0.001; ###p<0.0001 relative to negative controls.

4.10) Betulinic acid potentiates the SIRT3/PGC1α positive feedback loop

SIRT3 is a mitochondrial deacetylase, which activates various AO-related proteins, including SOD2 (Chen et al., 2011). NRF2, with the aid of its co-factor PGC1α, transcribes for SIRT3 (Song et al., 2017). Additionally, PGC1α forms a positive feedback loop with SIRT3 (Kong et al., 2010). Furthermore, PGC1α is also involved in many aspects of AO regulation, responsible for upregulations in CAT, SOD2, and UCP2 amongst others (Valle et al., 2005).

Betulinic acid elevated SIRT3 protein levels ($p<0.0001$) at both 5µM and 10 µM concentrations in HG conditions (Fig. 4.10B). Further qPCR revealed concomitant upregulations of *SIRT3* mRNA levels at both 5µM ($p<0.001$) and 10µM ($p<0.05$) BA in HG conditions (Fig. 4.10D).

PGC1α plays a role in AO induction. PGC1α protein levels were significantly upregulated ($p<0.05$) by 5µM BA HG conditions (Fig. 4.10F). Additionally, *PGC1α* mRNA levels were upregulated at both concentrations of BA in HG (Fig. 4.10H) conditions ($p<0.0001$).

In NG conditions, both *PGC1α* at 10µM ($p<0.0001$) and *SIRT3* ($p<0.05$) mRNA levels were upregulated (Fig. 4.10C; Fig. 4.10G), but their protein expressions were unchanged.

Thus, concomitant upregulations at 5µM BA in HG conditions, between both SIRT3 and PGC1α, at an mRNA and protein level suggests that BA potentiates their positive feedback loop and validates the enhanced expression of many AOs.
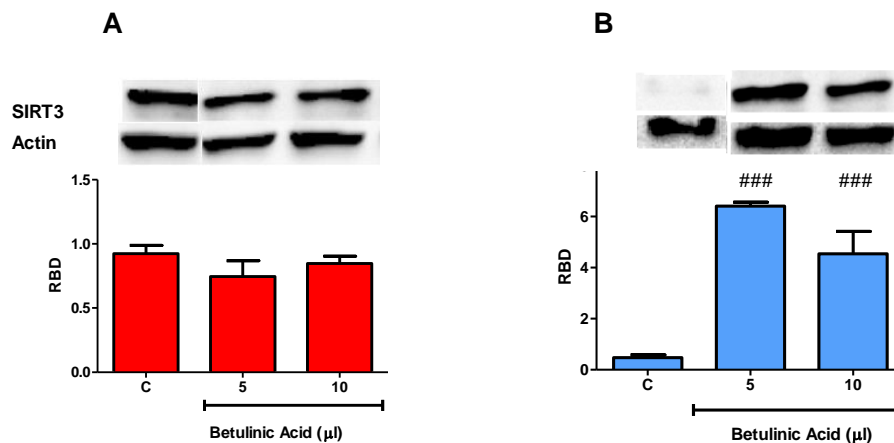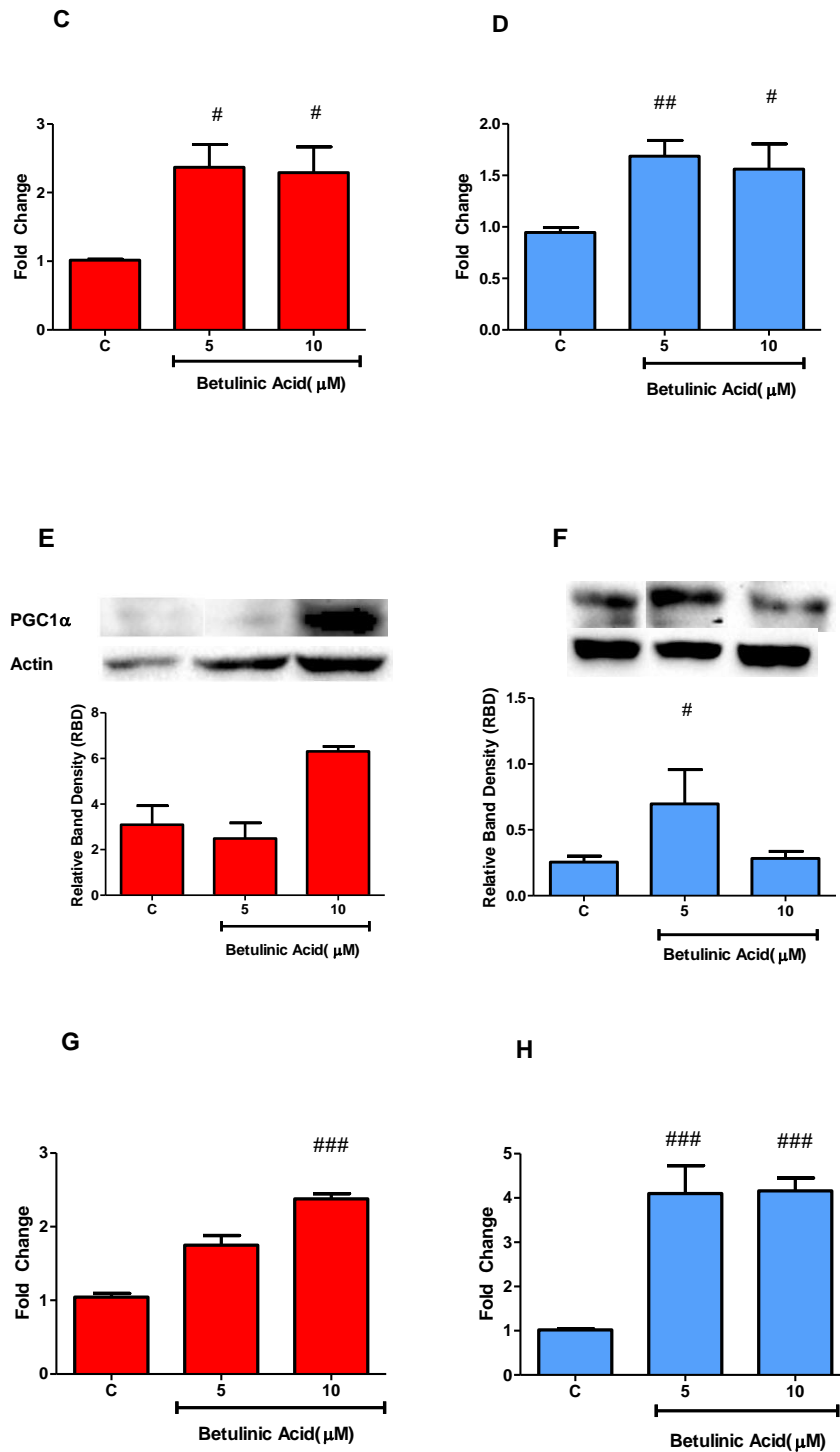
Figure 4.10 SIRT3 protein expression in A) normoglycaemic (p=0.1120) and B) hyperglycaemic(p<0.0001) conditions. SIRT3 mRNA levels in C) normoglycaemic (p<0.0001) and D) hyperglycaemic conditions (p<0.0001). PGC1α protein levels in E) normoglycaemic (p=0.0002) and F) hyperglycaemic (p=0.0025) media. PGC1α mRNA levels in G) normoglycaemic (p=0.0005) and H) hyperglycaemic (p<0.0001) media. #p<0.05; ##p<0.001; ###p<0.0001 relative to negative controls.

NORMOGLYCAEMIC CONDITIONS
HYPERGLYCAEMIC CONDITIONS

4.11) Betulinic acid promotes intramitochondrial degradation of oxidized proteins.

An extension of SIRT3's activities include its proven de-acetylation of LONP1 (Gibellini et al., 2014). LONP1's proteolytic digestive capabilities are vital to lower oxidized protein levels (Ngo et al., 2013).

At the optimal 5μM BA concentration (HG conditions)(Fig. 4.11B), LONP1 protein expression was significantly upregulated (p<0.05). Additionally, LONP1 levels in NG (Fig. 4.11A) conditions demonstrated upregulation at 10μM BA (p<0.05).

Thus, BA indirectly promoted LONP1 at an optimal concentration of 5μM BA in HG conditions to degrade oxidized proteins.

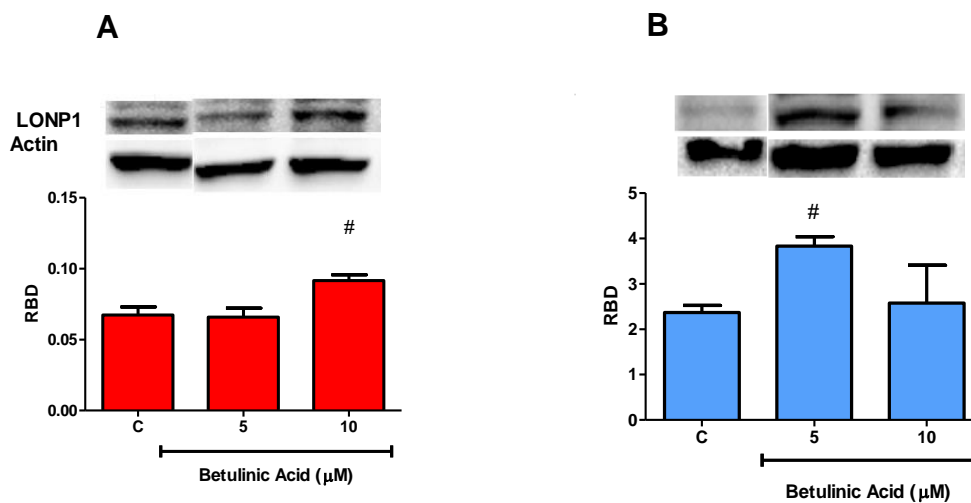*Figure 4.11: LONP1 protein expression in A) normoglycaemic (p=0.0005) and B) hyperglycaemic media (p<0.0001) #p<0.05; ##p<0.001; ###p<0.0001 relative to negative controls.*

NORMOGLYCAEMIC CONDITIONS
HYPERGLYCAEMIC CONDITIONS

CHAPTER 5: DISCUSSION

Oxidative stress, a state of redox imbalance favouring pro-oxidants, is a common pathological mechanism observed in diabetic complications (Asmat et al., 2016). Re-establishing the AO response may help alleviate OS, thus reducing the risk of diabetic complications. In this study, BA's established AO properties were extrapolated to the HG state, a good mimic of T2DM. It is of note, however, that despite its attempt to mimic the diabetic state, an *in vitro* model does, to some extent, eliminate normal human cellular and metabolic interactions from the equation.

Loboda et al. (2012) previously concluded that triterpenoids are concentration dependant, displaying anticancer activities at high concentrations, and anti-inflammatory and cytoprotective activities at low concentrations (Loboda et al., 2012). Betulinic acid's anticancer ability has been extensively researched. Fu et al. (2005) and Santos et al. (2009) established that BA exerts toxicity at concentrations ranging between 21μm and 36μm (Moghaddam et al., 2012, Fu et al., 2005, Santos et al., 2009). The MTT data in this study demonstrated no toxicity between 5μM and 150μM BA concentration (Fig. 4.1A; Fig. 4.1B). Thus, concentrations 5μM and 10μM were chosen for study, within the MTT range, but below the previously reported toxic levels. An ATP cell viability assay confirmed that both BA concentrations were non-toxic (Fig. 4.1C; Fig. 4.1D).

Although commonly regarded as viability assays, the MTT and ATP assays alternatively reveal complementary information with regards to the metabolic state of the cell. MTT cofactor, NADH is a substrate for the ETC, and a by-product of the TCA cycle, which is an important process linking lipid, protein and glucose metabolism (Riss et al., 2016). Furthermore, complex 2 of the ETC, succinate dehydrogenase, is the principle enzyme required for MTT conversion (Morgan, 1998). The ETC is coupled to OXPHOS, an ATP generator. Therefore, the MTT assay is a good indicator of the status of the redox potential of the cell. Constant MTT and ATP readings observed in this study alluded to BA being involved in the maintenance of a stable intramitochondrial metabolic environment (Fig. 4.1).

Due to BA's implications in anti-cancer activity, an LDH assay was warranted to ensure that BA did not exert any membrane damage (Zhang et al., 2016, Sánchez-Quesada et al., 2013). Additionally, HG induced OS results in the peroxidation of lipid-membranes, which, we hypothesized, may be prevented by the activity of BA (Cheeseman, 1993). In the HG model, BA downregulated levels of LDH (Fig. 4.2B). The NG model showed no difference (Fig. 4.2A). Thus, the results of the assay can be considered a two-fold preliminary indication to both BA's lack of toxicity, and possible presence of cytoprotective capacity to ROS-induced membrane damage.

Betulinic acid's anti-diabetic potential is well established (Brusotti et al., 2017, Castro et al., 2014, Castellano et al., 2013). A particular mechanism involves BA's phosphorylation of the β subunit of the IR (Castellano et al., 2013). Rhinesmith et al. (2017), however, concluded that a method of insulin

resistance involves HG conditions directly glycating the receptor, inhibiting its binding (Rhinesmith et al., 2017). To ensure that BA at concentrations of 5µM and 10µM had a direct effect on the HepG2 cell line, we tested this previously researched anti-diabetic scenario. Western blots of IRβ confirmed BA's phosphorylation of IRβ in NG conditions at both 5µM and 10µM BA, and also in HG conditions at 5µM (Fig. 4.3). Betulinic acid phosphorylates the IR in HG conditions to a lesser extent, due to possible glycation of IR. This 5µM BA HG concentration, however, demonstrated no significance relative to the insulin control (Fig. 4.3B), implying that BA phosphorylates the IR to a similar degree as insulin in HG conditions.

Phosphorylation of IR promotes insulin signalling pathways, resulting in GLUT4 membrane localization and resultant glucose uptake and disposal (Aronoff et al., 2004). Additionally, both PGC1α and PPARγ are proven to promote GLUT4 glucose uptake (Wu et al., 1998, Leick et al., 2010). Significant upregulations of both these proteins at 5µM in HG conditions, alongside IRβ, implies increased glucose uptake (Fig. 4.3B; Fig. 4.5B; Fig. 4.10F).

The HG state brings with it many deleterious effects, including excess superoxide production (Kaneto et al., 2010). Betulinic acid, however, is hypothesized to counterbalance this. Numerous studies have proven BA's ability to reduce ROS levels, however this has not been tested in response to HG-induced ROS (Szuster-Ciesielska and Kandefer-Szerszeñ, 2005). This current study reveals that BA significantly downregulated ROS in response to HG-induced stress, at both concentrations (Fig. 4.4B). Intriguingly, BA also downregulated ROS in the absence of OS, in the NG state (Fig. 4.4A).

The ROS damage to macromolecules in the HG state is associated with high levels of lipid peroxidation (Asmat et al., 2016). Lipid peroxidation levels were downregulated by BA, in both states, at both concentrations (Fig. 4.4C; Fig. 4.4D). Understandably, statistical analysis revealed a more significant MDA reduction in the HG state, by BA (Fig. 4.4D). Of further significance, is the ability of lipid peroxidation to directly attack cell membranes (Cheeseman, 1993). A significant decrease in MDA levels in HG conditions at 5µM and 10µM BA (Fig. 4.4D) coincided with a decrease in LDH levels (Fig. 4.2B), implying that BA reduced MDA-induced membrane damage, and subsequent LDH release.

MDA, the by-product of lipid peroxidation, post-translationally carbonylates proteins, resulting in irreversible damage (Hauck and Bernlohr, 2016). Betulinic acid's reduction of MDA levels understandably lead to concomitant reduction of protein carbonylation levels. This reduction was, likewise to MDA levels, more pronounced in the HG state (Fig. 4.4E; Fig. 4.4F).

HepG2 cells can be used to detect changes in toxicity at different glucose levels (Kamalian et al., 2015). The HG state is associated with increased OS biomarkers (MDA and carbonyl levels). Consequently, we hypothesize that BA would reduce MDA and protein carbonylation levels more

substantially in HG conditions. In line with this, both OS markers were more significantly reduced in the HG state, in response to BA treatment (Fig. 4.4D; Fig. 4.4F).

Although MDA and protein carbonyl levels are regarded as biomarkers of OS, ROS are implicated in many other situations. Basal ROS levels are required in the cell as signalling molecules, involved in gene transcription and protein synthesis etc. (Kaneto et al., 2010).

In NG media, BA reduced ROS significantly (Fig. 4.4A), but did not reduce OS biomarkers (MDA and protein carbonyls) as significantly (Fig. 4.4C; Fig. 4.4E). This further reduction of ROS beyond the baseline, however, may not be particularly deleterious as evidenced by constant TCA, ETC and OXPHOS readings present in NG media, implying stable energy levels (Fig. 4.1A; Fig. 4.1C). The NG state is not associated with OS, hence BA did not reduce OS markers as significantly in this state.

Taken together, these results indicate that BA significantly reduced ROS and OS biomarkers, thus combatting the highly oxidative state associated with hyperglycaemia.

The initial part of this study proved BA's lack of toxicity and anti-ROS activities. We then sought to discern the molecular mechanisms behind BA's anti-ROS action. Lee (2017) proposed a positive feedback model in which PPARγ and NRF2 reciprocally transcribe for each other. This model not only results in potentiation of the two transcription factors, but of a range of other AOs for which they transcribe (Lee, 2017). We hence proceeded to sequentially assess PPARγ and NRF2 levels in response to treatment with BA.

PPARγ upregulation has been widely proven in many HG studies. Additionally, BA binds tightly to PPARγ (Brusotti et al., 2017). We thus hypothesized PPARγ as the master regulator of BA's AO response to HG-induced OS. The PPARγ complex binds to specific PPREs on the promoter region of the common AO related genes, e.g. SOD2, CAT, UCP2, NRF2, activating their transcription (Lee, 2017, Kvandova et al., 2016, Pierelli et al., 2017, Polvani et al., 2012, Girnun et al., 2002). This current study revealed that BA upregulated PPARγ in both conditions at both concentrations, implying interaction (Fig. 4.5A; Fig. 4.5B). Furthermore, BA upregulated PPARγ more significantly in HG conditions at 5µM BA (Fig. 4.5B). This optimal upregulation coincided with upregulations in the above-mentioned AO-related proteins, implying that BA mounted an AO-response through PPARγ to HG stress (Fig. 4.7B; Fig. 4.7D; Fig. 4.8B; Fig. 4.5D).

Beyond the above proposed positive feedback loop, triterpenes also exert a direct effect on the activity of NRF2. Loboda et al. 2012 stated that triterpenoids can activate NRF2 indirectly via signal pathway phosphorylation, or via oxidative modification of SH groups (Loboda et al., 2012). Once phosphorylated, NRF2 is translocated to the nucleus to exert its AO transcription activity (Loboda et al., 2012). Evaluation of our results revealed that both BA treatments of 5µM and 10µM upregulated pNRF2 to maximum significance in response to HG stress (Fig. 4.6D).

NRF2 exerts its transcription of many AO proteins via direct binding to the ARE on the promoter region of their genes. Multiple lines of research revealed presence of ARE complex on many AO-related genes, e.g. PPARγ, SOD2, CAT, SIRT3, GPx1 (Lee, 2017, Cho et al., 2005, Cho et al., 2010, Jeong et al., 2016, Jin et al., 2016, Song et al., 2017). In keeping with this, our study demonstrated concomitant upregulations of all of the above proteins and genes, alongside NRF2 gene and protein expression (Fig. 4.5B; Fig. 4.5D; Fig. 4.5F; Fig. 4.7B; Fig. 4.7D; Fig. 4.7F; Fig. 4.10B; Fig. 4.10D). We can thus identify NRF2 as one of the factors involved in BA's heightening of the AO response to HG-induced stress.

An osmotic control of mannitol was included in the western blots of proteins pNRF2, localized to the nucleus, and total NRF2, localised in both the cytoplasm and nucleus. NRF2 is considered a master regulator and hence its levels determine the corresponding levels of many AO and AO-related proteins in this study. Thus, the inert sugar, mannitol, was added as a control to ensure that the effects in HG were rightly attributed to BA action, and not due to changed pressure in the cell. No significance was found between HG control and osmotic control in both NRF2 states, validating this result (Fig. 4.5D; Fig. 4.6D).

Taken together, our study serves as confirmatory evidence of this positive feedback loop phenomenon being enhanced by BA to combat HG induced stress at an optimum concentration of 5μM, evidenced by concomitant upregulations of NRF2 and PPARγ as well as the AOs for which they transcribe.

The link between NRF2 and PPARγ can be further explored via epigenetics. The apt miR124 is transcribed for by PPARγ, and exerts AO actions via indirect NRF2 phosphorylation, as well as anti-inflammatory effects via NFκB repression (Shu and Zhang, 2019, Wang et al., 2017). Upregulations of PPARγ, pNRF2 and miR124 coincided with a downregulation of NFκB at 5μM BA in HG conditions, suggesting miR124 activity in this study (Fig. 4.5B; Fig. 4.6B; Fig. 4.6D; Fig. 4.9B). This further strengthens the link between NRF2 and PPARγ, and is indicative of miR124 reducing ROS-induced inflammation and enhancing AO transcription.

The AO nature of BA has previously been explored with Yi et al., (2014) concluding that, in mice, BA stimulates the AO system (SOD2, GPx1, GSH), protecting against hepatoxicity and lowering MDA levels (Yi et al., 2014). SOD2 protein is responsible for detoxifying superoxide radicals into peroxides, to be consequently reduced to water by both CAT and the GSH mechanism (Noori, 2012). This current study confirmed that BA exerts an AO response to HG-stress, by demonstrating significant upregulations of both SOD2 and CAT at 5μM BA (Fig. 4.7B; Fig. 4.7D). These upregulations coincided with a downregulation of ROS and OS biomarkers, implying that these proteins successfully exerted their AO-activity (Fig. 4.4B; Fig. 4.4D; Fig. 4.4F).

The alternate peroxide reduction method involving GPx1 and GSH was also analysed. Upon HG stimulation, BA significantly upregulated GPx1 mRNA levels (Fig. 4.7F). Coinciding with this, BA

further upregulated GSH levels in HG media, at a prime concentration of 5µM BA (Fig. 4.7H). These results suggest that BA upregulated the GpX1/GSH AO mechanism, to reduce HG-induced peroxides to H_2O.

For the most part, BA did not upregulate AO activities in NG media. However, BA upregulated GPx1 mRNA levels in NG media at a concentration of 10µM BA (Fig. 4.7E). Lu et al. (2015) uncovered that, in unstressed hepatic conditions, NFκB induces GPx1 gene expression, without apparent inflammation (Lu et al., 2015). Concomitant upregulations of both GPx1 mRNA and NFκB at 10µM BA in NG conditions corroborate this observation (Fig. 4.7E; Fig. 4.9A).

It should be known that Szuster-Ciesielska and Kandefer-Szerszen (2005) suggested that the AO activity of BA is dependent on the level of ROS induction (Szuster-Ciesielska and Kandefer-Szerszeň, 2005). A consistent upregulation was evident in the entire AO response (SOD2, CAT, GPx1/GSH) at 5µM BA treatment in HG conditions, coinciding with lowered ROS, protein carbonyl and MDA levels (Fig. 4.4; Fig. 4.7). These results are in line with Szuster-Ciesielska and Kandefer-Szerszen's observation, suggesting the HG state brought high levels of ROS induction, stimulating an intensive AO response by BA (Szuster-Ciesielska and Kandefer-Szerszeň, 2005).

To further evaluate the AO profile, the transmembrane protein, UCP2, was assessed. UCP2 is associated with increased proton leakage, uncoupling ETC from OXPHOS, hence it is proven to modulate ATP synthesis and ROS levels (Su et al., 2017). Additionally, UCP2's effect on ATP and NAD+ levels allow it to maintain the mitochondrial steady state (Su et al., 2017). UCP2 fluctuations were observed in NG media in Fig. 4.8A. We can thus infer that any alterations in UCP2 levels assisted in the maintenance of constant ATP readings observed in Fig. 4.1C and Fig. 4.1D.

Betulinic acid's effect on UCP2 is not fully elucidated, with Heiss et al. (2014) concluding that, despite BA's upregulation of UCP2 in the MEF cell line, it is expressed to different degrees in different tissues, warranting further research in different cell lines (Heiss et al., 2014). Recent research into UCP2's anti-ROS activities demonstrated that UCP2 is upregulated in HG conditions to combat associated ROS (Sosa-Gutiérrez et al., 2018). This current study demonstrated an upregulation at 5µM BA, relative to the HG control (Fig. 4.8B). Therefore, we conclude that BA further upregulated UCP2 expression above this already heightened state, at 5µM concentration, to intensify cytoprotection to HG-induced ROS (Fig. 4.8B).

Although the modulation of UCP2 activity is poorly understood, recent research suggest that PPARγ can modulate UCP2 gene and protein levels, utilising it as a key method of ROS reduction (Wang et al., 2014). Research into this further elucidated the vital role of UCP2, by demonstrating that inhibiting UCP2 lead to a reduction of PPARγ agonist rosiglitazone's ROS-diminishing capacity. A concomitant upregulation at 5µM BA in HG conditions in both PPARγ and UCP2 demonstrated the presence of this link in this current study (Fig. 4.5B; Fig. 4.8B).

In addition to UCP's ROS-reducing role, exists its role to promote AO activity. Sosa-Gutierrez et al. (2018) suggests that UCP2's ability to modulate the NAD+/NADH ratio allows it to favour NAD, thus promoting SIRT3 deacetylase activity (Sosa-Gutiérrez et al., 2018).

SIRT3 is aptly titled a metabolic sensor, due to its intrinsic ability to sense NAD+ levels, as well as utilise them as a cofactor for its deacetylation function. SIRT3 exerts its AO functions via deacetylation of AO proteins, thus activating them (Hirschey et al., 2011a). It has been previously proven that OS conditions induce SIRT3. Furthermore, Gounden et al. (2015) demonstrated that HG conditions bring about an increase in SIRT3 expression and resultant AO defence in HepG2 cells (Gounden et al., 2015). In the current study, it was observed that BA upregulated SIRT3 protein expression significantly above the HG control (Fig. 4.10B). These findings imply that BA further upregulated an already enhanced SIRT3 at 5μM in HG conditions (Fig. 4.10B).

Additionally, we explore the SIRT3/PGC1α loop in potentiation of the AO response upon BA treatment. The hypothesized involvement of BA in the SIRT3/PGC1α loop in this study originates from the relation of NRF2 and SIRT3. PGC1α was found to interact directly with NRF2 at the ARE promoter region of SIRT3, enhancing SIRT3 transcription (Song et al., 2017). We propose that BA stimulates NRF2 to transcribe for SIRT3, which thus initiates the SIRT3/PGC1α/ERRα/CREB positive feedback mechanism. Betulinic acid's enhancement of both these observations were clearly evident at 5μM BA stimulation in HG conditions, where all 3 proteins (NRF2, SIRT3, PGC1α), and genes were upregulated (Fig. 4.5D; Fig. 4.10B; Fig. 4.10D; Fig. 4.10F; Fig. 4.10H). These observations suggest that BA potentiates the SIRT3/PGC1α positive feedback loop via NRF2 in response to HG-stress. This feedback loop enhances AO response, with SIRT3 promoting AO activity, and PGC1α promoting AO transcription.

We report on SIRT3 and PGC1α's AO involvement. Chen et al. (2011) revealed the concept of SIRT3-dependant deacetylation of SOD2, to activate its anti-superoxide capabilities (Chen et al., 2011). Our results demonstrate an upregulation of both proteins at 5μM BA, demonstrating that BA stimulation enhances SIRT3's deacetylation of SOD2 to further its AO activities (Fig. 4.7B; Fig. 4.10B). Additionally, many of SIRT3's AO abilities are indirect, stemming from its activation of PGC1α, amongst other proteins (Kong et al., 2010).

PGC1α is involved in the co-regulation of various AO-related proteins. Valle et al., (2005) demonstrated that PGC1α could be found associated with the regulatory promoter sequences of SOD2 and UCP2 (Valle et al., 2005). Additionally, research has established PGC1α's control of GPx1 and CAT (Iacovelli et al., 2016) . The current study revealed concomitant enhancement of PGC1α and the abovementioned AOs at a concentration of 5μM BA in HG conditions. This suggests that BA's upregulation of PGC1α assisted in the amplification of the AO response to combat HG stress (Fig. 4.7B; Fig. 4.7D; Fig. 4.7F; Fig. 4.8B; Fig. 4.10F).

Despite a lack of protein upregulation in NG conditions, mRNA levels of PGC1α and SIRT3 were significantly increased (Fig. 4.10A; Fig. 4.10C; Fig. 4.10E; Fig. 4.10G). Research into both proteins has demonstrated high levels of post-translational regulation, especially with regards to metabolic stress status (Flick and Lüscher, 2012, Luo et al., 2019). This strongly implies that post-translational repression occurs , due to lack of metabolic stress in NG conditions, in the current study, preventing an increase in protein expression, despite elevated mRNA levels (Fig. 4.10A; Fig. 4.10C; Fig. 4.10E; Fig. 4.10G).

The oxidation of proteins not only result in loss of function, but also result in crosslinking, forming aggregates, disrupting metabolism and homeostatic processes, being increasingly linked to T2DM (Dalle-Donne et al., 2006). Mitochondria are protein dense, high traffic organelles, exposed to constant levels of ROS, warranting a security mechanism to protein oxidation (Andreyev et al., 2005). LONP1 is a proteolytic digestor, implicated in the removal of oxidized proteins from the mitochondria (Ngo et al., 2013). Gibellini et al. (2014) concluded that LONP1 is directly deacetylated by SIRT3, resulting in its activation for protein degradation (Gibellini et al., 2014). Consistent with this, at 5µM BA in HG conditions, upregulations in SIRT3 and LONP1 coincided with significantly low protein carbonylation levels (Fig. 4.4F; Fig. 4.10B; Fig. 4.11B). BA's indirect upregulation of SIRT3 thus extends to promote LONP1s proteolysis of protein carbonyls, reducing the toxic environment induced by hyperglycaemia.

LONP1, however, is considered biphasic, and is also implicated in many other functions, including mitogenesis, chaperone systems and ETC and ATP maintenance (Ngo et al., 2013). An upregulation of LONP1 in NG conditions at 10µM did not correlate with SIRT3 levels, leading us to assume that the upregulation was due to other extraneous factors (Fig. 4.11A).

Another repercussion of HG-induced ROS is that of inflammation. In the HG setting, inflammation and ROS are intertwined in a positive feedback loop, with NFκB an important linking protein between the two, being stimulated by ROS, and reciprocally stimulating ROS and inflammation (Morgan and Liu, 2011, Sharma et al., 2018). NFκB is an easily inducible transcription factor involved in the induction of genes for various processes (Zhang et al., 2017). It is also proven to be repressed by all of PGC1α, NRF2 and PPARγ (Eisele et al., 2015, Wahli, 2008, Wardyn et al., 2015). Expectedly, low levels of NFκB coincided with high levels of PGC1α, NRF2 and PPARγ, its repressors, at 5µM BA in response to HG stress (Fig. 4.9B; Fig. 4.5B; Fig. 4.5D; Fig. 4.10F). Additionally, we speculate the NFκB downregulation at 5µM BA in HG conditions, may have assisted in reducing the ROS levels demonstrated in Figure 4.4B. Furthermore, multiple studies have indicated that LDH can be alternatively viewed as a biomarker of inflammation (Wu et al., 2016). NFκB downregulation at 5µM BA concentration correlated with previously noted LDH downregulations in this study (Fig. 4.2B; Fig. 4.9B). Thus, we deduce that BA's stimulation of PGC1α, NRF2 and PPARγ repressed NFκB, lessening ROS-induced inflammation and resultant membrane damage, noted via downregulation of LDH and ROS levels.

Previous research involving BA proved its inhibition of NFκB for anti-inflammatory purposes in a nontumor cell line and on a diabetic rat-model (Wang et al., 2016). Interestingly, it has also been concluded that BA activates NFκB to aid in anti-cancer activity in tumour cell lines (Kasperczyk et al., 2005). These confounding studies suggest a possible modulation of NFκB to suit specific circumstances (Wang et al., 2016). In the NG model, BA induced an upregulation of NFκB at both concentrations (Fig. 4.9A). Constant LDH levels (Fig. 4.2A), however, alluded to a lack of inflammation in NG model, hence we can assume that BA exerts differential regulation of NFκB, downregulating it to combat HG induced inflammation, and upregulating it otherwise, for extraneous purposes.

Taken together, our results highlight 5μM BA as an optimal concentration to enhance the cytoprotective machinery to HG induced OS. We further summarize these results and propose a model of the mechanism of BA's cytoprotective action.

As demonstrated by figure 5.1, BA upregulated PPARγ and phosphorylated NRF2. The PPARγ/NRF2 feedback loop potentiates transcription of many AO's including UCP2, SOD2, CAT and GPx1. SOD2 detoxifies ROS into peroxides, which CAT and GPx1 then reduce to water thus reducing HG-induced ROS and resultant OS. UCP2 acts to simultaneously reduce ROS and increase AO response, via promoting SIRT3 activity. NRF2 transcribes for SIRT3. SIRT3 deacetylates and activates SOD2 and LONP1, promoting AO activity and proteolysis of oxidized proteins. Furthermore, SIRT3 stimulates PGC1α, resulting in a positive feedback loop. PGC1α aids in transcription of SOD2, CAT, GPx1 and UCP2, further potentiating the AO-profile.
PPARγ additionally transcribes for miR124, which inhibits NFκB and promotes NRF2 phosphorylation. Furthermore, PPARγ, NRF2 and PGC1α also directly repress NFκB transcription. This combined inhibition of NFκB reduces HG-induced ROS and ROS-induced inflammation.

This mechanism acts to amplify the AO and anti-ROS response to combat an OS state associated with hyperglycaemia, with potential to be extrapolated to the diabetic state.
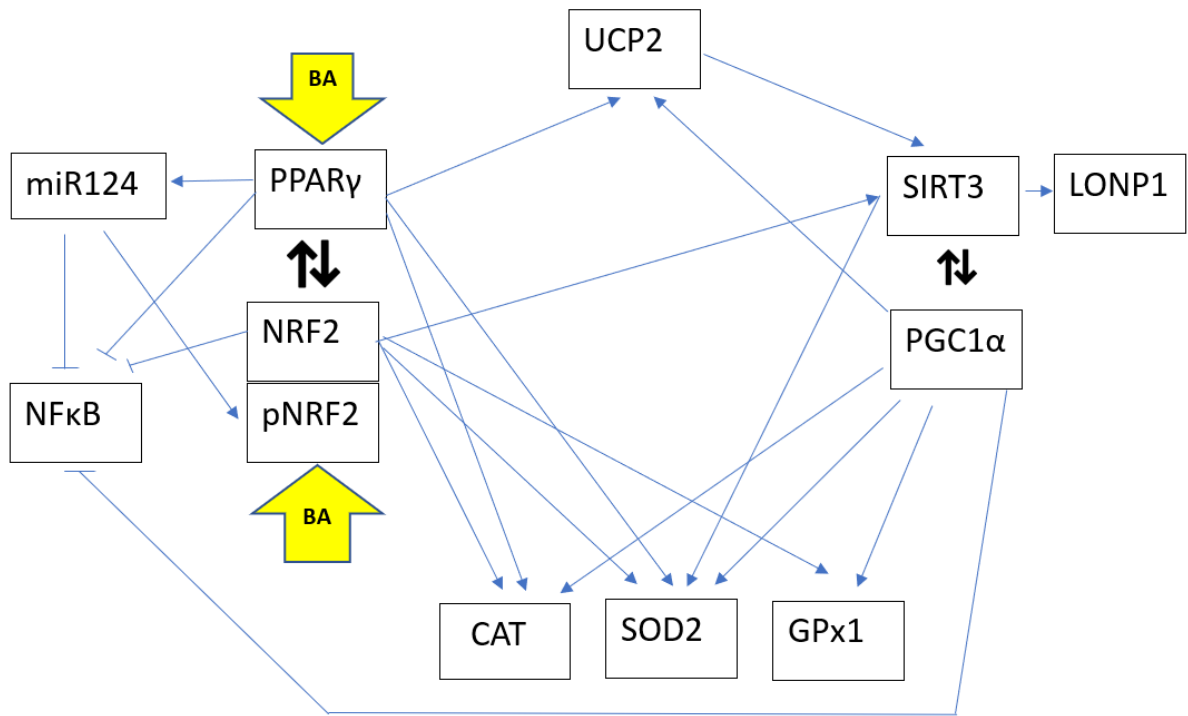
Figure 5.1: Proposed mechanism for BA's cytoprotective actions to hyperglycaemic induced ROS at 5µM BA concentration (prepared by author)

CHAPTER 6: CONCLUSION

6.1) Conclusion

Taken together, data of this study demonstrates that BA, a lupane-triterpene, has the ability to protect human hepatoma cells against HG-induced OS, via modulation of the AO profile at an optimal concentration of 5µM. Additionally, we propose a mechanism by which BA exerts its cytoprotective effect, originating from the NRF2/PPARγ positive feedback loop. These findings suggest BA as a potential adjunctive therapeutic agent for diabetes and diabetes-related complications, which is cost effective and readily available. This is of particular significance in developing countries like South Africa where the incidence of diabetes is rapidly rising. This study's limitation of an *in vitro* model opens avenues for further research in a murine model and human testing to consider overall metabolic interactions normally prevalent in the *in vivo* model.

6.2) Future Studies

Betulinic acid is an essential component of *Peltophorum africanum,* a traditional African medicinal plant. It would be relevant to examine this plant for additional pharmacologically active compounds.

Recent research suggests a paradigm shift away from the "adipocentric theory," in which adipose tissue is one of the primary causes of insulin resistance, towards an "endothelial dysfunction theory," in which oxidative stress brings about endothelial inflammation as the primary cause of insulin resistance. Thus, this study can be transposed onto a more relevant endothelial cell line to evaluate BA's ability to ameliorate endothelial cell OS in order to combat insulin resistance and CVS complications.

Betulinic acid's previously researched anti-diabetic effects make BA an interesting candidate to evaluate as adjunctive therapy with metformin to combat hyperglycaemia and prevent complications in T2DM. Additionally, the HG model could be expanded to include a palmitate-induced insulin resistance model to more closely mimic the *in vivo* diabetic state and thus provide a more accurate and appropriate cellular response to OS in response to BA treatment.

6.3) Limitations

In this study an *in vitro* HepG2 model was utilised to assess the AO response to HG induced OS in response to BA. Although this model allowed for detailed analysis, a shortcoming is that cells are far removed from their natural environment, thus eliminating cellular and metabolic interactions normally present in a whole organism. Future studies could entail using a diabetic mouse model in order to better elucidate a cellular response to OS upon treatment with BA.

References

ADELEKE, G. E. & ADARAMOYE, O. A. 2017. Betulinic acid protects against N-nitrosodimethylamine-induced redox imbalance in testes of rats. *Redox report,* 22**,** 556-562.

AHN, B.-H., KIM, H.-S., SONG, S., LEE, I. H., LIU, J., VASSILOPOULOS, A., DENG, C.-X. & FINKEL, T. 2008. A role for the mitochondrial deacetylase Sirt3 in regulating energy homeostasis. *Proceedings of the National Academy of Sciences,* 105**,** 14447-14452.

ALBANO, E., BELLOMO, G., PAROLA, M., CARINI, R. & DIANZANI, M. U. 1991. Stimulation of lipid peroxidation increases the intracellular calcium content of isolated hepatocytes. *Biochimica et Biophysica Acta (BBA)-Molecular Cell Research,* 1091**,** 310-316.

ANDREYEV, A. Y., KUSHNAREVA, Y. E. & STARKOV, A. 2005. Mitochondrial metabolism of reactive oxygen species. *Biochemistry (Moscow),* 70**,** 200-214.

ANSARI, A., RAHMAN, M. S., SAHA, S. K., SAIKOT, F. K., DEEP, A. & KIM, K. H. 2017. Function of the SIRT 3 mitochondrial deacetylase in cellular physiology, cancer, and neurodegenerative disease. *Aging cell,* 16**,** 4-16.

APEL, K. & HIRT, H. 2004. Reactive oxygen species: metabolism, oxidative stress, and signal transduction. *Annu. Rev. Plant Biol.,* 55**,** 373-399.

APPARI, M., CHANNON, K. M. & MCNEILL, E. 2018. Metabolic regulation of adipose tissue macrophage function in obesity and diabetes. *Antioxidants & redox signaling,* 29**,** 297-312.

ARONOFF, S. L., BERKOWITZ, K., SHREINER, B. & WANT, L. 2004. Glucose metabolism and regulation: beyond insulin and glucagon. *Diabetes spectrum,* 17**,** 183-190.

ARYA, M., SHERGILL, I. S., WILLIAMSON, M., GOMMERSALL, L., ARYA, N. & PATEL, H. R. 2005. Basic principles of real-time quantitative PCR. *Expert review of molecular diagnostics,* 5**,** 209-219.

ASMAT, U., ABAD, K. & ISMAIL, K. 2016. Diabetes mellitus and oxidative stress—a concise review. *Saudi Pharmaceutical Journal,* 24**,** 547-553.

BERG, A. H., COMBS, T. P. & SCHERER, P. E. 2002. ACRP30/adiponectin: an adipokine regulating glucose and lipid metabolism. *Trends in Endocrinology & Metabolism,* 13**,** 84-89.

BERMUDEZ, V., FINOL, F., PARRA, N., PARRA, M., PÉREZ, A., PENARANDA, L., VÍLCHEZ, D., ROJAS, J., ARRÁIZ, N. & VELASCO, M. 2010. PPAR-γ agonists and their role in type 2 diabetes mellitus management. *American journal of therapeutics,* 17**,** 274-283.

BIRBEN, E., SAHINER, U. M., SACKESEN, C., ERZURUM, S. & KALAYCI, O. 2012. Oxidative stress and antioxidant defense. *World Allergy Organization Journal,* 5**,** 9-19.

BONEN, A., HOLLOWAY, G. P., TANDON, N. N., HAN, X.-X., MCFARLAN, J., GLATZ, J. F. & LUIKEN, J. J. 2009. Cardiac and skeletal muscle fatty acid transport and transporters and triacylglycerol and fatty acid oxidation in lean and Zucker diabetic fatty rats. *American Journal of Physiology-Regulatory, Integrative and Comparative Physiology,* 297**,** R1202-R1212.

BOTA, D. A. & DAVIES, K. J. 2016. Mitochondrial Lon protease in human disease and aging: Including an etiologic classification of Lon-related diseases and disorders. *Free Radical Biology and Medicine,* 100**,** 188-198.

BROWNLEE, M. 2001. Biochemistry and molecular cell biology of diabetic complications. *Nature,* 414**,** 813.

BRUSOTTI, G., MONTANARI, R., CAPELLI, D., CATTANEO, G., LAGHEZZA, A., TORTORELLA, P., LOIODICE, F., PEIRETTI, F., BONARDO, B. & PAIARDINI, A. 2017. Betulinic acid is a PPARγ antagonist that improves glucose uptake, promotes osteogenesis and inhibits adipogenesis. *Scientific reports,* 7**,** 5777.

BRYAN, H. K., OLAYANJU, A., GOLDRING, C. E. & PARK, B. K. 2013. The Nrf2 cell defence pathway: Keap1-dependent and-independent mechanisms of regulation. *Biochemical pharmacology,* 85**,** 705-717.

CARVALHO, F. 2017. Role of Nrf2 in the Regulation of Ppar Expression in Mice.

CASTELLANO, J. M., GUINDA, A., DELGADO, T., RADA, M. & CAYUELA, J. A. 2013. Biochemical basis of the antidiabetic activity of oleanolic acid and related pentacyclic triterpenes. *Diabetes,* 62**,** 1791-1799.

CASTRO, A. J. G., FREDERICO, M. J. S., CAZAROLLI, L. H., BRETANHA, L. C., DE CARVALHO TAVARES, L., DA SILVA BUSS, Z., DUTRA, M. F., DE SOUZA, A. Z. P., PIZZOLATTI, M. G. & SILVA, F. R. M. B. 2014. Betulinic acid and 1, 25 (OH) 2 vitamin D3 share intracellular signal transduction in glucose homeostasis in soleus muscle. *The international journal of biochemistry & cell biology,* 48**,** 18-27.

CHEESEMAN, K. 1993. Mechanisms and effects of lipid peroxidation. *Molecular Aspects of Medicine,* 14**,** 191-197.

CHEN, Y.-L., FU, L., WEN, X., WANG, X. Y., LIU, J., CHENG, Y. & HUANG, J. 2014. Sirtuin-3 (SIRT3), a therapeutic target with oncogenic and tumor-suppressive function in cancer. *Cell death & disease,* 5**,** e1047.

CHEN, Y., ZHANG, J., LIN, Y., LEI, Q., GUAN, K. L., ZHAO, S. & XIONG, Y. 2011. Tumour suppressor SIRT3 deacetylates and activates manganese superoxide dismutase to scavenge ROS. *EMBO reports,* 12**,** 534-541.

CHO, H.-Y., GLADWELL, W., WANG, X., CHORLEY, B., BELL, D., REDDY, S. P. & KLEEBERGER, S. R. 2010. Nrf2-regulated PPARγ expression is critical to protection against acute lung injury in mice. *American journal of respiratory and critical care medicine,* 182**,** 170-182.

CHO, H.-Y., REDDY, S. P., DEBIASE, A., YAMAMOTO, M. & KLEEBERGER, S. R. 2005. Gene expression profiling of NRF2-mediated protection against oxidative injury. *Free Radical Biology and Medicine,* 38**,** 325-343.

CHO, N., SHAW, J., KARURANGA, S., HUANG, Y., DA ROCHA FERNANDES, J., OHLROGGE, A. & MALANDA, B. 2018. IDF Diabetes Atlas: Global estimates of diabetes prevalence for 2017 and projections for 2045. *Diabetes research and clinical practice,* 138**,** 271-281.

CHORLEY, B. N., CAMPBELL, M. R., WANG, X., KARACA, M., SAMBANDAN, D., BANGURA, F., XUE, P., PI, J., KLEEBERGER, S. R. & BELL, D. A. 2012. Identification of novel NRF2-regulated genes by ChIP-Seq: influence on retinoid X receptor alpha. *Nucleic acids research,* 40**,** 7416-7429.

COLLINS, K. H., HERZOG, W., MACDONALD, G. Z., REIMER, R. A., RIOS, J. L., SMITH, I. C., ZERNICKE, R. F. & HART, D. A. 2018. Obesity, metabolic syndrome, and musculoskeletal disease: common inflammatory pathways suggest a central role for loss of muscle integrity. *Frontiers in physiology,* 9**,** 112.

CONSOLI, A. 1992. Role of liver in pathophysiology of NIDDM. *Diabetes care,* 15**,** 430-441.

CZECH, M. P. 1985. The nature and regulation of the insulin receptor: structure and function. *Annual Review of Physiology,* 47**,** 357-381.

DALLE-DONNE, I., ALDINI, G., CARINI, M., COLOMBO, R., ROSSI, R. & MILZANI, A. 2006. Protein carbonylation, cellular dysfunction, and disease progression. *Journal of cellular and molecular medicine,* 10**,** 389-406.

DAVID, J. A., RIFKIN, W. J., RABBANI, P. S. & CERADINI, D. J. 2017. The Nrf2/Keap1/ARE pathway and oxidative stress as a therapeutic target in type II diabetes mellitus. *Journal of diabetes research,* 2017.

DE MELO, C. L. L., QUEIROZ, M. G. R., ARRUDA FILHO, A. C. V., RODRIGUES, A. M., DE SOUSA, D. F., ALMEIDA, J. G. L., PESSOA, O. D. L., SILVEIRA, E. R., MENEZES, D. B. & MELO, T. S. 2009. Betulinic acid, a natural pentacyclic triterpenoid, prevents abdominal fat accumulation in mice fed a high-fat diet. *Journal of agricultural and food chemistry,* 57**,** 8776-8781.

DEVASAGAYAM, T., BOLOOR, K. & RAMASARMA, T. 2003. Methods for estimating lipid peroxidation: an analysis of merits and demerits. *Indian journal of biochemistry & biophysics,* 40**,** 300-308.

DONATO, M. T., TOLOSA, L. & GÓMEZ-LECHÓN, M. J. 2015. Culture and functional characterization of human hepatoma HepG2 cells. *Protocols in In Vitro Hepatocyte Research.* Springer.

EISELE, P. S., FURRER, R., BEER, M. & HANDSCHIN, C. 2015. The PGC-1 coactivators promote an anti-inflammatory environment in skeletal muscle in vivo. *Biochemical and biophysical research communications,* 464**,** 692-697.

FERNANDES, J., WEDDLE, A., KINTER, C. S., HUMPHRIES, K. M., MATHER, T., SZWEDA, L. I. & KINTER, M. 2015. Lysine acetylation activates mitochondrial aconitase in the heart. *Biochemistry,* 54**,** 4008-4018.

FINLEY, L. W., HAAS, W., DESQUIRET-DUMAS, V., WALLACE, D. C., PROCACCIO, V., GYGI, S. P. & HAIGIS, M. C. 2011. Succinate dehydrogenase is a direct target of sirtuin 3 deacetylase activity. *PloS one,* 6**,** e23295.

FLICK, F. & LÜSCHER, B. 2012. Regulation of sirtuin function by posttranslational modifications. *Frontiers in pharmacology,* 3**,** 29.

FROHNERT, B. I. & BERNLOHR, D. A. 2013. Protein carbonylation, mitochondrial dysfunction, and insulin resistance. *Advances in nutrition,* 4**,** 157-163.

FU, L., ZHANG, S., LI, N., WANG, J., ZHAO, M., SAKAI, J., HASEGAWA, T., MITSUI, T., KATAOKA, T. & OKA, S. 2005. Three New Triterpenes from Nerium o leander and Biological Activity of the Isolated Compounds. *Journal of natural products,* 68**,** 198-206.

GIBELLINI, L., PINTI, M., BERETTI, F., PIERRI, C. L., ONOFRIO, A., RICCIO, M., CARNEVALE, G., DE BIASI, S., NASI, M. & TORELLI, F. 2014. Sirtuin 3 interacts with Lon protease and regulates its acetylation status. *Mitochondrion,* 18**,** 76-81.

GIRNUN, G. D., DOMANN, F. E., MOORE, S. A. & ROBBINS, M. E. 2002. Identification of a functional peroxisome proliferator-activated receptor response element in the rat catalase promoter. *Molecular Endocrinology,* 16**,** 2793-2801.

GORRINI, C., HARRIS, I. S. & MAK, T. W. 2013. Modulation of oxidative stress as an anticancer strategy. *Nature reviews Drug discovery,* 12**,** 931-947.

GOUNDEN, S. & CHUTURGOON, A. 2017. Curcumin upregulates antioxidant defense, lon protease, and heat-shock protein 70 under hyperglycemic conditions in human hepatoma cells. *Journal of medicinal food,* 20**,** 465-473.

GOUNDEN, S., PHULUKDAREE, A., MOODLEY, D. & CHUTURGOON, A. 2015. Increased SIRT3 expression and antioxidant defense under hyperglycemic conditions in HepG2 cells. *Metabolic syndrome and related disorders,* 13**,** 255-263.

GROTTO, D., MARIA, L. S., VALENTINI, J., PANIZ, C., SCHMITT, G., GARCIA, S. C., POMBLUM, V. J., ROCHA, J. B. T. & FARINA, M. 2009. Importance of the lipid peroxidation biomarkers and methodological aspects for malondialdehyde quantification. *Quimica Nova,* 32**,** 169-174.

GUZIK, T. J. & COSENTINO, F. 2018. Epigenetics and immunometabolism in diabetes and aging. *Antioxidants & redox signaling,* 29**,** 257-274.

HAUCK, A. K. & BERNLOHR, D. A. 2016. Oxidative stress and lipotoxicity. *Journal of lipid research,* 57**,** 1976-1986.

HEISS, E. H., KRAMER, M. P., ATANASOV, A. G., BERES, H., SCHACHNER, D. & DIRSCH, V. M. 2014. Glycolytic switch in response to betulinic acid in non-cancer cells. *PloS one,* 9**,** e115683.

HIRSCHEY, M., SHIMAZU, T., HUANG, J.-Y., SCHWER, B. & VERDIN, E. SIRT3 regulates mitochondrial protein acetylation and intermediary metabolism. Cold Spring Harbor symposia on quantitative biology, 2011a. Cold Spring Harbor Laboratory Press, 267-277.

HIRSCHEY, M. D., SHIMAZU, T., JING, E., GRUETER, C. A., COLLINS, A. M., AOUIZERAT, B., STANČÁKOVÁ, A., GOETZMAN, E., LAM, M. M. & SCHWER, B. 2011b. SIRT3 deficiency and mitochondrial protein hyperacetylation accelerate the development of the metabolic syndrome. *Molecular cell,* 44**,** 177-190.

HUANG, J., TABBI-ANNENI, I., GUNDA, V. & WANG, L. 2010a. Transcription factor Nrf2 regulates SHP and lipogenic gene expression in hepatic lipid metabolism. *American Journal of Physiology-Gastrointestinal and Liver Physiology,* 299**,** G1211-G1221.

HUANG, T., LONG, M. & HUO, B. 2010b. Competitive binding to cuprous ions of protein and BCA in the bicinchoninic acid protein assay. *The open biomedical engineering journal,* 4**,** 271.

IACOVELLI, J., ROWE, G. C., KHADKA, A., DIAZ-AGUILAR, D., SPENCER, C., ARANY, Z. & SAINT-GENIEZ, M. 2016. PGC-1α induces human RPE oxidative metabolism and antioxidant capacity. *Investigative ophthalmology & visual science,* 57**,** 1038-1051.

IGHODARO, O. & AKINLOYE, O. 2018. First line defence antioxidants-superoxide dismutase (SOD), catalase (CAT) and glutathione peroxidase (GPX): Their fundamental role in the entire antioxidant defence grid. *Alexandria Journal of Medicine,* 54**,** 287-293.

JÄGER, S., TROJAN, H., KOPP, T., LASZCZYK, M. & SCHEFFLER, A. 2009. Pentacyclic triterpene distribution in various plants–rich sources for a new group of multi-potent plant extracts. *Molecules,* 14**,** 2016-2031.

JEONG, Y.-H., PARK, J.-S., KIM, D.-H. & KIM, H.-S. 2016. Lonchocarpine increases Nrf2/ARE-mediated antioxidant enzyme expression by modulating AMPK and MAPK signaling in brain astrocytes. *Biomolecules & therapeutics,* 24**,** 581.

JIN, C. H., SO, Y. K., HAN, S. N. & KIM, J.-B. 2016. Isoegomaketone upregulates heme oxygenase-1 in RAW264. 7 cells via ROS/p38 MAPK/Nrf2 pathway. *Biomolecules & therapeutics,* 24**,** 510.

KABEL, A. M. 2014. Free radicals and antioxidants: role of enzymes and nutrition. *World Journal of Nutrition and Health,* 2**,** 35-38.

KALYANARAMAN, B., DARLEY-USMAR, V., DAVIES, K. J., DENNERY, P. A., FORMAN, H. J., GRISHAM, M. B., MANN, G. E., MOORE, K., ROBERTS II, L. J. & ISCHIROPOULOS, H. 2012. Measuring reactive oxygen and nitrogen species with fluorescent probes: challenges and limitations. *Free Radical Biology and Medicine,* 52**,** 1-6.

KAMALIAN, L., CHADWICK, A. E., BAYLISS, M., FRENCH, N. S., MONSHOUWER, M., SNOEYS, J. & PARK, B. K. 2015. The utility of HepG2 cells to identify direct mitochondrial dysfunction in the absence of cell death. *Toxicology in vitro,* 29**,** 732-740.

KANETO, H., KATAKAMI, N., MATSUHISA, M. & MATSUOKA, T.-A. 2010. Role of reactive oxygen species in the progression of type 2 diabetes and atherosclerosis. *Mediators of inflammation,* 2010.

KASPERCZYK, H., LA FERLA-BRÜHL, K., WESTHOFF, M. A., BEHREND, L., ZWACKA, R. M., DEBATIN, K.-M. & FULDA, S. 2005. Betulinic acid as new activator of NF-κB: molecular mechanisms and implications for cancer therapy. *Oncogene,* 24**,** 6945.

KEY, J., KOHLI, A., BÁRCENA, C., LÓPEZ-OTÍN, C., HEIDLER, J., WITTIG, I. & AUBURGER, G. 2019. Global Proteome of LonP1+/− Mouse Embryonal Fibroblasts Reveals Impact on Respiratory Chain, but No Interdependence between Eral1 and Mitoribosomes. *International journal of molecular sciences,* 20**,** 4523.

KIM, J.-H., NA, H.-J., KIM, C.-K., KIM, J.-Y., HA, K.-S., LEE, H., CHUNG, H.-T., KWON, H. J., KWON, Y.-G. & KIM, Y.-M. 2008. The non-provitamin A carotenoid, lutein, inhibits NF-κB-dependent gene expression through redox-based regulation of the phosphatidylinositol 3-kinase/PTEN/Akt and NF-κB-inducing kinase pathways: role of H2O2 in NF-κB activation. *Free Radical Biology and Medicine,* 45**,** 885-896.

KIM, K.-D., JUNG, H.-Y., RYU, H., KIM, B., JEON, J., YOO, H., PARK, C., CHOI, B.-H., HYUN, C.-K. & KIM, K.-T. 2019. Betulinic acid inhibits high-fat diet-induced obesity and improves energy balance by activating AMPK. *Nutrition, Metabolism and Cardiovascular Diseases,* 29**,** 409-420.

KONG, X., WANG, R., XUE, Y., LIU, X., ZHANG, H., CHEN, Y., FANG, F. & CHANG, Y. 2010. Sirtuin 3, a new target of PGC-1α, plays an important role in the suppression of ROS and mitochondrial biogenesis. *PloS one,* 5**,** e11707.

KUMAR, P., NAGARAJAN, A. & UCHIL, P. D. 2018. Analysis of cell viability by the lactate dehydrogenase assay. *Cold Spring Harbor Protocols,* 2018**,** pdb. prot095497.

KURIEN, B. T. & SCOFIELD, R. H. 2006. Western blotting. *Methods,* 38**,** 283-293.

KVANDOVA, M., MAJÚNOVÁ, M. & DOVINOVÁ, I. 2016. The Role of PPAR [gamma] in Cardiovascular Diseases. *Physiological research,* 65**,** S343.

LEE, C. 2017. Collaborative power of Nrf2 and PPARγ activators against metabolic and drug-induced oxidative injury. *Oxidative medicine and cellular longevity,* 2017.

LEICK, L., FENTZ, J., BIENSØ, R. S., KNUDSEN, J. G., JEPPESEN, J., KIENS, B., WOJTASZEWSKI, J. F. & PILEGAARD, H. 2010. PGC-1α is required for AICAR-induced expression of GLUT4 and mitochondrial proteins in mouse skeletal muscle. *American Journal of Physiology-Endocrinology and Metabolism,* 299**,** E456-E465.

LEYVRAZ, C., SUTER, M., VERDUMO, C., CALMES, J. M., PAROZ, A., DARIMONT, C., GAILLARD, R., PRALONG, F. & GIUSTI, V. 2010. Selective effects of PPARγ agonists and antagonists on human pre-adipocyte differentiation. *Diabetes, Obesity and Metabolism,* 12**,** 195-203.

LI, Z., GENG, Y.-N., JIANG, J.-D. & KONG, W.-J. 2014. Antioxidant and anti-inflammatory activities of berberine in the treatment of diabetes mellitus. *Evidence-Based Complementary and Alternative Medicine,* 2014.

LIU, J., LI, J., LI, W.-J. & WANG, C.-M. 2013. The role of uncoupling proteins in diabetes mellitus. *Journal of diabetes research,* 2013.

LIU, Y., FISKUM, G. & SCHUBERT, D. 2002. Generation of reactive oxygen species by the mitochondrial electron transport chain. *Journal of neurochemistry,* 80**,** 780-787.

LIU, Z., DOU, W., ZHENG, Y., WEN, Q., QIN, M., WANG, X., TANG, H., ZHANG, R., LV, D. & WANG, J. 2016. Curcumin upregulates Nrf2 nuclear translocation and protects rat hepatic stellate cells against oxidative stress. *Molecular medicine reports,* 13**,** 1717-1724.

LIVAK, K. J. & SCHMITTGEN, T. D. 2001. Analysis of relative gene expression data using real-time quantitative PCR and the 2− ΔΔCT method. *methods,* 25**,** 402-408.

LOBODA, A., ROJCZYK-GOLEBIEWSKA, E., BEDNARCZYK-CWYNAR, B., LUCJUSZ, Z., JOZKOWICZ, A. & DULAK, J. 2012. Targeting Nrf2-mediated gene transcription by triterpenoids and their derivatives. *Biomolecules & therapeutics,* 20**,** 499.

LOVEN, D., SCHEDL, H., WILSON, H., DAABEES, T. T., STEGINK, L. D., DIEKUS, M. & OBERLEY, L. 1986. Effect of insulin and oral glutathione on glutathione levels and superoxide dismutase activities in organs of rats with streptozocin-induced diabetes. *Diabetes,* 35**,** 503-507.

LU, H., LEI, X. & ZHANG, Q. 2015. Moderate activation of IKK2-NF-kB in unstressed adult mouse liver induces cytoprotective genes and lipogenesis without apparent signs of inflammation or fibrosis. *BMC gastroenterology,* 15**,** 94.

LÜ, J. M., LIN, P. H., YAO, Q. & CHEN, C. 2010. Chemical and molecular mechanisms of antioxidants: experimental approaches and model systems. *Journal of cellular and molecular medicine,* 14**,** 840-860.

LUO, X., LIAO, C., QUAN, J., CHENG, C., ZHAO, X., BODE, A. M. & CAO, Y. 2019. Posttranslational regulation of PGC-1α and its implication in cancer metabolism. *International journal of cancer*.

LUSHCHAK, V. I. 2012. Glutathione homeostasis and functions: potential targets for medical interventions. *Journal of amino acids,* 2012.

MAHMOOD, T. & YANG, P.-C. 2012. Western blot: technique, theory, and trouble shooting. *North American journal of medical sciences,* 4**,** 429.

MERCIER, Y., GATELLIER, P. & RENERRE, M. 2004. Lipid and protein oxidation in vitro, and antioxidant potential in meat from Charolais cows finished on pasture or mixed diet. *Meat Science,* 66**,** 467-473.

MERSCH-SUNDERMANN, V., KNASMÜLLER, S., WU, X.-J., DARROUDI, F. & KASSIE, F. 2004. Use of a human-derived liver cell line for the detection of cytoprotective, antigenotoxic and cogenotoxic agents. *Toxicology,* 198**,** 329-340.

MOGHADDAM, M. G., AHMAD, F. B. H. & SAMZADEH-KERMANI, A. 2012. Biological activity of betulinic acid: a review. *Pharmacology & Pharmacy,* 3**,** 119.

MOKABBER, H., NAJAFZADEH, N. & MOHAMMADZADEH VARDIN, M. 2019. miR-124 promotes neural differentiation in mouse bulge stem cells by repressing Ptbp1 and Sox9. *Journal of cellular physiology,* 234**,** 8941-8950.

MORGAN, D. M. 1998. Tetrazolium (MTT) assay for cellular viability and activity. *Polyamine protocols.* Springer.

MORGAN, M. J. & LIU, Z.-G. 2011. Crosstalk of reactive oxygen species and NF-κB signaling. *Cell research,* 21**,** 103.

MUKHERJEE, A., MORALES-SCHEIHING, D., BUTLER, P. C. & SOTO, C. 2015. Type 2 diabetes as a protein misfolding disease. *Trends in molecular medicine,* 21**,** 439-449.

NGO, J. K., POMATTO, L. C. & DAVIES, K. J. 2013. Upregulation of the mitochondrial Lon Protease allows adaptation to acute oxidative stress but dysregulation is associated with chronic stress, disease, and aging. *Redox biology,* 1**,** 258-264.

NISHIKAWA, T., EDELSTEIN, D., DU, X. L., YAMAGISHI, S.-I., MATSUMURA, T., KANEDA, Y., YOREK, M. A., BEEBE, D., OATES, P. J. & HAMMES, H.-P. 2000. Normalizing mitochondrial superoxide production blocks three pathways of hyperglycaemic damage. *Nature,* 404**,** 787.

NISHIKORI, M. 2005. Classical and alternative NF-κB activation pathways and their roles in lymphoid malignancies. *Journal of clinical and experimental hematopathology,* 45**,** 15-24.

NOORI, S. 2012. An overview of oxidative stress and antioxidant defensive system. *Open access scientific reports,* 1**,** 1-9.

ORGANIZATION, W. H. 2018. Global health estimates 2016: disease burden by cause, age, sex, by country and by region, 2000–2016. *Geneva: World Health Organization.*

PATEL, S. & SANTANI, D. 2009. Role of NF-κB in the pathogenesis of diabetes and its associated complications. *Pharmacological Reports,* 61**,** 595-603.

PESTANA, E., BELAK, S., DIALLO, A., CROWTHER, J. R. & VILJOEN, G. J. 2010. *Early, rapid and sensitive veterinary molecular diagnostics-real time PCR applications*, Springer Science & Business Media.

PHANIENDRA, A., JESTADI, D. B. & PERIYASAMY, L. 2015. Free radicals: properties, sources, targets, and their implication in various diseases. *Indian journal of clinical biochemistry,* 30**,** 11-26.

PHEIFFER, C., PILLAY-VAN WYK, V., JOUBERT, J. D., LEVITT, N., NGLAZI, M. D. & BRADSHAW, D. 2018. The prevalence of type 2 diabetes in South Africa: a systematic review protocol. *BMJ open,* 8**,** e021029.

PIERELLI, G., STANZIONE, R., FORTE, M., MIGLIARINO, S., PERELLI, M., VOLPE, M. & RUBATTU, S. 2017. Uncoupling protein 2: A key player and a potential therapeutic target in vascular diseases. *Oxidative medicine and cellular longevity,* 2017.

PINTI, M., GIBELLINI, L., NASI, M., DE BIASI, S., BORTOLOTTI, C. A., IANNONE, A. & COSSARIZZA, A. 2016. Emerging role of Lon protease as a master regulator of mitochondrial functions. *Biochimica et Biophysica Acta (BBA)-Bioenergetics,* 1857**,** 1300-1306.

POLVANI, S., TAROCCHI, M. & GALLI, A. 2012. PPARγ and oxidative stress: Con (β) catenating NRF2 and FOXO. *PPAR research,* 2012.

POWELL, S. R., WANG, P., DIVALD, A., TEICHBERG, S., HARIDAS, V., MCCLOSKEY, T. W., DAVIES, K. J. & KATZEFF, H. 2005. Aggregates of oxidized proteins (lipofuscin) induce apoptosis through proteasome inhibition and dysregulation of proapoptotic proteins. *Free Radical Biology and Medicine,* 38**,** 1093-1101.

PURDEL, N. C., MARGINA, D. & ILIE, M. 2014. Current methods used in the protein carbonyl assay. *Annual Research & Review in Biology,* 4**,** 2015-2026.

QIU, S., FENG, Y., LESAGE, G., ZHANG, Y., STUART, C., HE, L., LI, Y., CAUDLE, Y., PENG, Y. & YIN, D. 2015. Chronic morphine-induced microRNA-124 promotes microglial immunosuppression by modulating P65 and TRAF6. *The Journal of Immunology,* 194**,** 1021-1030.

RAHMAN, I., KODE, A. & BISWAS, S. K. 2006. Assay for quantitative determination of glutathione and glutathione disulfide levels using enzymatic recycling method. *Nature protocols,* 1**,** 3159.

REDDY, R. C. & STANDIFORD, T. J. 2010. Nrf2 and PPARγ: PPARtnering against oxidant-induced lung injury. American Thoracic Society.

REISMAN, S. A., ALEKSUNES, L. M. & KLAASSEN, C. D. 2009. Oleanolic acid activates Nrf2 and protects from acetaminophen hepatotoxicity via Nrf2-dependent and Nrf2-independent processes. *Biochemical pharmacology,* 77**,** 1273-1282.

RHINESMITH, T., TURKETTE, T. & ROOT-BERNSTEIN, R. 2017. Rapid Non-Enzymatic Glycation of the Insulin Receptor under Hyperglycemic Conditions Inhibits Insulin Binding In Vitro: Implications for Insulin Resistance. *International journal of molecular sciences,* 18**,** 2602.

RISS, T. L., MORAVEC, R. A., NILES, A. L., DUELLMAN, S., BENINK, H. A., WORZELLA, T. J. & MINOR, L. 2016. Cell viability assays. *Assay Guidance Manual [Internet].* Eli Lilly & Company and the National Center for Advancing Translational Sciences.

ROLO, A. P. & PALMEIRA, C. M. 2006. Diabetes and mitochondrial function: role of hyperglycemia and oxidative stress. *Toxicology and applied pharmacology,* 212**,** 167-178.

ROSEN, E. D. & SPIEGELMAN, B. M. 2001. PPARγ: a nuclear regulator of metabolism, differentiation, and cell growth. *Journal of Biological Chemistry,* 276**,** 37731-37734.

RUI, L. 2011. Energy metabolism in the liver. *Comprehensive physiology,* 4**,** 177-197.

SAHA, S. S. & GHOSH, M. 2012. Antioxidant and anti-inflammatory effect of conjugated linolenic acid isomers against streptozotocin-induced diabetes. *British Journal of Nutrition,* 108**,** 974-983.

SÁNCHEZ-QUESADA, C., LÓPEZ-BIEDMA, A., WARLETA, F., CAMPOS, M., BELTRÁN, G. & GAFORIO, J. J. 2013. Bioactive properties of the main triterpenes found in olives, virgin olive oil, and leaves of Olea europaea. *Journal of Agricultural and Food Chemistry,* 61**,** 12173-12182.

SANTOS, R. C., SALVADOR, J. A., MARÍN, S. & CASCANTE, M. 2009. Novel semisynthetic derivatives of betulin and betulinic acid with cytotoxic activity. *Bioorganic & medicinal chemistry,* 17**,** 6241-6250.

SCHRECK, R., RIEBER, P. & BAEUERLE, P. A. 1991. Reactive oxygen intermediates as apparently widely used messengers in the activation of the NF-kappa B transcription factor and HIV-1. *The EMBO journal,* 10**,** 2247-2258.

SEFRIED, S., HÄRING, H.-U., WEIGERT, C. & ECKSTEIN, S. S. 2018. Suitability of hepatocyte cell lines HepG2, AML12 and THLE-2 for investigation of insulin signalling and hepatokine gene expression. *Royal Society Open Biology,* 8**,** 180147.

SEKHAR, R. V., MCKAY, S. V., PATEL, S. G., GUTHIKONDA, A. P., REDDY, V. T., BALASUBRAMANYAM, A. & JAHOOR, F. 2011. Glutathione synthesis is diminished in patients with uncontrolled diabetes and restored by dietary supplementation with cysteine and glycine. *Diabetes care,* 34**,** 162-167.

SEVER, R. & GLASS, C. K. 2013. Signaling by nuclear receptors. *Cold Spring Harbor perspectives in biology,* 5**,** a016709.

SHARMA, A., TATE, M., MATHEW, G., VINCE, J. E., RITCHIE, R. H. & DE HAAN, J. B. 2018. Oxidative stress and NLRP3-inflammasome activity as significant drivers of diabetic cardiovascular complications: therapeutic implications. *Frontiers in physiology,* 9**,** 114.

SHARMA, P., JHA, A. B., DUBEY, R. S. & PESSARAKLI, M. 2012. Reactive oxygen species, oxidative damage, and antioxidative defense mechanism in plants under stressful conditions. *Journal of botany,* 2012.

SHU, K. & ZHANG, Y. 2019. Protodioscin protects PC12 cells against oxygen and glucose deprivation-induced injury through miR-124/AKT/Nrf2 pathway. *Cell Stress and Chaperones***,** 1-9.

SHULMAN, M. & NAHMIAS, Y. 2012. Long-term culture and coculture of primary rat and human hepatocytes. *Epithelial Cell Culture Protocols.* Springer.

SILVA, F. S., OLIVEIRA, P. J. & DUARTE, M. F. 2016. Oleanolic, ursolic, and betulinic acids as food supplements or pharmaceutical agents for type 2 diabetes: promise or illusion? *Journal of agricultural and food chemistry,* 64**,** 2991-3008.

SOMEYA, S., YU, W., HALLOWS, W. C., XU, J., VANN, J. M., LEEUWENBURGH, C., TANOKURA, M., DENU, J. M. & PROLLA, T. A. 2010. Sirt3 mediates reduction of oxidative damage and prevention of age-related hearing loss under caloric restriction. *Cell,* 143**,** 802-812.

SONG, C., FU, B., ZHANG, J., ZHAO, J., YUAN, M., PENG, W., ZHANG, Y. & WU, H. 2017. Sodium fluoride induces nephrotoxicity via oxidative stress-regulated mitochondrial SIRT3 signaling pathway. *Scientific reports,* 7**,** 672.

SOSA-GUTIÉRREZ, J., VALDÉZ-SOLANA, M., FORBES-HERNÁNDEZ, T., AVITIA-DOMÍNGUEZ, C., GARCIA-VARGAS, G., SALAS-PACHECO, J., FLORES-HERRERA, O., TÉLLEZ-VALENCIA, A., BATTINO, M. & SIERRA-CAMPOS, E. 2018. Effects of Moringa oleifera leaves extract on high glucose-induced metabolic changes in HepG2 cells. *Biology,* 7**,** 37.

SOUSA, J. L., FREIRE, C. S., SILVESTRE, A. J. & SILVA, A. 2019. Recent developments in the functionalization of betulinic acid and its natural analogues: a route to new bioactive compounds. *Molecules,* 24**,** 355.

SOUZA, B. M. D., ASSMANN, T. S., KLIEMANN, L. M., GROSS, J. L., CANANI, L. H. & CRISPIM, D. 2011. The role of uncoupling protein 2 (UCP2) on the development of type 2 diabetes mellitus and its chronic complications. *Arquivos Brasileiros de Endocrinologia & Metabologia,* 55**,** 239-248.

SU, J., LIU, J., YAN, X.-Y., ZHANG, Y., ZHANG, J.-J., ZHANG, L.-C. & SUN, L.-K. 2017. Cytoprotective effect of the UCP2-SIRT3 signaling pathway by decreasing mitochondrial oxidative stress on cerebral ischemia–reperfusion injury. *International journal of molecular sciences,* 18**,** 1599.

SUKALSKI, K. A., PINTO, K. A. & BERNTSON, J. L. 1993. Decreased susceptibility of liver mitochondria from diabetic rats to oxidative damage and associated increase in α-tocopherol. *Free Radical Biology and Medicine,* 14**,** 57-65.

SZALECZKY, E., PRECHL, J., FEHER, J. & SOMOGYI, A. 1999. Alterations in enzymatic antioxidant defence in diabetes mellitus– a rational approach. *Postgraduate medical journal,* 75**,** 13-17.

SZUSTER-CIESIELSKA, A. & KANDEFER-SZERSZEÑ, M. 2005. Protective effects of betulin and betulinic acid against ethanol-induced cytotoxicity in HepG2 cells. *Pharmacol Rep,* 57**,** 588.

THEO, A., MASEBE, T., SUZUKI, Y., KIKUCHI, H., WADA, S., OBI, C. L., BESSONG, P. O., USUZAWA, M., OSHIMA, Y. & HATTORI, T. 2009. Peltophorum africanum, a traditional South African medicinal plant, contains an anti HIV-1 constituent, betulinic acid. *The Tohoku journal of experimental medicine,* 217**,** 93-99.

VALLE, I., ÁLVAREZ-BARRIENTOS, A., ARZA, E., LAMAS, S. & MONSALVE, M. 2005. PGC-1α regulates the mitochondrial antioxidant defense system in vascular endothelial cells. *Cardiovascular research,* 66**,** 562-573.

VENKATESH, S., LEE, J., SINGH, K., LEE, I. & SUZUKI, C. K. 2012. Multitasking in the mitochondrion by the ATP-dependent Lon protease. *Biochimica et Biophysica Acta (BBA)-Molecular Cell Research,* 1823**,** 56-66.

WAHLI, W. 2008. A gut feeling of the PXR, PPAR and NF-κB connection. *Journal of internal medicine,* 263**,** 613-619.

WANG, D., SHI, L., XIN, W., XU, J., XU, J., LI, Q., XU, Z., WANG, J., WANG, G. & YAO, W. 2017. Activation of PPARγ inhibits pro-inflammatory cytokines production by upregulation of miR-124 in vitro and in vivo. *Biochemical and biophysical research communications,* 486**,** 726-731.

WANG, P., LI, B., CAI, G., HUANG, M., JIANG, L., PU, J., LI, L., WU, Q., ZUO, L. & WANG, Q. 2014. Activation of PPAR-γ by pioglitazone attenuates oxidative stress in aging rat cerebral arteries through upregulating UCP2. *Journal of cardiovascular pharmacology,* 64**,** 497-506.

WANG, S., YANG, Z., XIONG, F., CHEN, C., CHAO, X., HUANG, J. & HUANG, H. 2016. Betulinic acid ameliorates experimental diabetic-induced renal inflammation and fibrosis via inhibiting the activation of NF-κB signaling pathway. *Molecular and cellular endocrinology,* 434**,** 135-143.

WARDYN, J. D., PONSFORD, A. H. & SANDERSON, C. M. 2015. Dissecting molecular cross-talk between Nrf2 and NF-κB response pathways. *Biochemical society transactions,* 43**,** 621-626.

WEN, J.-J. & GARG, N. 2004. Oxidative modification of mitochondrial respiratory complexes in response to the stress of Trypanosoma cruzi infection. *Free Radical Biology and Medicine,* 37**,** 2072-2081.

WOHAIEB, S. A. & GODIN, D. V. 1987. Alterations in free radical tissue-defense mechanisms in streptozocin-induced diabetes in rat: effects of insulin treatment. *Diabetes,* 36**,** 1014-1018.

WU, L.-W., KAO, T.-W., LIN, C.-M., YANG, H.-F., SUN, Y.-S., LIAW, F.-Y., WANG, C.-C., PENG, T.-C. & CHEN, W.-L. 2016. Examining the association between serum lactic dehydrogenase and all-cause mortality in patients with metabolic syndrome: a retrospective observational study. *BMJ open,* 6**,** e011186.

WU, Y., DING, Y., TANAKA, Y. & ZHANG, W. 2014. Risk factors contributing to type 2 diabetes and recent advances in the treatment and prevention. *International journal of medical sciences,* 11**,** 1185.

WU, Z., XIE, Y., MORRISON, R. F., BUCHER, N. & FARMER, S. R. 1998. PPARgamma induces the insulin-dependent glucose transporter GLUT4 in the absence of C/EBPalpha during the conversion of 3T3 fibroblasts into adipocytes. *The Journal of clinical investigation,* 101**,** 22-32.

YAO, Q., LIU, J., ZHANG, Z., LI, F., ZHANG, C., LAI, B., XIAO, L. & WANG, N. 2018. Peroxisome proliferator–activated receptor γ (PPARγ) induces the gene expression of integrin αVβ5 to promote macrophage M2 polarization. *Journal of Biological Chemistry,* 293**,** 16572-16582.

YARIAN, C. S., REBRIN, I. & SOHAL, R. S. 2005. Aconitase and ATP synthase are targets of malondialdehyde modification and undergo an age-related decrease in activity in mouse heart mitochondria. *Biochemical and biophysical research communications,* 330**,** 151-156.

YI, J., XIA, W., WU, J., YUAN, L., WU, J., TU, D., FANG, J. & TAN, Z. 2014. Betulinic acid prevents alcohol-induced liver damage by improving the antioxidant system in mice. *Journal of veterinary science,* 15**,** 141-148.

YILDIRIM, S. S., AKMAN, D., CATALUCCI, D. & TURAN, B. 2013. Relationship between downregulation of miRNAs and increase of oxidative stress in the development of diabetic cardiac dysfunction: junctin as a target protein of miR-1. *Cell biochemistry and biophysics,* 67**,** 1397-1408.

YOGEESWARI, P. & SRIRAM, D. 2005. Betulinic acid and its derivatives: a review on their biological properties. *Current medicinal chemistry,* 12**,** 657-666.

YU, M., LIU, Y., ZHANG, B., SHI, Y., CUI, L. & ZHAO, X. 2015. Inhibiting microRNA-144 abates oxidative stress and reduces apoptosis in hearts of streptozotocin-induced diabetic mice. *Cardiovascular Pathology,* 24**,** 375-381.

YU, W., DITTENHAFER-REED, K. E. & DENU, J. M. 2012. SIRT3 protein deacetylates isocitrate dehydrogenase 2 (IDH2) and regulates mitochondrial redox status. *Journal of Biological Chemistry,* 287**,** 14078-14086.

ZHANG, P., ZHANG, X., BROWN, J., VISTISEN, D., SICREE, R., SHAW, J. & NICHOLS, G. 2010. Global healthcare expenditure on diabetes for 2010 and 2030. *Diabetes research and clinical practice,* 87**,** 293-301.

ZHANG, Q., LENARDO, M. J. & BALTIMORE, D. 2017. 30 years of NF-κB: a blossoming of relevance to human pathobiology. *Cell,* 168**,** 37-57.

ZHANG, X., HU, J. & CHEN, Y. 2016. Betulinic acid and the pharmacological effects of tumor suppression. *Molecular medicine reports,* 14**,** 4489-4495.

ZHONG, H., LU, J., XIA, L., ZHU, M. & YIN, H. 2014. Formation of electrophilic oxidation products from mitochondrial cardiolipin in vitro and in vivo in the context of apoptosis and atherosclerosis. *Redox biology,* 2**,** 878-883.

Bicinchoninic Acid (BCA) Assay

$y = 0{,}7966x + 0{,}1554$
$R^2 = 0{,}988$
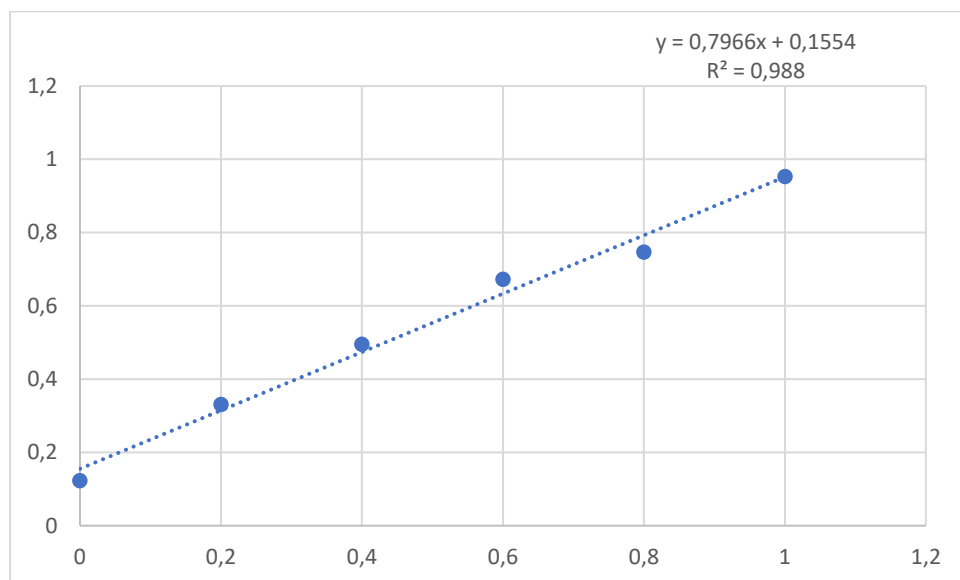
Figure 6: Standard curve displaying known concentrations of bovine serum albumin (BSA) used to extrapolate the concentration of protein present in sample.

Table 6: Standardisation of proteins (final volume = 200μl; concentration 1.8mg/ml)

Mean absorbance	Protein concentration (mg/ml)	Volume of sample (μl)	Volume of CytoBuster (μl)
2,4255	2,849736	126,3275	73,67253
2,3005	2,692819	133,6889	66,31113
2,2105	2,579839	139,5436	60,45643
2,321	2,718554	132,4233	67,57665
2,5765	3,039292	118,4486	81,55136
2,4365	2,863545	125,7183	74,28171
2,458	2,890535	124,5444	75,45557
2,443	2,871705	125,3611	74,63892
2,2385	2,614989	137,6679	62,3321
2,217	2,587999	139,1036	60,89639
2,4539	2,885388	124,7666	75,23341

25µM Betulinic Acid treatment

Literature proved presence of toxicity above 21µM, however, our MTT assay did not reproduce that observation, proving to be viable at all concentrations between 5 and 150µM. Hence, we additionally tested a 25µM BA concentration for the majority of our assays, as supplementary information to assess its cytoprotective capacity. It did not demonstrate toxicity, however it did not upregulate cytoprotective machinery to the same degree as 5µM and 10µM.
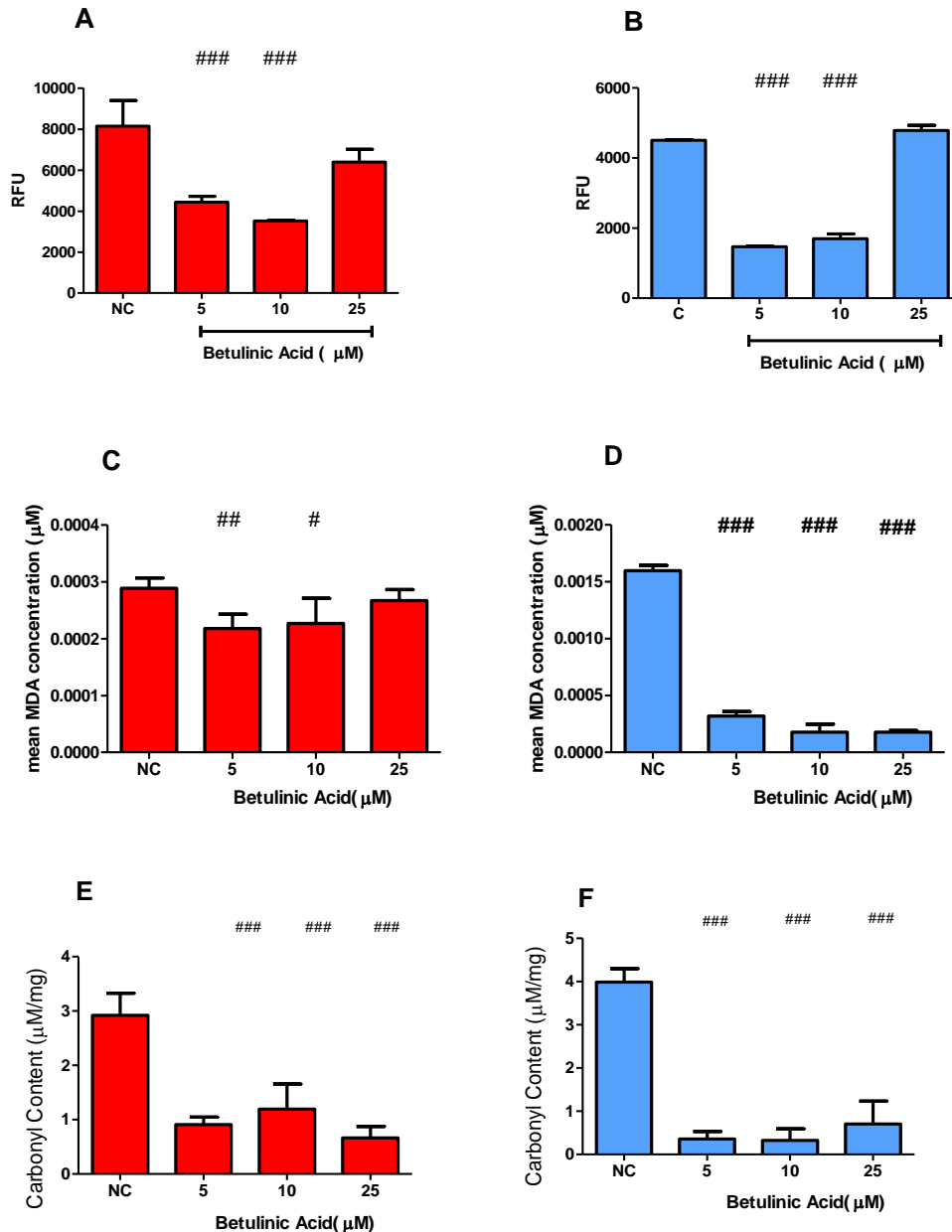
Figure 7: The H₂DCF-DA assay quantifying intracellular ROS levels in response to BA administration in a A) normoglycaemic and B) hyperglycaemic model. Lipid peroxidation by-product, MDA, quantified via a TBARS assay in both C) normoglycaemic and D) hyperglycaemic media. PCA assay quantifying protein carbonyl concentrations as an effect of ROS and lipid peroxidation, in E)

normoglycaemic (p<0.0001) and F) hyperglycaemic media. #p<0.05; ##p<0.001; ###p<0.0001 relative to negative controls.
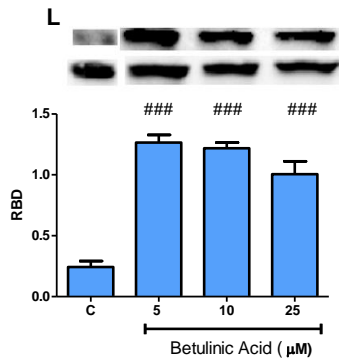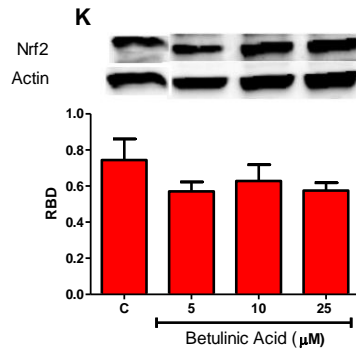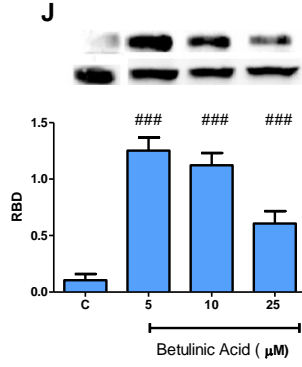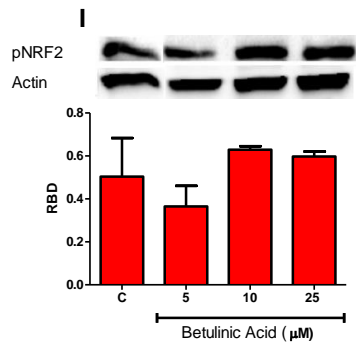
mRNA expression
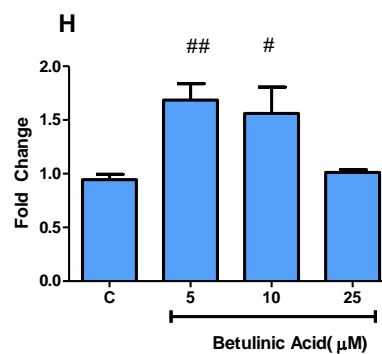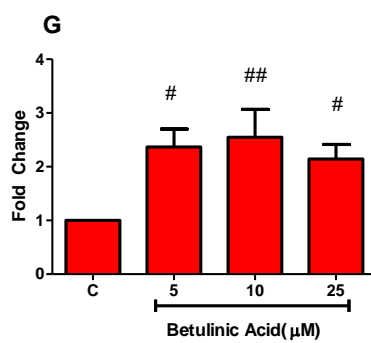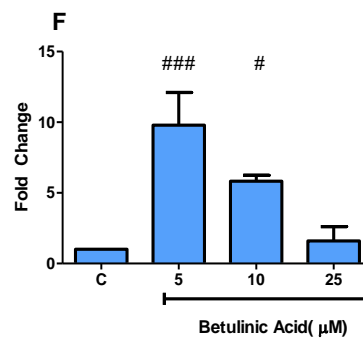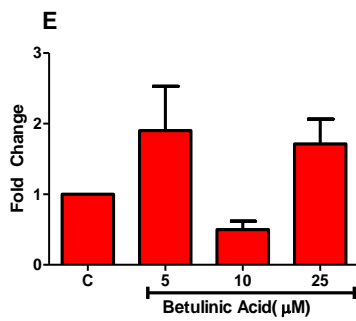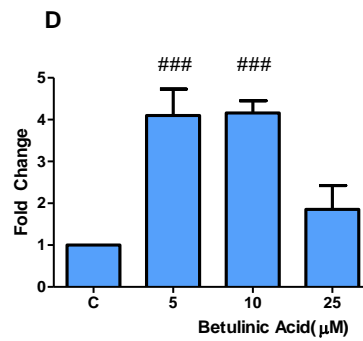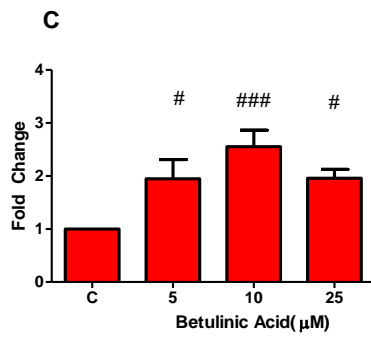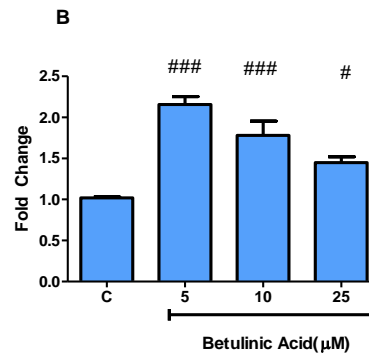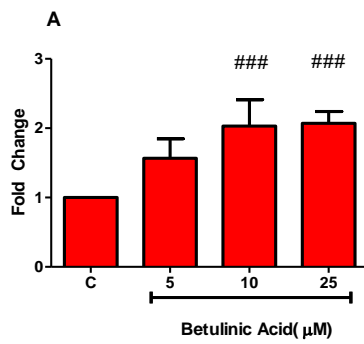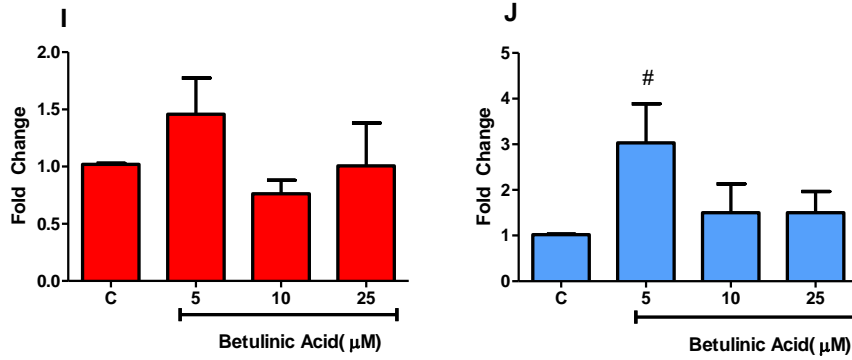
Figure 8: mRNA expression of GPx1 in A) normoglycaemic and B) hyperglycaemic conditions, PGC1α in C) normoglycaemic and D) hyperglycaemic conditions, NRF2 in E) normoglycaemic and F) hyperglycaemic conditions, SIRT3 in G) normoglycaemic and H) hyperglycaemic conditions, miR124 in I) normoglycaemic and J) hyperglycaemic conditions $^{\#}p<0.05;$ $^{\#\#}p<0.001;$ $^{\#\#\#}p<0.0001$ relative to negative controls.

Western Blots
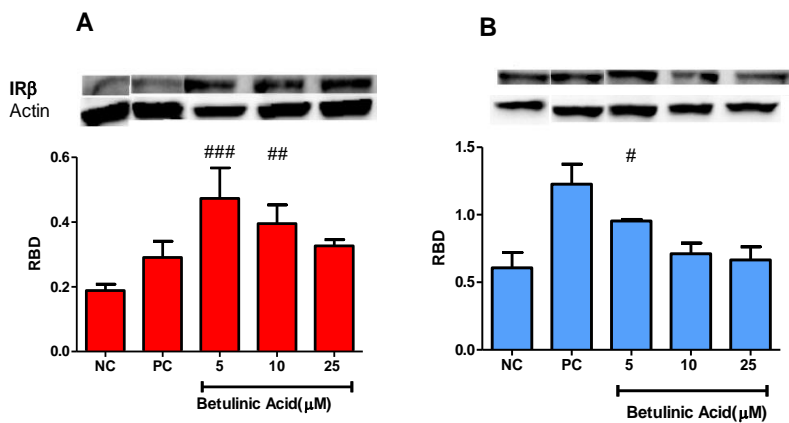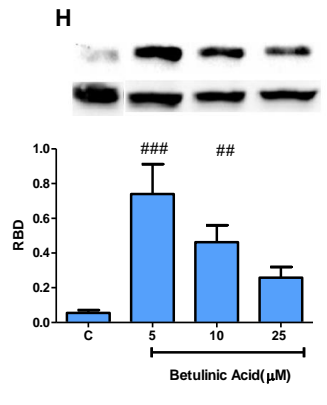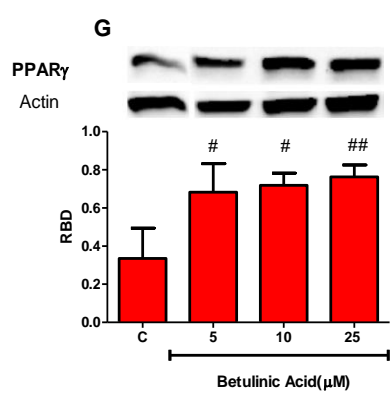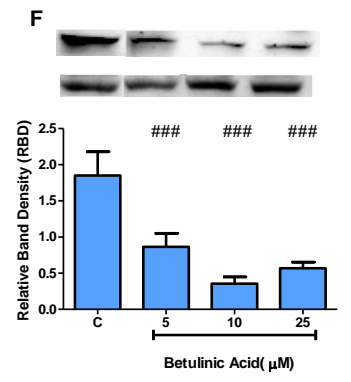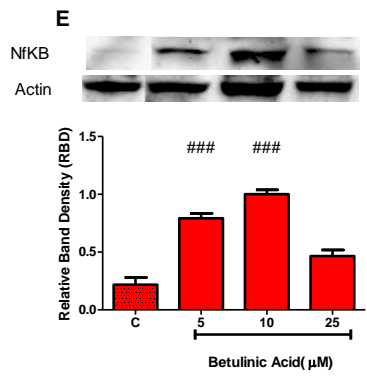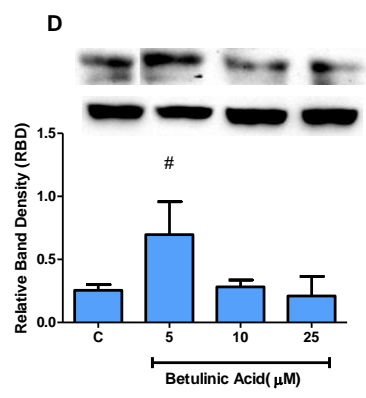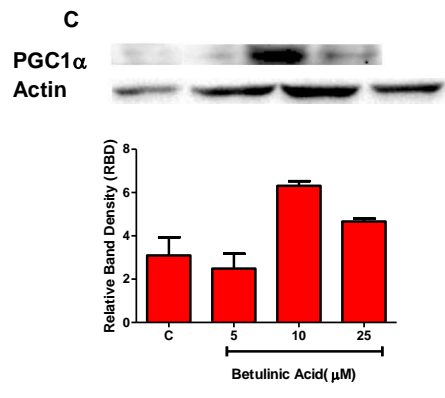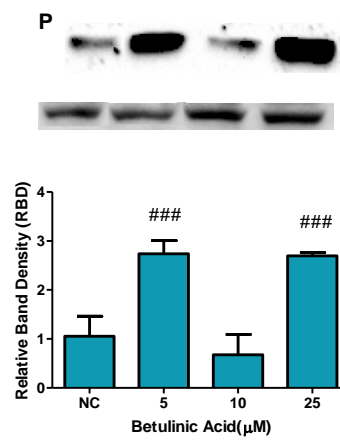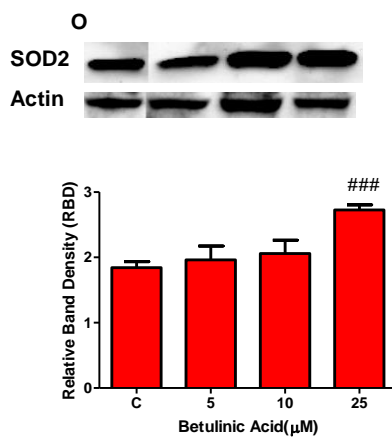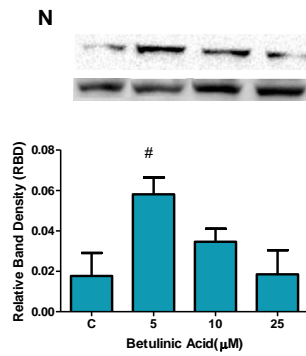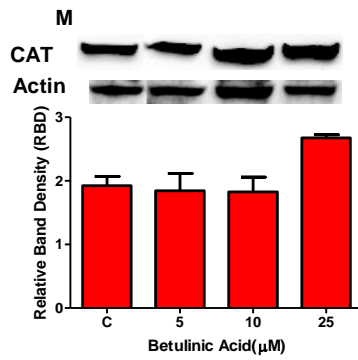
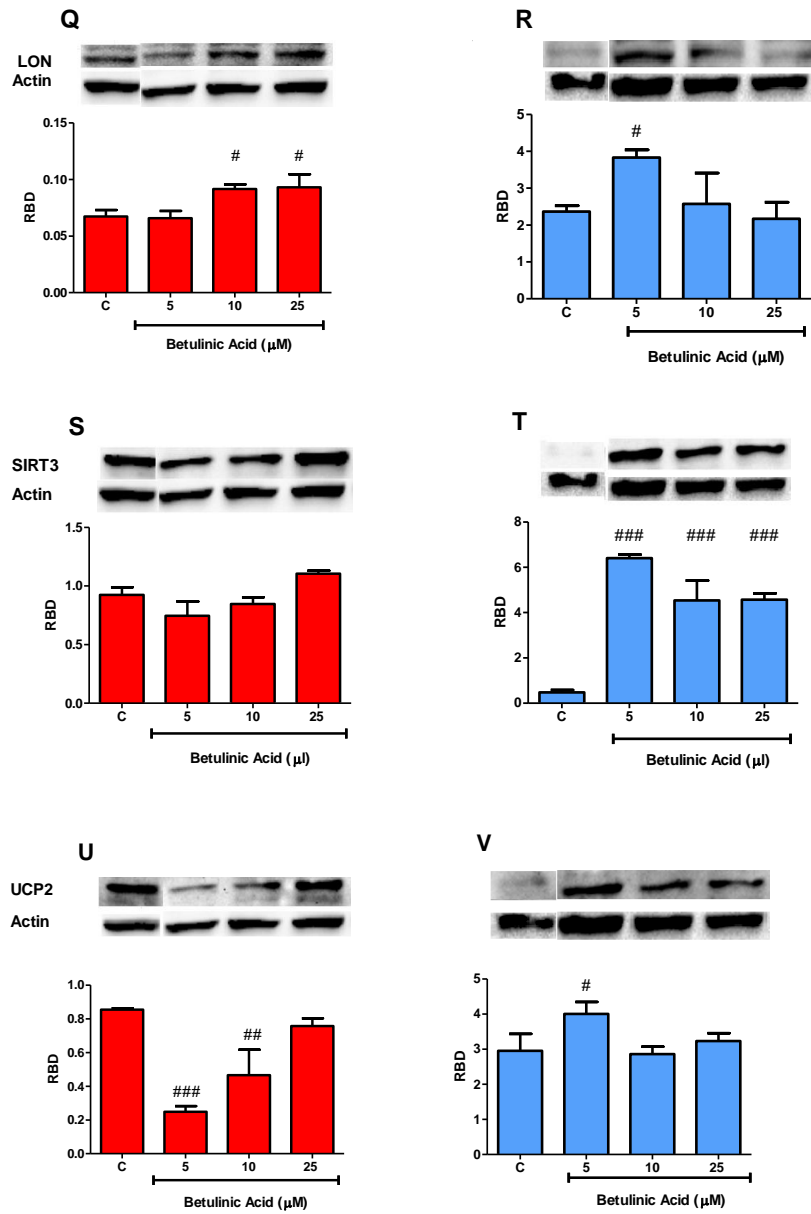*Figure 9: Protein expression of IRβ in A) normoglycaemic and B) hyperglycaemic conditions, PGC1α in C) normoglycaemic and D) hyperglycaemic conditions, NFκB in E) normoglycaemic and F) hyperglycaemic conditions, PPARγ in G) normoglycaemic and H) hyperglycaemic conditions, pNRF2 in I) normoglycaemic and J) hyperglycaemic conditions, NRF2 in K) normoglycaemic and L) hyperglycaemic conditions, CAT in M) normoglycaemic and N) hyperglycaemic conditions, SOD2 in O) normoglycaemic and P) hyperglycaemic conditions, LONP1 in Q) normoglycaemic and R) hyperglycaemic conditions, SIRT3 in S) normoglycaemic and T) hyperglycaemic conditions, UCP2 in U) normoglycaemic and V) hyperglycaemic conditions. #p<0.05; ##p<0.001; ###p<0.0001 relative to negative controls*